1-1-1989

Ordering processes in thermotropic liquid crystal polymers/

Sergio R. Rojstaczer
University of Massachusetts Amherst

ORDERING PROCESSES IN THERMOTROPIC LIQUID CRYSTAL POLYMERS

A Dissertation Presented

by

SERGIO R. ROJSTACZER

Submitted to the Graduate School of the
University of Massachusetts in partial fulfillment
of the requirements for the degree of

DOCTOR OF PHILOSOPHY

February 1989

Department of Polymer Science and Engineering

ORDERING PROCESSES IN THERMOTROPIC LIQUID CRYSTAL POLYMERS

A Dissertation Presented
by
SERGIO R. ROJSTACZER

Approved as to style and content by:

Richard S. Stein, Chairperson of Committee

Robert W. Lenz, Member

Murugappan Muthukumar, Member

Edwin L. Thomas, Member

William J. McKnight, Department Head
Polymer Science and Engineering

ACKNOWLEDGMENTS

I wish to thank my advisor, Professor Richard S. Stein, for providing guidance and support during this research project. I am particularly grateful for his ecouragement to develop new ideas in this interesting field. I am also grateful to the members of my committe, Professors R. W. Lenz, M. Muthukumar and in particular to Professor E. L. Thomas, for their insightful comments and suggestions. I would also like to thank Professor T. Hashimoto for the close collaboration in part of the project.

My colleagues in the research group provided a very nice environment to work in. First, I acknowledge Ellen Goldman for the participation in the project as a summer student. Special thanks go to Paula Hahn for introducing me to this project, and to Mike Satkowsky, Osamu Aoki and Russ Composto, for their collaboration and encouregement. I would like to mention the particularly enlightening interaction with Herve Marand and Greg Beaucage (not just for lighting-up). I am specially greateful to my classmate Jean Phillipe Autran for the close friendship and for the good moments we shared since arriving in Amherst. I must also mention my gratitude to Yachin Cohen for his friendship and for being always there when needed.

Above all, this dissertation is possible because of the moral support and exceptional patience of my wife Nurit, who, along with my sons Mattan and Eyal provided a loving home which was the inspiration for getting the work done.

ABSTRACT

ORDERING PROCESSES IN THERMOTROPIC
LIQUID CRYSTAL POLYMERS
FEBRUARY 1989
SERGIO R. ROJSTACZER, B.Sc., HEBREW UNIVERSITY OF JERUSALEM
M.Sc., HEBREW UNIVERSITY OF JERUSALEM
Ph.D., UNIVERSITY OF MASSACHUSETTS
Directed by: Professor Richard S. Stein

The morphology of a nematic thermotropic liquid crystal polyester composed of alternating mesogenic and flexible units is characterized by small-angle light scattering (SALS) and optical microscopy. The scattering from the polydomain textures is analyzed in terms of an average domain size related to the density of disclinations defects.

The effect of thermal history on the nematic state is investigated by quenching thin films from the isotropic phase down to various temperatures within the nematic range, followed by isothermal aging. The initial textures obtained immediately after the phase transition are characterized by a large density of disclination lines. The average domain size of the initial textures measured by SALS was found to be independent of the degree of undercooling. The temperature independence of the initial defect density is discussed in terms of a model describing a mechanism for the formation of disclinations during the formation of the

nematic phase. During annealing, a coarsening of the initial fine textures takes place by the annihilation of defects, this process being accompanied with an increase in the local anisotropy of the system. A kinetic study of the texture coarsening suggests that in the range of temperatures studied, the temperature dependence of the process is controlled by the mobility of the defects in the medium. Thermal analysis studies show that the ordering induced by annealing can lead to an increase of up to 10°C in the nematic to isotropic transition temperature.

In a study of the effect of shear, the texture obtained at small deformations was found to be composed of elongated domains with their long axis oriented perpendicular to the shear direction. Following the cessation of the shear after reaching a shear strain of 100 shear units, a banded texture was observed to form only upon cooling. During further heating and cooling cycles, the banded texture is seen to respectively form and fade-out without the application of additional deformation, suggesting the banded texture being a metastable thermodynamical state.

TABLE OF CONTENTS

Chapter

LIST OF TABLES

LIST OF FIGURES

CHAPTER 1

INTRODUCTION

1.1 Scope of the Dissertation

The role of liquid crystallinity in the high mechanical performance achievable in polymers was recognized in the early 1970s. The long range orientational order characteristic of the liquid crystalline phase facilitates the high degree of molecular alignment required for realizing high tensile modulus and strength materials. However, liquid crystal polymers (LCPs) usually form complex and relatively unstable superstructures or textures. The study of the relationship between chemical structure and physical properties requires a fundamental understanding of how the latter are affected by the textures. This is one of the reasons for the increasing number of morphological studies of LCPs carried out in recent years. The complete characterization of the polymeric textures requires the development of new experimental techniques along with theoretical models for their interpretation.

A liquid crystalline phase can be induced by a change in solvent concentration (lyotropic liquid crystals) or by a change in temperature (thermotropic liquid crystals). While polymers composed of rodlike structures show lyotropic behavior only, thermotropic liquid crystal polymers (TLCPs) were achieved during the last decade by various different approaches, such as the introduction of flexible units or unsymmetrically substituted

aromatic groups. The major part of the present thesis concerns the investigation of a main chain thermotropic polyester containing mesogenic units alternated by flexible spacers. A second system studied consists of a fully aromatic para-linked polyester in which the low melting temperature is attributed to the presence of large unsymmetrical substituents.

Some physical[1] and rheological[2] properties of TLCPs are known to be affected thermal history. One objective of this thesis is to characterize the textures occurring in TLCPs, and to investigate how these are affected by thermal history and deformation. The emphasis in this thesis is put on the quantitative characterization of the textures by SALS, based on the correlation between the scattering and the direct visualization of the structures by optical microscopy. By first establishing the relationship between the angular distribution of the scattered intensities and the corresponding morphologies, the SALS technique is then used to monitor the dynamics of structural changes occurring upon the formation of the nematic phase.

The scattering of light by liquid crystals is their most distinctive feature which differentiate them from ordinary isotropic liquids. In the first reported observation of liquid crystallinity, Reinitzer[3] states

" . . . *it struck me that the substance melted not into a clear transparent but always into a cloudy only translucent liquid, which I initially considered to be a sign of impurities, although both microscopic and crystallographic examinations of the compound revealed no signs of nonuniformity.*".

Another topic which is the focus of an increasing number of investigations carried-out in academic as well as in industrial laboratories is the deformation of the macroscopically unoriented textures into highly oriented structures, because of its implications in the processing of the high performance materials. The rheo-optical techniques pioneered by Stein[4] were found to be a powerful method for studying the deformation of semicrystalline polymers. The application of optical methods to complement the rheological characterization of lyotropic LCPs was introduced by Kiss and Porter[5], who utilized an optical microscope to observe the structure developing during and after shear by using a transparent cone and plate rheometer. Another rheo-optical technique increasingly used involves the continuous measurement of the birefringence during shear.[6] However, being a macroscopic property, the birefringence does not provide detail information about the structure. The inclusion of scattering measurements can be used to supplement the quantitative characterization of the structures induced by deformation. Recently, such studies were carried out on lyotropic systems by Hashimoto et al.[7], who introduced the term "Flow Small Angle Light Scattering". The analogous studies on TLCPs involve some technical difficulties due to the high turbidity and viscosity of the systems, which impart the necessity of thin specimens and high temperatures. This thesis includes a first report on the study of the deformation of a TLCP by SALS.

1.2 Organization of the Dissertation

Having established the main goals of the thesis, the rest of the present chapter presents an overview of the theories concerned with the liquid crystal phenomenon. The purpose is to introduce the concepts which will be used in the discussion of the experimental observations. Also included is a condensed overview of LCPs.

A description of the substances investigated along with the details of the experimental techniques used are presented in chapter 2. Chapter 3 outlines the basic theories concerned with the SALS from orientation fluctuations, followed by a description of the observed SALS patterns from the macroscopically unoriented textures. A proposed analysis of the SALS from the nematic textures is presented in terms of an average "domain" size and a local degree of order. The major part of the thesis concerns the study of the evolution of the nematic state following the phase transition from the isotropic precursor. Chapter 4 describes the effect of annealing on the textures and the corresponding SALS patterns. The kinetics of the relaxation of the initial structure are characterized by the time evolution of the angular dependence of the scattered intensities.

Chapter 5 presents the results of a preliminary study concerning the textures induced when the quiescent state is subjected to shear flow. It illustrates the SALS patterns observed during the deformation performed on a simple adaptation of the Flow-SALS technique. The reported results include a peculiar

effect of temperature on the banded texture observed after the cessation of the shear.

Chapter 6 presents a discussion of the experimental results described in chapters 3 through 5. As some of the experimental observations made can not be rigorously analyzed due to the lack of theoretical models, part of the interpretation falls in the context of speculations. The conclusions drawn are given in chapter 7, along with suggestions for future investigations, proposed in view of questions raised by the present work.

1.3 Literature Review

1.3.1 The Nematic Phase

The term liquid crystallinity refers to mesomorphic states characterized by long range orientational order. Following the nomenclature proposed by Friedel[8], liquid crystals are classified into three main groups: smectic, cholesteric and nematic. Smectic liquid crystals are characterized by layered structures. According to the molecular arrangement within the layers, several smectic modifications are defined. Nematic liquid crystals, as studied in this thesis, exhibit orientational order, but no long range translational order. The cholesteric phase is a twisted variation of the nematic class induced by an asymmetric center in the molecule. Thermodynamically, cholesterics are very similar to nematics, as the energy of twist is only a very small fraction of the total energy associated with the parallel alignment of the molecules.[9]

The long range orientational order occurring in nematics is characterized by a unit vector **n**, termed the director, representing the axis of preferred orientation. Nematics are apolar, meaning that the directions **n** and -**n** are equivalent. If the distribution function of the molecular orientation is cylindrically symmetric (uniaxial nematics), the degree of alignment can be defined by the order parameter *s*, first introduced by Tsvetkov[10],

$$s = \frac{1}{2} < 3\ \cos^2\theta - 1> \ , \qquad (1.1)$$

where θ is the angle the molecular axis makes with **n**, and the angular brackets represent a statistical average. For perfect parallel alignment $s=1$, while for the uncorrelated orientations characteristic of the isotropic state, $s=0$. In the nematic phase *s* has an intermediate value which is temperature dependent. The experimental determination of the order parameter requires homogeneously aligned samples, the so called monodomain texture. Neglecting thermal fluctuations of the director, the order parameter is obtained by relating a macroscopic anisotropic property such as birefringence or the diamagnetic anisotropy to the respective molecular anisotropy.[11] An important tool increasingly used for determining the molecular order is nuclear magnetic resonance spectroscopy.[12,13]

The following paragraphs present a qualitative summary of the main theoretical approaches proposed for explaining the bases for the stability of the nematic phases. A more detailed description of the various theories, including their quantitative

aspects, can be found in the textbooks by de Gennes[14] and Chandrasekhar.[15]

The first model for the nematic to isotropic (N-I) transition is due to Onsager[16], who considered a gas composed of ideal rigid rods, without any potential between them other than the repulsive forces preventing their interpenetration. Onsager proved, based on an exact density expansion of the free energy, a spontaneous transformation from an isotropic to a nematic order occurring at a critical concentration of the rods. Flory[17] proposed the treatment of hard rods using the lattice theory developed for polymer solutions, by replacing flexible chains with rigid rods, and predicted the formation of an anisotropic phase at a critical volume fraction of the rods, its value depending on the axial ratio of the rods.

The original Onsager and Flory theories indicated that steric interactions can be sufficient for the formation of liquid crystalline phases. Later versions of the lattice theory, however, include both isotropic and anisotropic interactions, after Flory[18] recognized the important role they may play in concentrated solutions and thermotropic melts.

A different approach was taken by Maier and Saupe[19], by considering dispersion forces only. The Maier-Saupe treatment consists of a mean field theory in which each molecule is subject to an internal field which is independent of any short range ordering. The orientational energy of a molecule is assumed to be proportional to the order parameter s, and a function of the angle between the molecular axis and the director. The calculation of the

free energy predicts a stable nematic phase with a decreasing order parameter at increasing temperatures. A first order transition occurs at a critical value of the order parameter s_c=0.44 , in fair agreement with the experimentally determined values for a large number of compounds. However, significant discrepancies are observed in some properties such as the isotropization enthalpy.

All the models presented above predict an abrupt vanishing of the order parameter at the nematic to isotropic transition temperature (T_{N-I}). This is in disagreement with the experimental evidence of anomalous effects in the isotropic phase which indicate some extent of short range order at temperatures close to T_{N-I}. An example of these pretransitional effects are the unusually high values of the magnetic[20] and flow[21] birefringence. The magnetic birefringence Δn_m in the isotropic phase follows a $(T-T^*)^{-1}$ dependence, where T* is the temperature obtained by extrapolating Δn_m to infinity. In small molecule liquid crystals (SMLC)[20], T* is found to be in the order of 1°C lower than T_{N-I}. While the $(T-T^*)^{-1}$ relationship can be obtained from the mean field theory, the predicted T* is in the order of 40 - 50°C below T_{N-I}.[15]

A more satisfactory description of the pretransitional phenomena was reached by de Gennes[22], by treating the N-I transition on the basis of the Landau theory of phase transitions.[23,24] This phenomenological approach predicts a first order transition at a critical temperature T_c (T_{N-I}) and a second

order transition at a temperature T*. For weak transitions, such as the N-I transition, T_c -T* is a very small quantity, in accordance to the experimental evidence. The Landau-de Gennes model has been used to treat the light scattering from the isotropic phase in terms of fluctuations of the order parameter about its equilibrium value (zero). The predictions are found to agree well with the experimentally measured temperature dependence of the scattered intensity and correlation length.[25]

1.3.2 Continuum Theory of Curvature Elasticity

The thermodynamical theories described in the preceding section predict a nematic phase in which the preferred alignment is represented by a single axis **n**. In real nematics, particular orientations can be imposed by the surfaces or by the effect of external forces such as magnetic fields. If these boundary conditions impose orientations other than parallel alignment, the local director will change gradually or abruptly from point to point. Abrupt variations in the director are made possible by defects corresponding to the rotation of one part of the mesophase with respect to the other. In order to find the equilibrium form of the director, i.e., the directorfield, a continuum model was initially proposed by Oseen in 1933.[26] Twenty five years later, Frank[27] derived Oseen's treatment on a more general bases as a theory of curvature elasticity. The theory defines a curvature strain involving a change in the direction of the director, which unlike the strain deformation in solids, does not involve a change in the

distance between points in the continuum. The director orientation can change continuously from point to point, except at singularities. Frank originally named these singularities "disinclinations", but the term was later changed to "disclinations". In analogy to the forces opposing the strain in a solid medium, in a liquid crystal the curvature is opposed by restoring torques.

The curvature is described in terms of splay, twist and bend deformation, associated with the elastic constants k_{11} , k_{22} and k_{33}, respectively (Frank constants). The three modes of deformation are schematically represented in figure 1.1. The excess free energy per unit volume due to the distortion of the directorfield is given by

$$F_d = \frac{1}{2} \{ k_{11} (\text{div } \mathbf{n})^2 + k_{22} (\mathbf{n} \text{ curl } \mathbf{n})^2 + k_{33} (\mathbf{n} \times \text{curl } \mathbf{n})^2 \} \quad .(1.2)$$

For a planar geometry, in which the director is parallel to the x-y plane and not a function of the normal to the plane (z), only splay and bend deformation are relevant.

The first attempt to relate the values of the elastic constants to molecular parameters is due to Saupe.[28] Using the mean field theory, Saupe obtained quantitative expressions for the elastic constants in which k_{ii} is proportional to s^2 (s being the order parameter). This prediction was found to agree with the experimentally determined temperature dependence of the elastic constants of various systems. Theoretical efforts were since then made in an attempt to predict the ratio between the various elastic constants. Models developed for long rodlike particles[29,30]

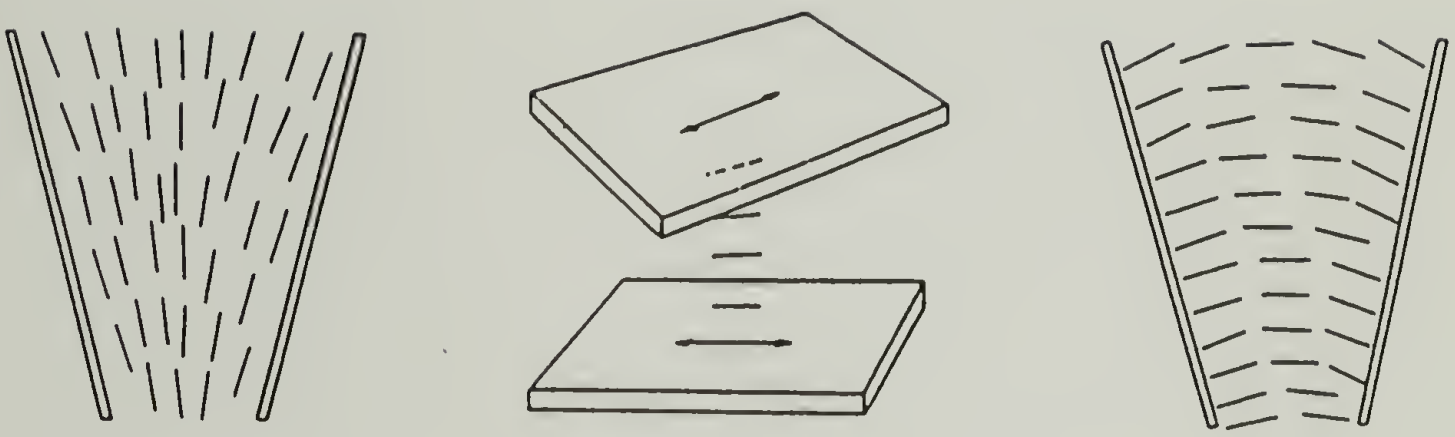

splay twist bend

Figure 1.1 Main modes of deformation in liquid crystals. (after ref. 14)

were able to predict the general observation of the bend constant k_{33} being larger than the splay constant k_{11}, both in lyotropic[31] as well as in thermotropic[32] nematics.

The difference in the values of the various elastic constants is referred to as "elastic anisotropy". The solution for the directorfield can be simplified by assuming isotropic elasticity, often called the "one constant approximation" ($k_{11}=k_{33}=k$). In cylindrical coordinates, the orientation of the director is represented in terms of the angle Φ, the director makes with the x axis. Minimization of the energy leads to a set of solutions for Φ as a function of the polar angle α and radius r. A trivial solution corresponds to Φ = constant , representing a uniformly oriented state. Other singular solutions are given by

$$\Phi = S\,\alpha + c\ , \qquad (1.3)$$

where c is a constant and S is defined as the strength of the disclination. In order to comply with the apolarity of the nematic phase, S can take the values

$$S = \pm\frac{1}{2}\ , \pm 1\ , \pm\frac{3}{2}\ , \ldots$$

with $0 < c < \pi$. The directorfield in the x-y plane in the neighborhood of disclination of various strengths is shown in figure 1.2. The disclination lines lie in the z axis. For disclinations of strength other than S=1 , a change in the constant c corresponds to a rotation of the directorfield around the disclination line. For S=1, a variation of c changes the shape of the directorfield.

$s=\frac{1}{2}$

$s=-\frac{1}{2}$

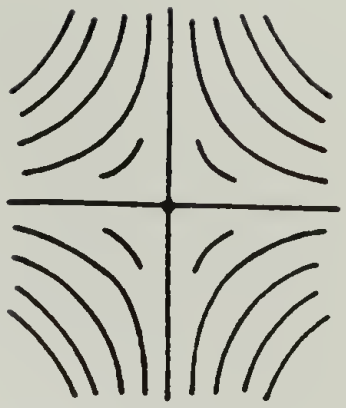

$s=-1$

$s=1, c=0$

$s=1, c=\pi/4$

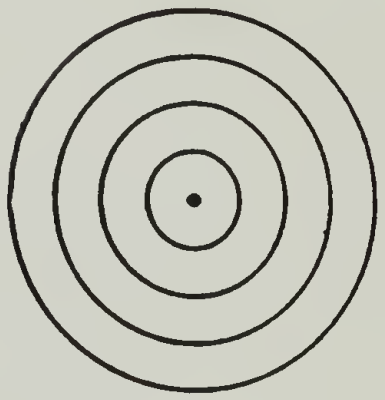

$s=1, c=\pi/2$

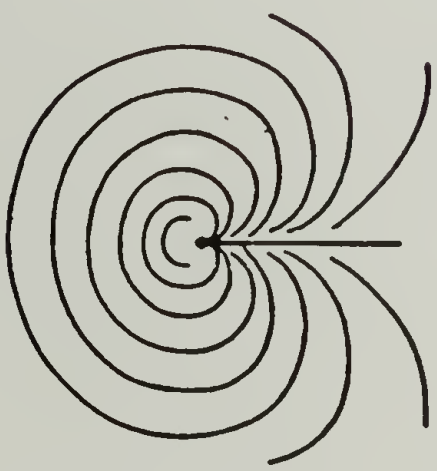

$s=3/2$

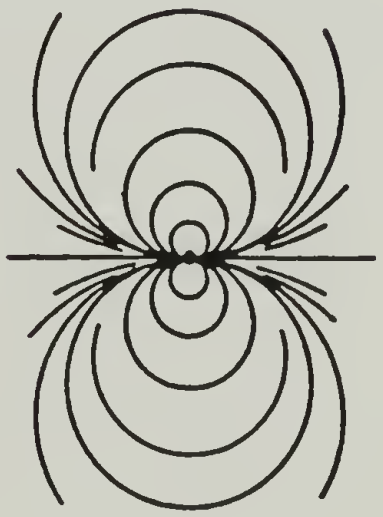

$s=2$

Figure 1.2 Directorfield in the neighborhood of disclinations. (after ref. 27)

The Schlieren textures observed between cross polarizers when a thin sample (10 to 50 μm) is placed between untreated glass plates consists of black brushes originating at points, which correspond to end-on views of the disclination lines. The absolute value of the disclination strength is

$$|S| = \frac{\text{number of brushes}}{4} . \qquad (1.4)$$

The sign of a disclination can be obtained by simultaneously rotating the polarizers in the crossed position. The brushes originating at positive disclinations follow the direction of rotation of the polarizers while those originating at negative disclinations rotate in the opposite direction.

The energetics of defects in liquid crystals are discussed in detail in a recent review by Chandrasekhar.[33] The deformation energy of an isolated disclination in a circular layer of radius R is given by

$$E = \pi k S^2 \ln(R/r_c) \qquad (1.5)$$

where r_c is the radius of the core. The S^2 dependence of the energy indicates that $S=\pm 1/2$ disclinations are more stable than those of higher strength. In small molecule liquid crystals, however, $S=\pm 1$ disclinations are usually the more abundant. It has been shown[34] that the $S=\pm 1$ disclinations are stabilized by a departure from planarity, leading to nonsingular, more stable $S=\pm 1$ disclinations. Equation 1.5 implies that as $R \rightarrow \infty$, $E \rightarrow \infty$,

meaning that a single disclination should have infinite energy. Such a situation does not arise in practice due to the presence of pairs of disclinations of opposite sign. The energy of a pair of disclinations separated by a distance $r_{1,2}$ is

$$E = \pi\, k\, (S_1+S_2)^2\, \ln(R/r_c) - 2\pi\, k\, S_1\, S_2\, \ln\,(r_{1,2}/2r_c)\,. \qquad (1.6)$$

Thus, if $S_1 = -S_2$, the energy is independent of R. Based on equation 1.6, the force between two disclinations is

$$f_{1,2} = 2\,\pi\, k\, S_1\, S_2 \,/\, r_{1,2}\,. \qquad (1.7)$$

Accordingly, disclinations of like sign repel while those of opposite sign attract with a force inversely proportional to the distance. Disclinations can merge, either creating a new disclination of strength $S'=S_1+S_2$, or annihilating, if $S_1 = -S_2$. Example of these processes are reported in reference 35.

The effect of elastic anisotropy ($k_{11} \neq k_{33}$) results in deviations from the picture presented above. Elastic anisotropy affects both the director patterns around disclinations and their energies.

For $S=\pm 1/2$, the directorfield around the disclinations departs from the elastic isotropic solutions to accommodate the lower energy deformation. One manifestation of this effect is the non-homogeneous rotation of the various brushes during the rotation of the polarizers. Frank[27] suggested that it might be possible to evaluate k_{11}/k_{33} from the non uniform rotation of the brushes of a disclination when the polarizers are rotated uniformly. One limitation of this technique, besides its experimental difficulty, is

the disturbances of the directorfield caused by neighboring disclinations. Recently, a more sophisticated method based on the same principle was developed by Hudson[36], for evaluating k_{11}/k_{33} in polymeric systems. For $S=\pm 1$ disclinations, the configuration of the directorfield is not affected by the elastic anisotropy, but their energy becomes a function of the constant c. Elastic anisotropy also induces a relative stability of the S=+1/2 disclinations in relation to the S=-1/2 ones.

Ranganath[37] realized that if $k_{11} \neq k_{33}$, the interaction between disclinations depends not only on the distance between their cores, as in the isotropic case, but also on the relative rotation of the directorfield around them. The effect is illustrated in figure 1.3, which shows the directorfield patterns for two pairs of opposite sign defects (+1/2, -1/2) and (+1, -1), each in two different situations. For the configurations shown in the upper part of the figure, the region connecting the disclinations is predominantly bend, while in the other configuration, the central region consists of mostly splay deformation. Depending on the relative values of k_{11} and k_{33} , one or the other pair of configurations will be the energetically favored.

1.3.3 Light Scattering from Monodomain Nematics

The first systematic study of the Rayleigh scattering from liquid crystals was carried out by Chatelain[38] in 1948. Studying homogeneously aligned samples of p-azoxyanizole, he observed that the scattering was highly depolarized and particularly strong

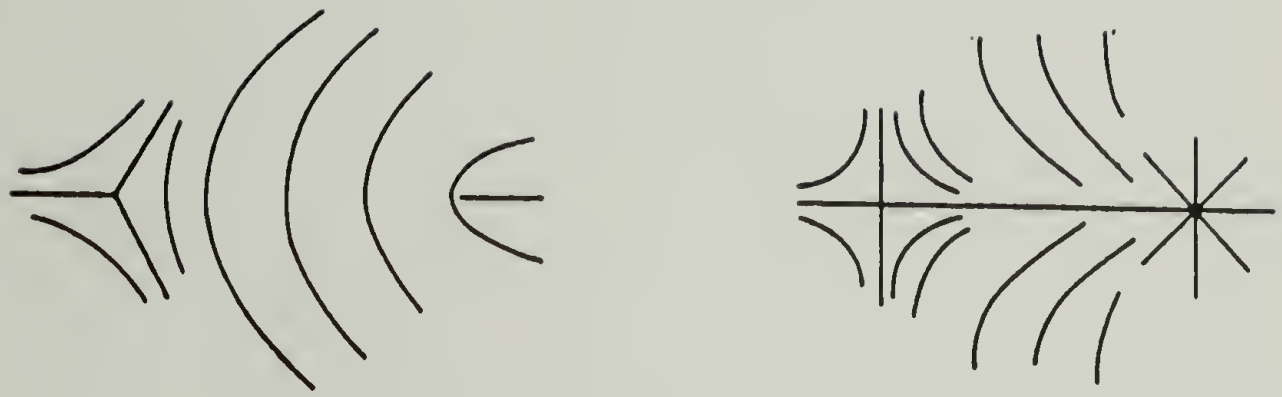

(1/2, -1/2)

(1, -1)

Figure 1.3 Directorfield for (1/2, -1/2) and (1, -1) disclination pairs. (after ref. 37)

at small angles. The temperature dependence of the intensity was found to be very small. The observations were initially interpreted in terms of scattering from anisotropic objects about 0.2 μm in size. With the development of the continuum approach, the concept of such objects or domains with abrupt changes in orientation was replaced by the idea of continuum distortions of the director. In this context, de Gennes[39] treated the theory of light scattering from homogeneously aligned nematics in terms of thermal fluctuations of the director. In this approach, the Frank elastic constants play an analogous role to the compressibility in isotropic liquids, where the scattering is a consequence of density fluctuations. Analysis of the angular dependence of the scattering under various polarization conditions allows for the evaluation of the ratio of the elastic constants. By including the dampening effect of a magnetic field, the absolute values of the various elastic constants can be obtained. After probing its reliability[40], the method became a standard procedure for measuring the elastic constants.

The scattering cross section can be approximated by

$$\frac{d\sigma}{d\Omega} \equiv \frac{\pi^2}{\lambda^4} \delta^2 \frac{k_B T}{k_{eff} q^2} \quad , \qquad (1.8)$$

where λ represents the wavelength of the radiation, q is the magnitude of the scattering vector and k_{eff} is an average of the elastic constants. The effect of temperature on the intensity can be evaluated by considering the temperature dependence of the

various terms. The macroscopic anisotropy of polarizability δ is proportional to the order parameter s, while according to the mean field theory, k_{eff} is proportional to s^2. The effect of $k_B T$ is very small in the nematic range, leading to a nearly temperature independent scattering, in accordance with Chatelain's original measurements and other recent evidence.[41] In other words, the effect of increasing fluctuations with increasing temperature is cancelled out by the decrease in the anisotropy.

The quasielastic light scattering is analyzed in terms of the relaxation rate of the orientation fluctuations. The theoretical treatment calculates a relaxation rate[42]

$$u = \frac{k_{eff}}{\eta_{eff}} \cdot q^2 \quad , \qquad (1.9)$$

where k_{eff} represents the restoring force of the fluctuation and η_{eff} is an effective viscosity related to the friction opposing the distortion of the director. The ratio k/η has been interpreted by de Gennes[14] as a diffusion coefficient for the orientation.

1.3.4 Liquid Crystal Polymers

The first contribution to the field of liquid crystal polymers can be attributed to Vorlander.[43] In 1923, studying the effect of molecular shape on liquid crystallinity, he stated that " . . . *infinitely long mesogens would be compatible with the molecular organizational constrains in liquid crystals*". It was not until the early 1940s that the ability of long rodlike molecules to form anisotropic phases was recognized. These consisted of lyotropic

biopolymers such as the tobacco mosaic virus. The research in the area of synthetic LCPs was throughout the history industrially motivated. The synthetic polypeptide poly (γ)-benzyl -l-glutamate (PBLG) was comprehensively studied in the 1950s in an industrial laboratory seeking to obtain fibers with properties comparable to the excellent properties of naturally occurring polypeptides such as wool. The development of linear, mainchain LCPs was a result of research focused on obtaining high thermal stability and high mechanical properties. The importance of the mesophase formation was recognized following the observation of unusually high tensile strength exhibited by fibers spun from concentrated solutions of poly(aryl-amides).[44] The difficulty in the processability of these polyaramides gave rise to an increasing extent of industrial and academic research focused on the tailoring of TLCPs which would be processable in the melt state at temperatures below degradation. A variety of approaches have been used in an attempt to obtain structures with relatively low melting points while preserving the liquid crystalline character.[45]

Although the polymeric nature of LCPs results in some unique characteristics not found in SMLCs, the basic features of the polymeric mesophases can be fitted under the classification developed for the small molecule counterparts.

Concerning the thermodynamical aspects, one major difference is the contribution of the configurational entropy to the various phase transitions. The overall entropy change in the transition from a three dimensional crystal to the isotropic liquid

can be separated into three contributions: positional, orientational and configurational entropy[46]

$$\Delta S_f = \Delta S_{pos} + \Delta S_{or} + \Delta S_{conf} \ . \qquad (1.10)$$

The values of the first two terms are found to be nearly constant for a large number of compounds indicating that the positional and the orientational contributions are independent of molecular size. In SMLCs, the N-I transition is dominated by ΔS_{or} . The experimentally determined values of ΔS_{or} are usually at least one order of magnitude smaller than the total entropy of fusion ΔS_f , indicating that the nematic phase retains only a small extent of the orientational order existing in the crystalline phase.

The configurational entropy ΔS_{con} is the one that dominates the melting of semicrystalline flexible polymers. The entropy of isotropization of LCPs is in general larger than for SMLCs. The difference is particularly large for polymers containing flexible spacers.

As the T_{N-I} is a function of molecular weight, the polydispersity of polymeric systems can cause a broad N-I transition in which stable biphases occur by the segregation of different molecular weight fractions into the isotropic and nematic regions.[47]

Molecular size also affects the distortion energy associated with the various modes of deformation. de Gennes[48] predicted that as molecular length increases from a small value, all the elastic constants should show some initial increase. For rodlike

molecules, the effect should be stronger on the splay deformation, because the requirement of constant density can only be satisfied by accommodating chain ends.

The study of the textures displayed by LPCs started in the last few years.[49-54] The general observation is that TLCPs form fine scale textures characterized by large defect densities, making their characterization by optical methods a difficult task. There is also an experimental difficulty due to the thinner film thickness required for the analysis of the textures in the planar geometry. Wood[53] developed a "lamellar decoration" technique in which the directorfield is traced by Transmission Electron Microscopy (TEM) imaging of a partially crystallized nematic state. The imaging of textures of a semiflexible TLCP in the quiescent state indicated the presence of disclinations, mostly of strength $S=\pm 1/2$. The director patterns in the vicinity of disclinations were fount to correlate well with the results of the continuum theory of elasticity. This observation suggests that the difference in the optical appearance of polymeric and SMLC resides in the quantitative aspect concerning the disclination densities.

The large viscosities characteristic of macromolecular systems give rise to unique behavior of the textures when LCPs are subjected to shear deformation. One example is the banded texture occurring in various LCPs, both lyotropic[56-58] and thermotropic.[59-62] The banded texture is characterized by long, dark extinction lines perpendicular to the shear direction, when viewed under a polarized light optical microscope. The bands develop usually after the cessation of the shear. Systematic

studies of the necessary conditions for the formation of the banded texture were carried out in anisotropic solutions of hydroxypropylcellulose (HPC) by Cifferri[63] and by Navard.[64] The results indicate that there is a minimum shear rate and shear deformation necessary for the formation of the bands. The time it takes for the bands to form as well as the period of stability of the texture were also found to depend on the shear conditions.

CHAPTER 2

MATERIALS AND EXPERIMENTAL TECHNIQUES

2.1 Materials

The major part of the thesis focuses on the investigation of a thermotropic polyester based on a triad mesogenic unit containing an arylsulfonyl hydroquinone group and a decamethylene spacer (referred to as PSHQ) as shown below

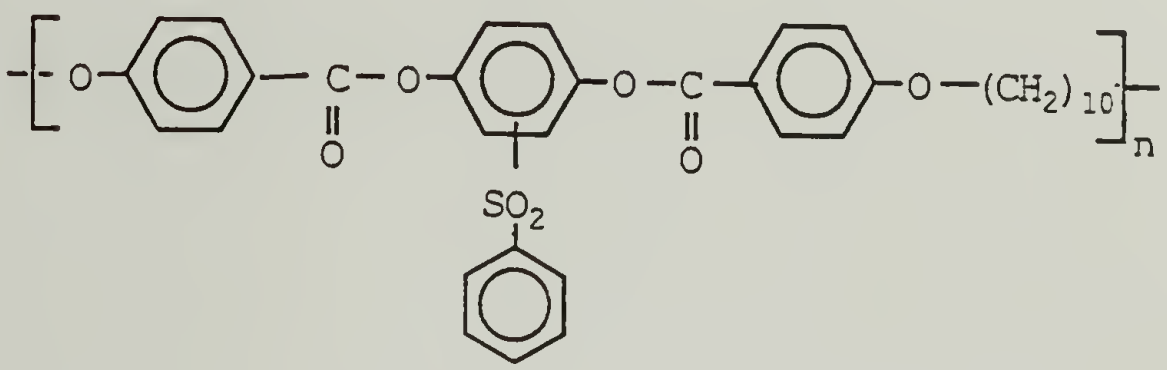

This is one of a series of homologous polymers synthesized by Furukawa and Lenz.[65] The polymer was reported to form a nematic phase at a melting point of 100°C, with a N-I transition occurring at 170°C. Thermal analysis indicated a glass transition temperature at 87°C. The moderate T_{N-I} suggested the PSHQ polymer as a good candidate for studying the nematic phase by quenching from its isotropic precursor without expecting significant extent of degradation. The relatively broad nematic range also allowed to study the effect of temperature on the nematic state. The relatively low transition temperatures are a result of the combined effect of both the flexible decamethylene spacer and the bulky unsymmetrical sulfonyl substituent in the

mesogenic unit. The occurrence of a glass transition at 87°C leads to a narrow window for crystallization suggesting, as it was experimentally corroborated, that the nematic state can be easily "frozen-in" at room temperature.

The structure of the second polymer studied consists of a completely aromatic, para-linked backbone of the form

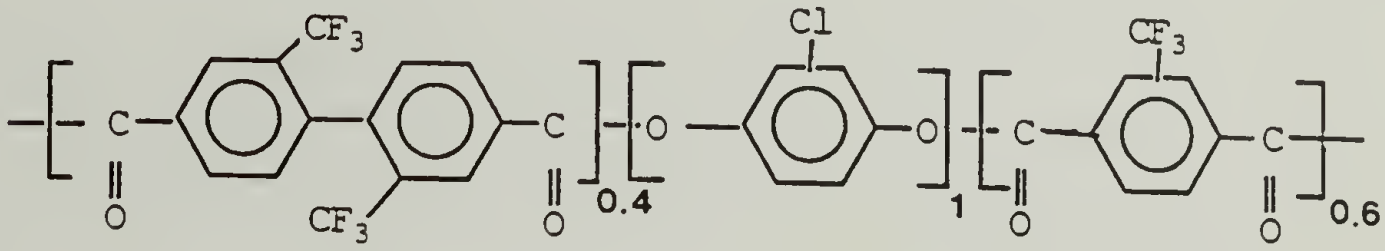

This polymer was synthesized[66] and provided by the Polaroid Corporation. Due to the random distribution of the biphenyl units and the bulky 2-2' substituents, the Polaroid polymer was found as unable to crystallize under normal circumstances.[66] The initial state of the polymer was defined as amorphous. The reported thermal analysis results indicated a glass transition at 110°C, while optical microscopy indicated the onset of birefringence at 150°C. The nematic phase, once formed, is locked-in whatever thermal treatment is performed. Thermal decomposition takes place at around 430°C, before a stable isotropic phase develops. The estimated molecular weight from Gel Permeation Chromatography (GPC) based on polystyrene standards is M_n=7,000 with a polydispersity index of 2.1.[67] The molecular weight obtained by Hsiao[68] from light scattering measurements is M_w=21,800.

2.2 Sample Preparation

A key factor for obtaining reliable quantitative SALS from TLCPs is to avoid a significant effect of multiple scattering. Neglecting any absorption of the incident light, the extent of multiple scattering can evaluated by the percent transmittance T defined as

$$T = 100 \cdot \frac{I}{I_0} \quad , \tag{2.1}$$

where I is the intensity at zero scattering angle and I_0 is the incident intensity. The turbidity τ is related to the transmittance by

$$\tau = \frac{1}{d} \ln\left(\frac{100}{T}\right) \quad , \tag{2.2}$$

where d is the sample thickness. While procedures for the correction for multiple scattering have been worked out[69,70], these are rather complex and the conclusion is that the corrections can be avoided by keeping T above 80%.[71] The intrinsic turbidity of the materials studied limited the sample thickness to the range of up to one micron.

The procedure chosen for obtaining homogeneous thin film was solution casting. Films of both the PSHQ and the Polaroid polymers were cast by placing a couple of drops of the respective 0.8% THF solutions onto microscope cover glasses. The latter were inserted into a closed chamber to allow slow evaporation of the solvent (typically two hours). The as-cast film were transparent and optically isotropic under the observation of the optical

microscope. The same sample preparation technique was used for the optical microscopy studies.

The specimens used in the deformation study (PSHQ polymer) were prepared by melting a previously press-molded 10 μm thick film between microscope slides. The sandwiched polymer was then heated to 200°C (in the isotropic phase) to erase any possible distortion of the quiescent texture due to the pressure exerted by the microscope slides. Multiple scattering from this thicker films was not significant for the qualitative description of the patterns during deformation, as the application of the shear deformation was accompanied by a significant decrease in the turbidity.

2.3 Small-Angle Light Scattering

The SALS patterns were photographically recorded using Polaroid type 55 film. The quantitative scattered intensities were measured by an Optical Multichannel Analyzer (OMAIII) system, EG&G Princeton Applied Research. The detector consists of a two dimensional array of photodiodes (vidicon) controlled by a 1460-V microprocessor unit. Figure 2.1 shows a diagram of the SALS apparatus. Its basic components are a 2 mW He-Ne laser (λ = 632.8nm), a sample stage and a system of three lenses with the purpose of focusing the scattering onto the detector area (12.5 by 12.5 mm). Table 2.1 lists the properties of the lenses used. These were chosen so to allow the measurement of scattering up to angles of 15°. Two Polaroid linear polarizers are used to select the polarization plane of the incident and scattered light (termed

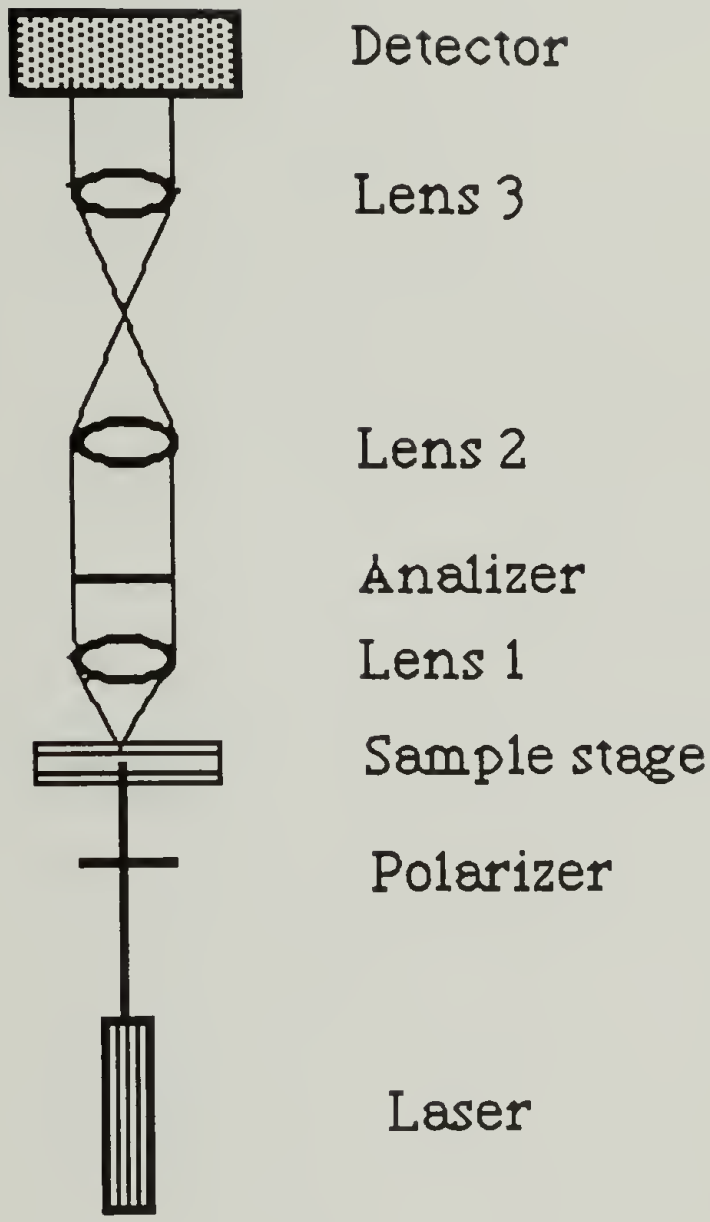

Figure 2.1 Schematic diagram of the small-angle light scattering apparatus.

Table 1

Constants of the lenses used in the SALS apparatus

Lens number	Diameter (mm.)	Focal Length (mm)
1	50.8	50.8
2	75.0	200.0
3	50.0	80.0

polarizer and analyzer, respectively). The scattering angles were calibrated by a diffraction grating.

The absolute values of the scattered intensities were determined by calibration with a Lambertian diffuser,

$$I=\frac{C_s}{C_d}\cdot\frac{RGTG}{d\cdot A}\quad , \qquad (2.3)$$

where C_S is the counts measured from the sample, C_d is the counts measured from the diffuser in the absence of the analyzer, RGTG is the constant of the diffuser, A is the attenuation factor of the analyzer and d is the sample thickness. The scanning conditions of the detector were selected so to optimize the signal to noise ratio. In order to maximize the dynamic range in the time dependent

measurements, the detector was scanned along a single line containing the main beam. This corresponds to measuring the scattering at a constant pre-set azimuthal angle. A single scattering curve in the dynamic experiments consisted of the accumulation of counts for a period of 2 seconds (100 scans of 20 msec).

2.4 Optical Microscopy

Polarized light optical microscopy studies were performed on a Zeiss microscope. Unpolarized micrographs were obtained by removing the polarizer from the optical path. The observation of the textural changes in the annealing studies were done by incorporating a Mettler FP-2 heating unit, in which case long length objectives were used. A larger magnification objective lens was used to observe quenched samples. Images were recorded on a 35mm Kodak T-Max black and white film.

2.5 Differential Scanning Calorimetry

Thermal analysis was performed on a Perkin-Elmer DSC-2 differential scanning calorimeter. Calibration of the temperature scale and transition enthalpies was done using indium and lead standards. The melting and isotropization temperatures were taken as the onset of the respective endotherm peaks obtained at a heating rate of 20°C/min.

2.6 Complementary Techniques

The thickness of the films studied by SALS were measured by an interference light microscope model 6JA Shangai Optical Instruments with monochromatic light (λ = 520nm).

The molecular weight and molecular weight distribution of the PSHQ polymer were determined by Gel Permeation Chromatography using an Ultrastyragel column calibrated with polystyrene standards.

CHAPTER 3
CHARACTERIZATION OF NEMATIC TEXTURES BY SMALL-ANGLE LIGHT SCATTERING

This chapter focuses on the description of the nematic textures of the PSHQ polymer in the quiescent state and their characterization by small-angle light scattering. The objective is to obtain parameters from the scattering measurements for the quantitative characterization of the corresponding textures. Section 3.1 outlines the basic small-angle light scattering theories with emphasis on the scattering from anisotropic systems. A possible model for the description of the scattering from textured nematics is given in section 3.2. Section 3.3 describes the characteristic SALS patterns and textures observed from the quiescent nematic state. Finally, section 3.4 presents a procedure proposed for characterizing the nematic textures by small angle light scattering.

3.1 Small Angle Light Scattering from Anisotropic Systems

Scattering occurs in heterogeneous systems due to the fluctuation in scattering power from point to point in the medium. The scattered amplitude is given by[72]

$$E_s = C \int_{-\infty}^{\infty} \rho(\mathbf{r})\, e^{-i\mathbf{q}\cdot\mathbf{r}}\, d\mathbf{r}^3 \quad , \qquad (3.1)$$

where $\rho(\mathbf{r})$ is the scattering power of the volume element located

at position **r**, and **q** is the scattering vector defined by

$$\mathbf{q} = \frac{2\pi}{\lambda}(\mathbf{s}_1 - \mathbf{s}_0) \quad , \tag{3.2}$$

where λ is the wavelength in the medium and $\mathbf{s}_1$ and $\mathbf{s}_0$ are unit vectors along the incident and scattered rays, respectively. The magnitude of **q** is given by

$$q = |\mathbf{q}| = \frac{4\pi}{\lambda} \cdot \sin\left(\frac{\theta}{2}\right) \quad , \tag{3.3}$$

where θ represents the scattering angle (between $\mathbf{s}_1$ and $\mathbf{s}_0$). For light radiation, the scattering power depends upon the polarizability tensor of the volume element by the following equation

$$\rho(\mathbf{r}) = |\alpha(\mathbf{r})|\ \mathbf{E} \cdot \mathbf{O} \quad , \tag{3.4}$$

where **E** is the field of the radiation at the volume element **r** and **O** is a unit vector in the direction of polarization of the analyzer. In the Rayleigh-Gans-Debye approximation[73], the internal field effects are neglected, and **E** is approximated by the external field.

The scattered light can be decomposed into its polarization components and the intensity can be a function of the azimuthal angle μ even in unoriented systems. Figure 3.1 presents a diagram showing the geometry of the scattering experiment, including the angles θ and μ. The incident and scattered beams can be parallel to each other (V_V) or perpendicular (H_V).

The various scattering theories can be classified into two groups, namely, the "model approach" and the "statistical

approach". The model approach can be used to calculate the scattering from structures of well defined geometry by using the appropriate $\rho(\mathbf{r})$ functions. This is suitable for systems containing particles of given shape such as isotropic[72] or anisotropic[74] spheres. Once the scattered amplitude is known, the intensities are calculated by

$$I = E\,E^{*} \quad , \tag{3.5}$$

where E^{*} is the conjugated complex of the scattering amplitude.

For complex systems lacking a well defined geometry, the statistical approach can be used. The first statistical theory was introduced by Debye and Bueche[75] to calculate the scattering from fluctuations in polarizability in isotropic systems. A correlation function $\gamma(\mathbf{r})$ is defined by

$$\gamma(\mathbf{r}) = \frac{< \eta_1\,\eta_2 >_{r1,2}}{\overline{\eta^2}} \quad , \tag{3.6}$$

where η_i is the difference in polarizability between point i and the average of the medium. The scattering intensity is given by

$$I(\mathbf{q}) = C\,\overline{\eta^2} \int_{-\infty}^{\infty} \gamma(\mathbf{r})\; e^{-i\,\mathbf{q}\cdot\mathbf{r}}\; d^3\mathbf{r} \quad . \tag{3.7}$$

Goldstein and Michalek[76] and Stein and Wilson[77] have generalized the statistical treatment to include anisotropic systems. In this case, two extra correlation functions are needed to describe the possible fluctuations in anisotropy and in the orientation. In this terms, the H_V and V_V intensities are given

by[77]

$$I_{V_v} = K \left\{ \overline{\eta^2} \int_0^\infty \gamma(r) \frac{\sin(qr)}{q\,r} r^2\, dr + \frac{4}{45} \delta^2 \int_0^\infty f(r)\, \mu(r) \frac{\sin(qr)}{q\,r} r^2\, dr \right\} \quad (3.8)$$

$$I_{H_v} = \frac{1}{15} K \delta^2 \int_0^\infty f(r)\, \mu(r) \frac{\sin(qr)}{q\,r} r^2\, dr \quad (3.9)$$

where $\mu(r)$ is related to the fluctuation in anisotropy and δ represents the anisotropy in polarizability. The function f(r) is an orientation correlation defined by

$$f(r) = \frac{1}{2} < 3\ \cos^2\theta - 1>_r \quad . \quad (3.10)$$

where θ is the angle between the optic axes of two volume elements separated by a distance r.

In equations 3.8 and 3.9 the scattered intensities are independent of the azimuthal angle μ, meaning that the scattering patterns are cylindrically symmetric. This is a consequence of the "random orientation fluctuations" assumption, which implies a spherical symmetry of the correlated regions. In other words, the correlation in orientation is assumed to depend only on the distance between the volume elements, irrespective of the angle β, the separation vector makes with the optic axis (figure 3.2a). Stein et. al.[78] showed that an azimuthal dependence of the scattering can be accounted for if the orientation correlation function is described in terms of both r and β. In the two-dimensional derivation the correlation function f(r,b) can be expanded in the following form

$$f(r,\beta)=f_o(r) + f_2(r)\ \cos(2\beta) + f_4(r)\ \cos(4\beta) +... \quad , \qquad (3.11)$$

where the functions $f_2(r)$ and $f_4(r)$ describe the shape of the non-spherical correlated regions. This theory can describe any arbitrary correlation geometry. Figure 3.2b shows examples of fiber and disk-like correlations. This approach involves a large number of parameters which are difficult to evaluate. The description of non-random anisotropic systems such as spherulitic or rodlike geometries is more readily done by the model approach.

3.2 Scattering from Random Disclinations

The theoretical treatment of the light scattering from liquid crystalline textures has received little attention, probably due to the complexity of the systems. The description of the directorfield can be feasible if the textures have regularity. One such example is the focal conic texture of cholesteric phases[79], characterized by a well defined three dimensional arrangement of defects. The trajectory of the director follows a complex but regular path, and the calculation of the light scattering from the system can be done by using the model approach, as the polarizability tensor at each point is known.

In the case of the less ordered nematic Schlieren texture, although the geometry of the directorfield in the neighborhood of a disclination is known, the disclinations do not occur in a regular way, and the models to describe the directorfield should account

for all the possible conformations through the use of statistical theories. A first step in solving the problem was made by de Gennes[80], who considered the scattering from random disclinations in a nematic texture. The model considers a planar geometry and the three Frank elastic constants are assumed to be equal. Another important point is that the correlation between disclinations are neglected. The distortion of the directorfield is described in terms of two effects: one is the disclination density ν, the second one being the orientation fluctuations due to the shape of a single disclination line. The latter is quantified by defining a "persistence length" of a line b, in analogy to the definition of the persistence length of a flexible polymer. The parameter b also represents the distance over which a disclination line affects the directorfield. The statistical calculation leads to a correlation function of the form

$$f(r) = \left(\frac{b}{K}\right)^{K r} \quad , \tag{3.13}$$

where $K = 8 \pi S^2 \nu b$, S being the disclination strength. Equation 3.13 is approximated to an exponential function of the form

$$f(\mathbf{r}) = e^{-\frac{r}{\xi}} \quad , \tag{3.14}$$

where the correlation length ξ is given by

$$\xi = \frac{c}{S^2 \nu b} \quad , \tag{3.15}$$

c being a constant. The resulting distribution of the scattering

intensity is

$$I(q) = \frac{8 \pi \eta^3}{(1 + q^2 \eta^2)} \quad . \qquad (3.16)$$

It is also shown that the scattering due to thermal fluctuations, which is the principal contribution to the scattering in single domain nematics, is negligibly small compared to the scattering due to the distortions of the director in the presence of disclinations.

In the treatment described above, the resulting scattering intensity is independent of the azimuthal angle, which is a result of the assumed "randomness" of the disclinations. It predicts, however, an explicit relationship between the orientation correlation length and parameters such as the disclination density and the "stiffness" of a disclination line.

3.3 The Nematic Textures and Their SALS Patterns

Figure 3.3 presents a polarized micrograph of a 0.5 μm thick PSHQ film quenched from the nematic state. The texture is composed of thin dark threads of irregular shape corresponding to positions where the director lies parallel to either the polarizer or analyzer. The trajectory of single threads in terms of locating their origin is not evident due to their abundance. The texture can be classified as a fine Schlieren texture, a term often used to describe textures of similar appearance.[82] Figure 3.4 presents two magnified views obtained by simultaneously rotating the polarizer

and analyzer in the crossed position. As the polarizers are rotated the threads move, indicating a continuous change in the orientation of the optic axes or director. The total intensity of light transmitted between cross polarizers remains constant, indicating the lack of overall orientation in the field of view. Some points which remain dark upon rotation of the polarizers are believed to correspond to disclination lines perpendicular to the film. In figure 3.4a, some points (such as *a* and *b*) appear to connect four threads. Rotation of the polarizers indicates that most of them (such as point *b*) are actually two threads which at some point their distance approaches the resolution limit of the optical microscope. Point *a*, however, corresponds to a disclination of strength S=+1, as the four threads follow the rotation direction of the polarizers. While the large density of the threads prevents from quantifying the distribution of disclination strength, the effect of rotating the polarizers suggests that the majority of disclinations correspond to S=±1/2 disclinations. Figure 3.5 shows a micrograph from a different section of the sample obtained in the absence of the polarizer. By removing the polarizer, only dark points appear on the bright background. Similar dark points corresponding to disclinations lines lying perpendicular to the film have been observed in various systems, including small molecule [35] as well as polymeric [48,81] nematics. The dark appearance of the defects is believed to be a consequence of the strong scattering of light occurring in the vicinity of the disclinations. An attempt to quantify the textures by counting the number of disclinations as dark points in the unpolarized micrographs failed,

as not all the points observed are equally distinct. Also, the number of dark points counted per unit area was found to depend on the magnification used. Even at large magnification, it is not obvious whether some points which appear larger consist of more than a single disclination. Disclination densities as high as 25 disclinations per μm^2 (unresolvable by optical microscopy) were determined in a semiflexible TLCP studied by Hudson and Thomas[55] using the lamellar decoration technique. As it will be discussed in chapter 4, the disclination density of the textures was determined by thermal history.

Figure 3.6 presents the H_V (crossed polarization) and V_V (parallel polarization) SALS patterns recorded from a 1.0 μm thick PSHQ film quenched from the nematic phase. The H_V pattern has a four leaf clover shape with intensity maxima at azimuthal angles $\mu = \mu_{max} = 0°, 90°, \ldots$ .The V_V pattern shows maxima occurring at azimuthal angles $\mu = \mu_{max} = 45°, 135°, \ldots$. Figure 3.7 shows a quantitative representation of the H_V and V_V intensity distributions at their respective μ_{max} as a function of the scattering vector q. The position of the maximum H_V intensity (q_{max}) coincides with the local maximum of the V_V curve, indicating that the scattering can be characterized by a single correlation length. Moreover, the ratio of the H_V/V_V intensity at q_{max} is in the order of 0.80, suggesting the scattering being primarily due to orientation fluctuations, as it would be expected in a nematic system. Figure 3.8 presents the azimuthal dependence of the H_V and V_V intensity at q_{max}. The shape of the

SALS patterns in terms of its azimuthal dependence was found to be independent of $1/q_{max}$.

3.4 Quantification of the Nematic Textures by SALS

3.4.1 Size of the Structural Units

It is desirable to define a size parameter to characterize the macroscopically unoriented nematic textures by SALS. Unlike systems containing particles, the areas of homogeneous orientation in the nematic textures are not separated by sharp boundaries. It seems then more appropriate to use the concept of an orientation correlation length representing the average distance over which the local orientation is correlated. The definition of a correlation length is usually done based on a specific correlation function. As at the present time no suitable model is available to describe the fluctuations in the orientation of the director in the fine Schlieren textures, the definition of a correlation length will be done on a semiempirical basis. For simplicity , the characteristic size of the correlated regions will be referred to as a "domain size".

The experimentally measured value of q_{max} was found to be related to the coarseness of the respective textures, with smaller q_{max} values corresponding to coarser textures (lower disclination densities). For scattering curves with an intensity maximum at a scattering angle θ_{max} , the quantity U_{max} is defined by

$$U_{max} = \frac{4\pi}{\lambda} a \sin\frac{\theta_{max}}{2} = a\, q_{max} \quad , \qquad (3.17)$$

where a is a characteristic size of the scattering entity (the radius in the case of spheres). The SALS theory suggests that U_{max} is characteristic of the structural unit and its dimensionality, independent of its size. Values of U_{max} for various structures range between 2.0 and 4.1.

In the case of the fine Schlieren textures, the average size of a domain is related to the disclination density. However, the exact relationship between disclination density and q_{max} could not be established, preventing from experimentally evaluating U_{max}. The average domain size will be defined as $1/q_{max}$ (in units of microns).

In a study of the X7-G Tennesee Eastman TLCP, Hashimoto[83] found a linear relationship between $1/q_{max}$ and the average distance between disclinations d, defined as the square root of the average area per disclination. This implies the following relationship between $1/q_{max}$ and the the disclination density ν:

$$\frac{1}{q_{max}} \approx \frac{1}{\sqrt{\nu}} \quad , \qquad (3.18)$$

for $3\mu m < d < 8\mu m$. This regime can be called a dense regime, in which the parameter b, defining the distance over which a disclination affects the directorfield, is in the order of the distance between neighboring disclinations, i.e., $b \approx d$. It is recalled that in the "dilute" regime treated by de Gennes[80], where $b << d$, the

orientation correlation length is expected to be inversely proportional to ν. The textures displayed by the PSHQ polymer can be classified as dense systems, with disclination densities slightly larger than those measured on the X7-G polymer by Hashimoto.[81]

3.4.2 Degree of Order

While the information concerning the domain size depends on the shape of the scattering curves, their intensity can be analyzed in terms of the "efficiency" of the scattering process. The latter is related to the amplitude of the fluctuations giving rise to the scattering phenomenon. In isotropic systems, the efficiency of the scattering is determined by the mean square of the fluctuation in polarizability, which in two phase systems, depends on the difference in polarizability between the components. The analogous parameter controlling the scattering from anisotropic systems is the anisotropy of the polarizability. In macroscopically unoriented systems such as the quiescent nematic textures under study, the anisotropy of the polarizability depends upon the size scale of the probe used to measure it. The anisotropy determining the scattering intensity can be defined as the anisotropy of a volume element "sensed" by a light wave of wavelength λ. This corresponds approximately to the effective anisotropy on a scale of λ/10 (~0.05μm).

For a systems composed of uniaxially oriented rodlike molecules, δ is given by

$$\delta = p\ \delta_{mol} \quad , \tag{3.19}$$

where δ_{mol} is the molecular anisotropy and p is an orientation function which in three dimensions is given by

$$p = \frac{1}{2} < 3\ \cos^2\theta - 1> \quad , \tag{3.20}$$

where θ is the angle between the molecular axis and the optic axis of the volume element. In monodomain textures, the orientation function p is identical to the thermodynamic order parameter *s*.

In SMLCs, it is usually assumed that the distortion of the director occurring in textured nematics does not affect the degree of local molecular alignment, which Maier and Saupe refer to as the "true nematic order".[11] This assumption implies that the local orientation function in textured nematics should be equal to the thermodynamic order parameter *s*, which is defined only in homogeneously oriented systems. In molecules containing flexible segments, the molecular polarizability depends upon the molecular conformation. For such molecules, separate orientation functions are used for describing the degree of order of the various segments. The overall molecular anisotropy will be a function of the various order parameters and its respective anisotropy of polarizabilities. Regardless of its components, the parameter δ measured by SALS can be used for evaluating a "degree of local order".

In the Rayleigh-Gans-Debye regime, the scattered intensity depends not only on the efficiency of the scattering δ but also on the size of the structural units. For scattering from orientation fluctuations, the dependence of the intensity on the various

parameters can be generalized as

$$I_{H_V}(q) \approx \delta^2 a^n P(q) \quad , \qquad (3.21)$$

where a is the a correlation length or the size of the scattering particles and P(q) is the normalized intensity distribution function, independent of a. Values of the exponent n for various systems are given in table 2. For continuous anisotropic systems such as volume filled spherulites and systems described by exponential correlation functions, the exponent n is equal to the dimensionality.

The scattering from the nematic textures presently studied can be analyzed by taking a as the domain size $1/q_{max}$. Thus, for planar textures, in which the director is confined to the plane of the film, the local anisotropy of polarizability δ is proportional to $(I_{max})^{0.5} q_{max}$.

Table 2

Values of the exponent n in equation 3.21 for various systems.

System	Dimensionality	Exponent (n)	Reference
random fluctuations	3	3	83
random fluctuations	2	2	83
volume filling spherulites	3	3	74
volume filling spherulites	2	2	85
isolated spherulites	3	6	74
isolated spherulites	2	4	85

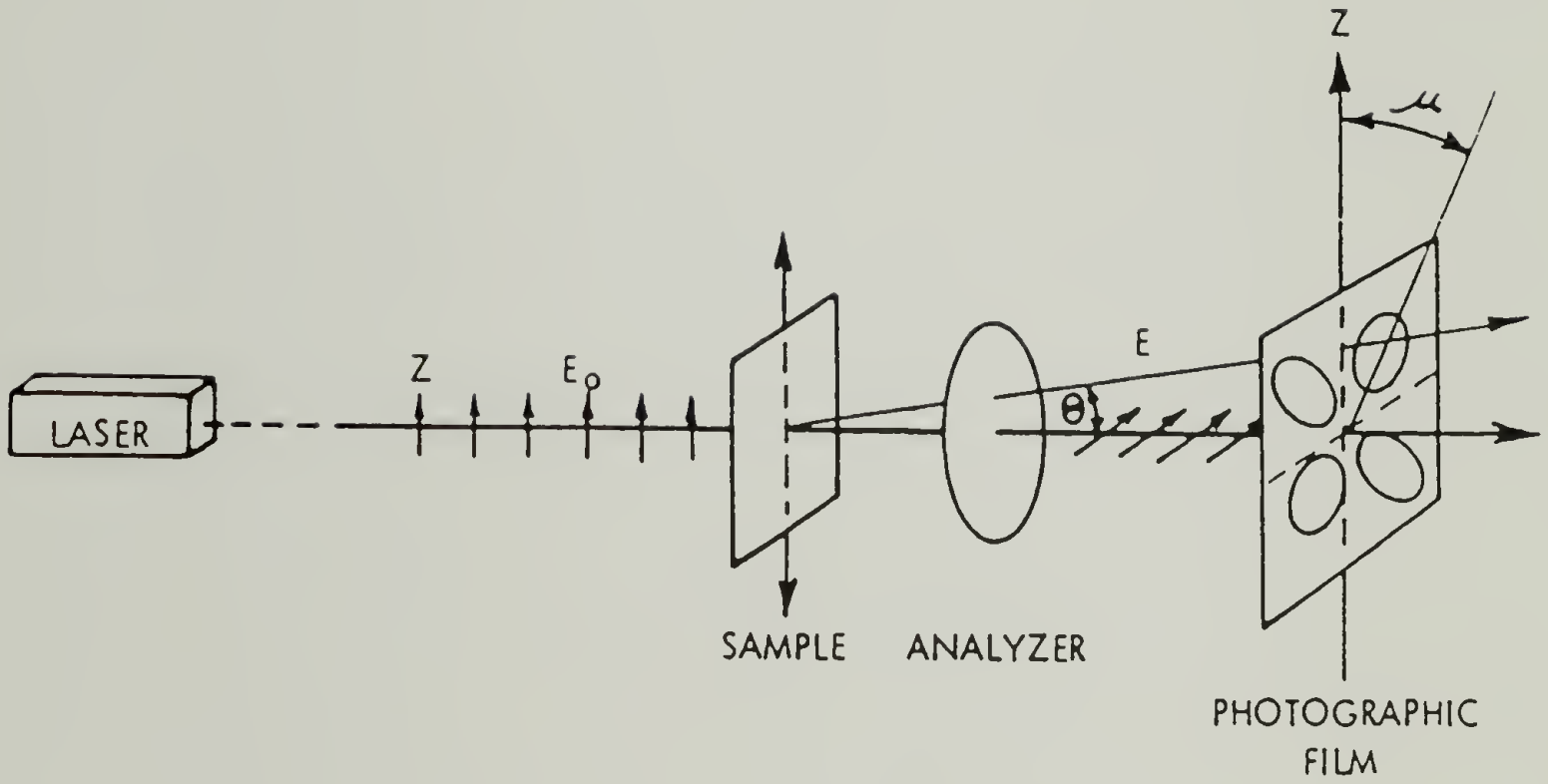

Figure 3.1 The light scattering angles θ and μ.

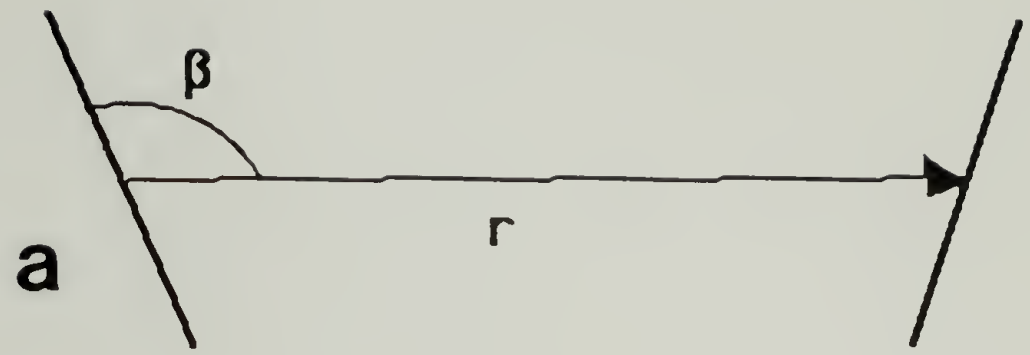

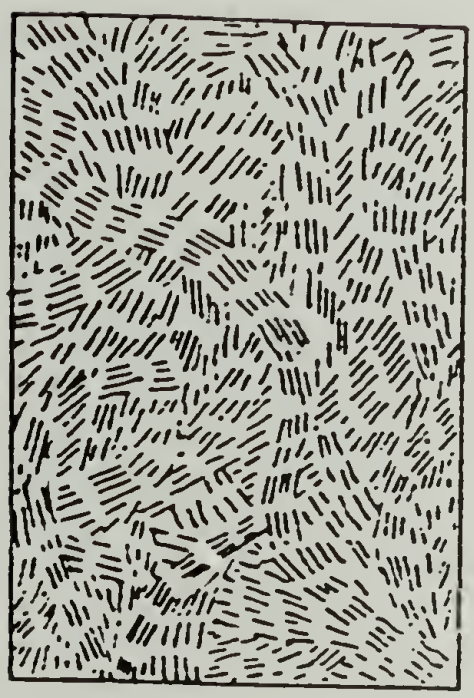

b

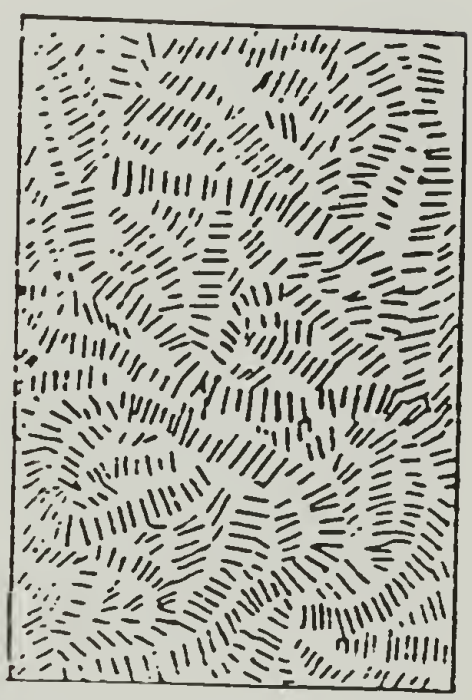

c

Figure 3.2 (a) the angle β; (b) fiber and (c) disk-like correlation in orientation. (after ref. 78).

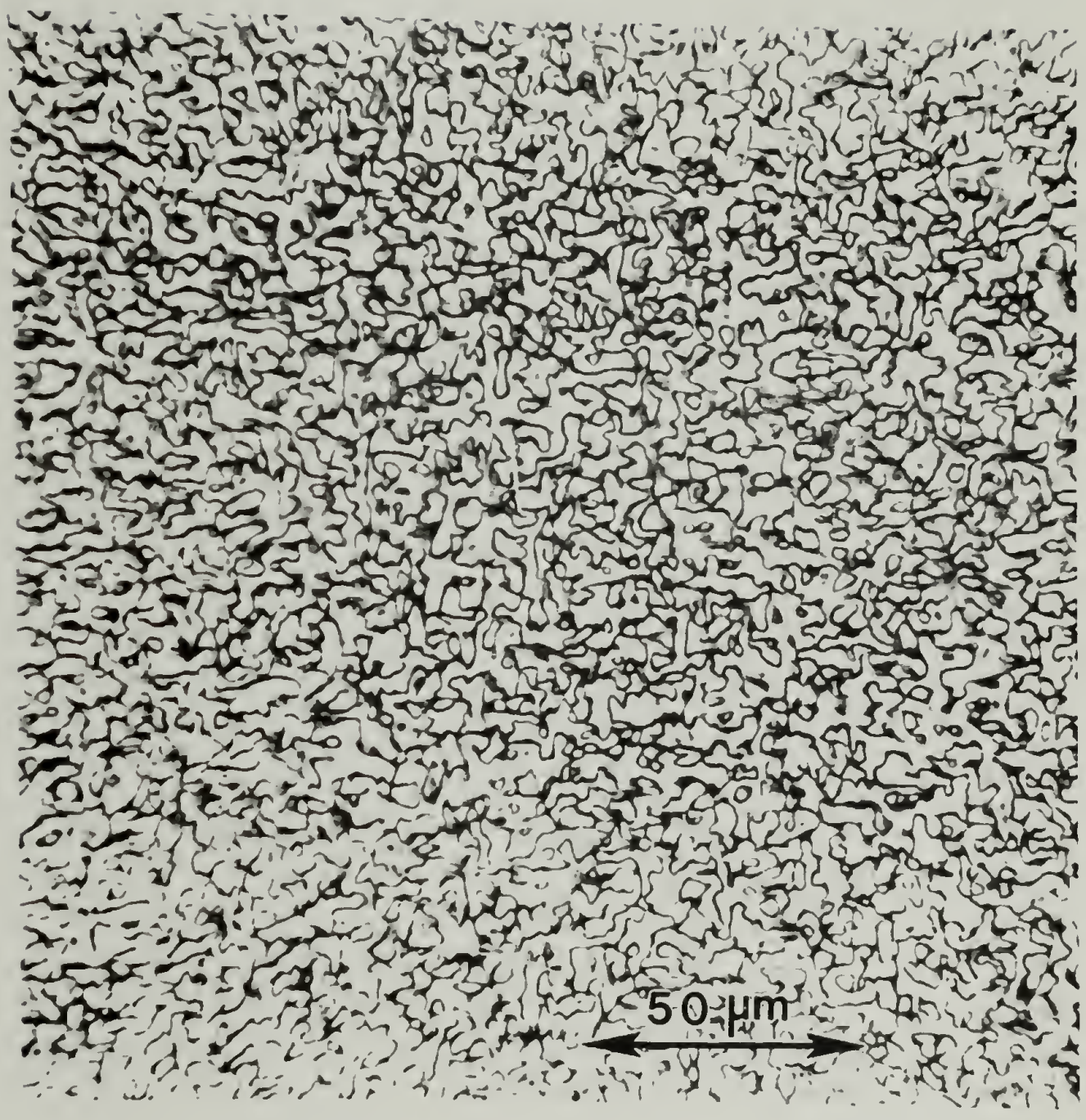

Figure 3.3 Fine Schlieren texture of the PSHQ polymer.

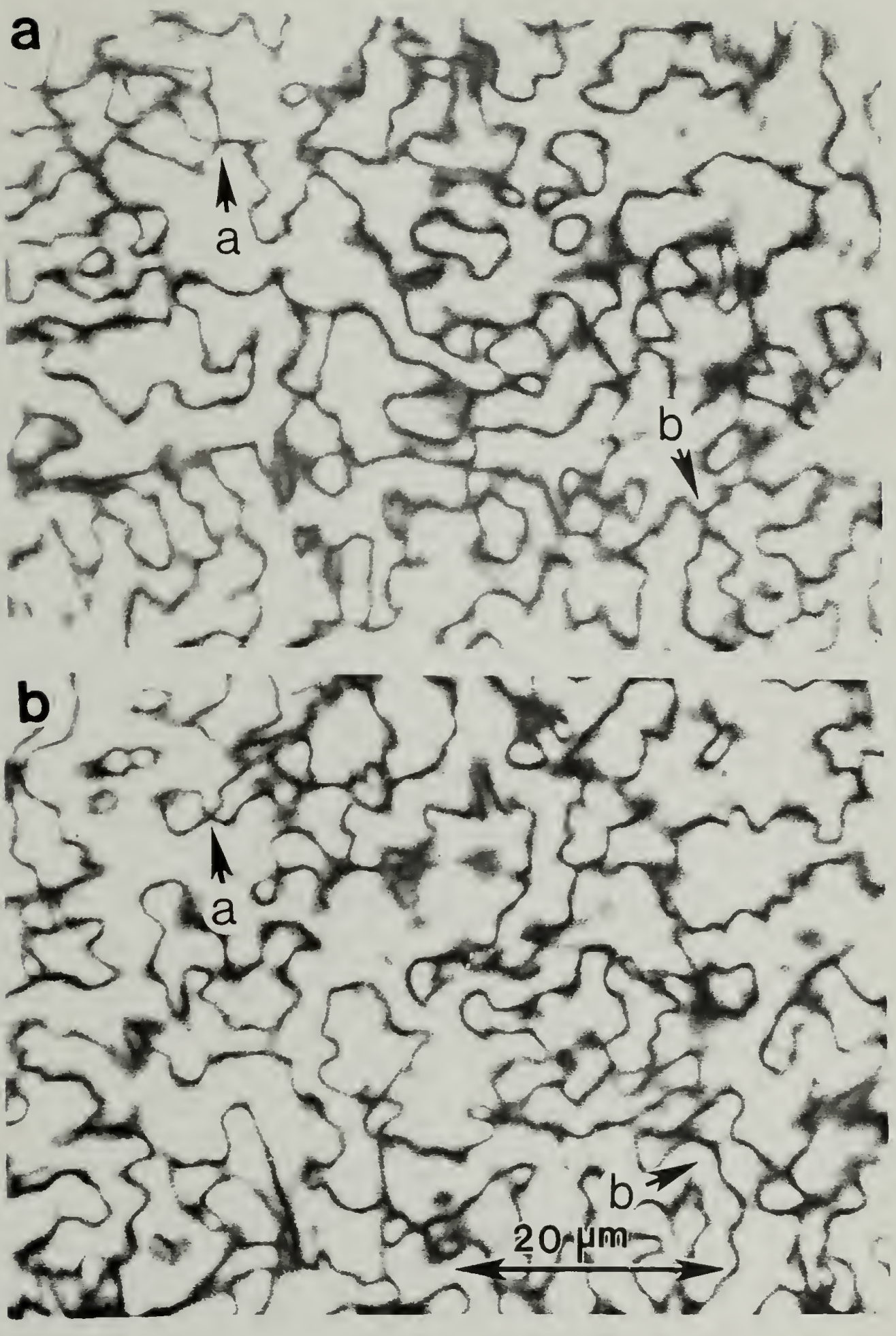

Figure 3.4 Micrographs of a section of the fine Schlieren texture. (a) Polarizer vertical; (b) polarizers rotated 30° clockwise.

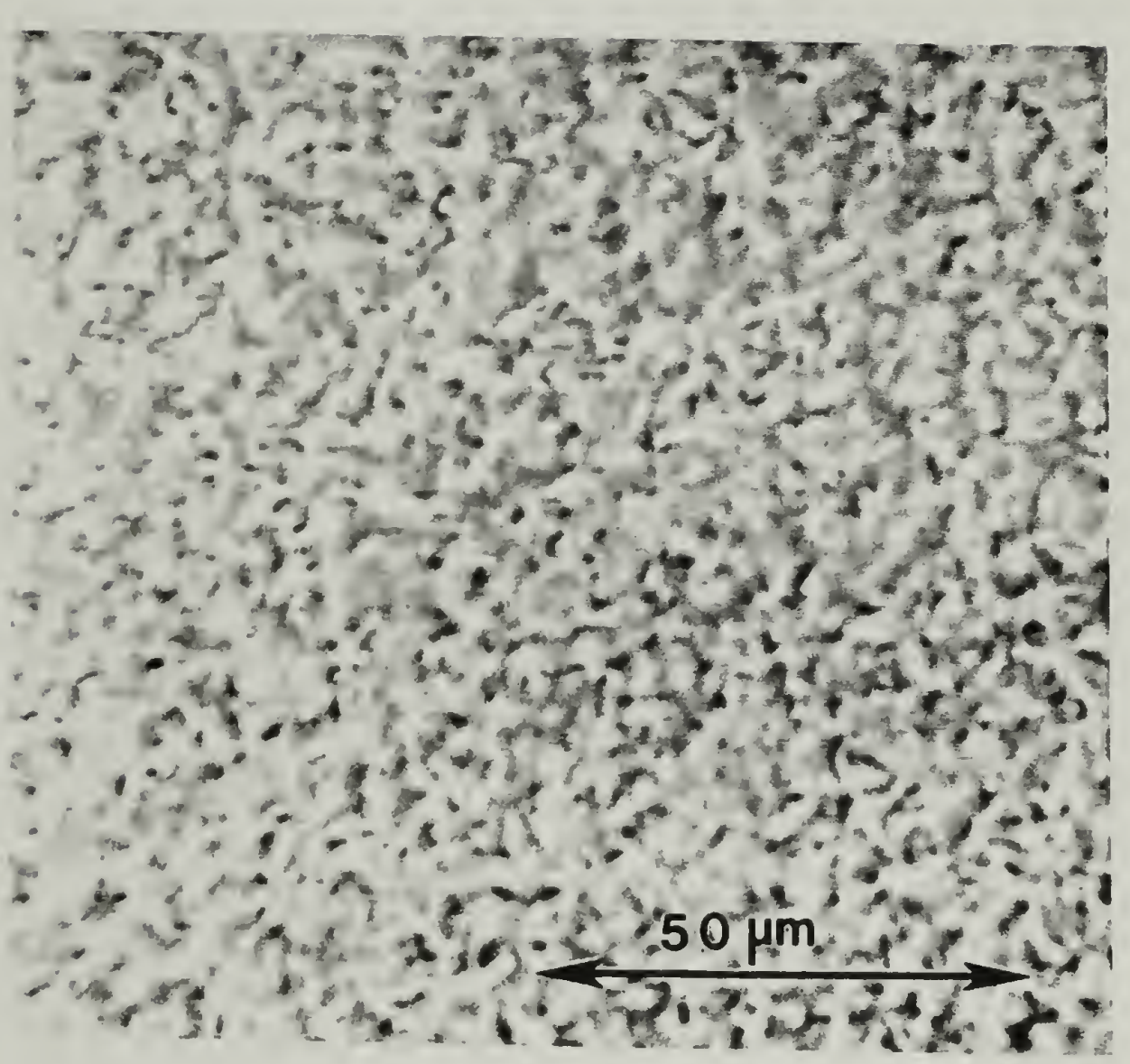

Figure 3.5 Unpolarized micrograph of a PSHQ film quenched from the nematic phase.

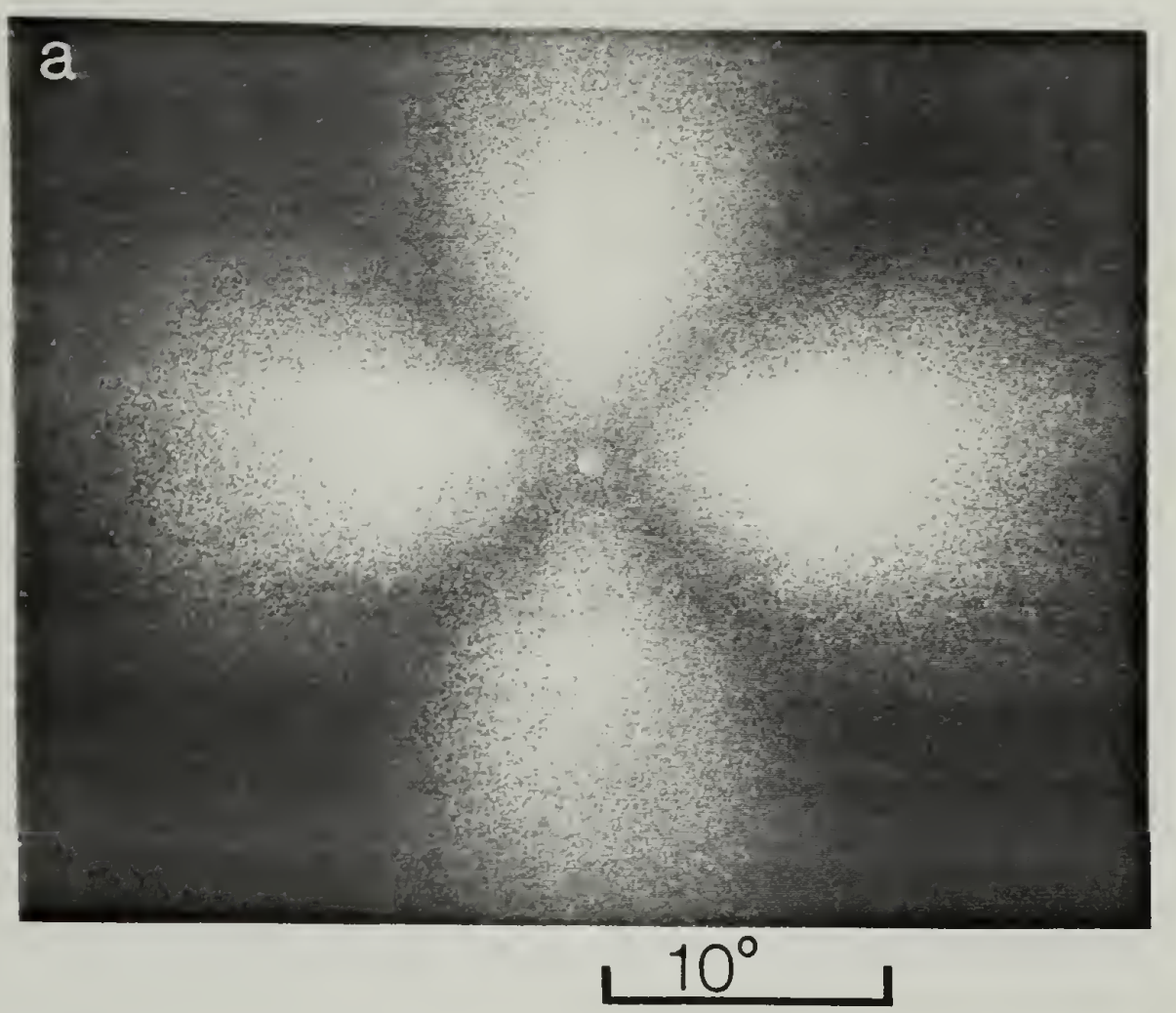

Figure 3.6 SALS patterns from a PSHQ film quenched from the nematic phase. (a) H_V ; (b) V_V (incident polarization is vertical).

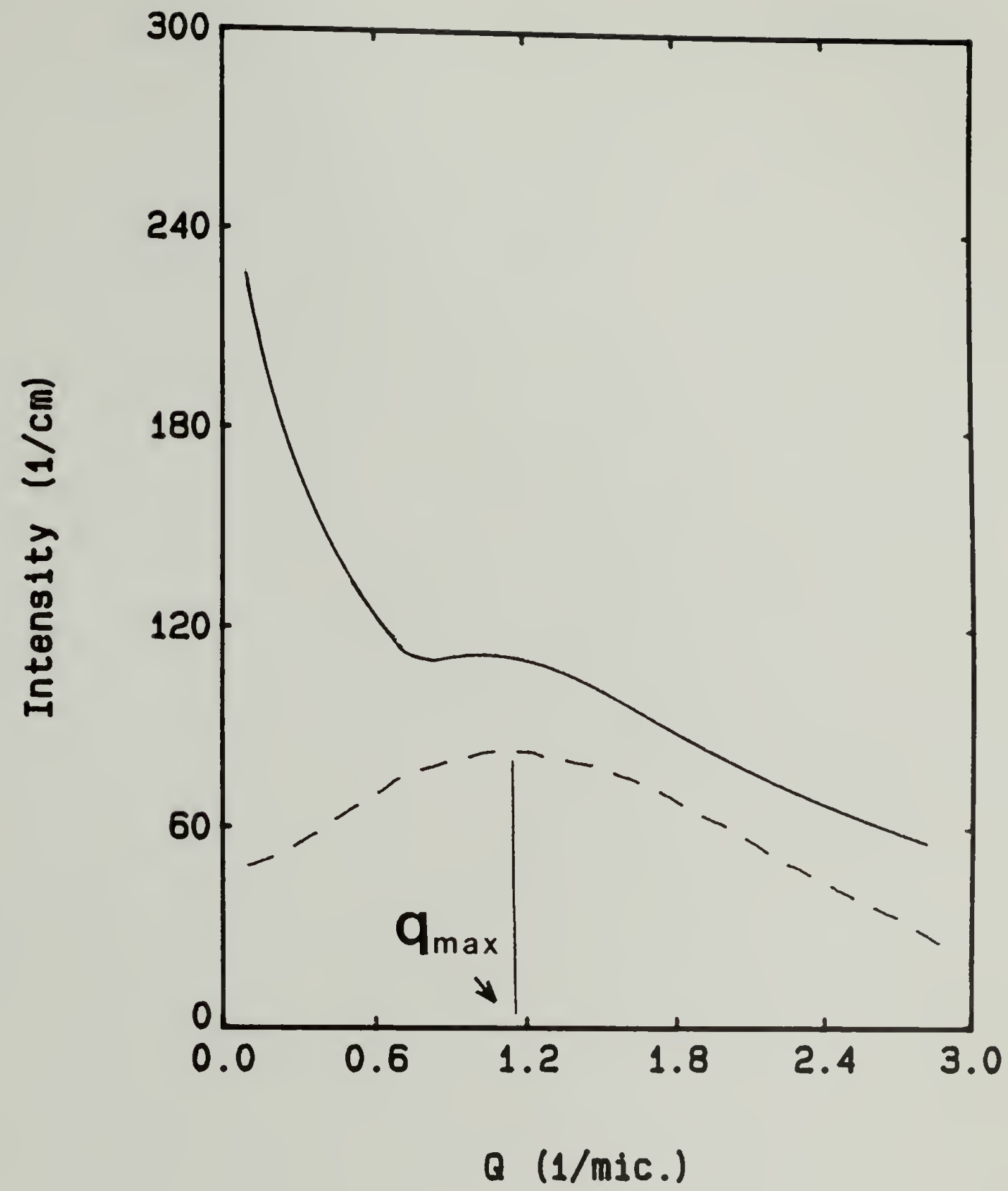

Figure 3.7 H_V (- - -) and V_V (——) intensity distribution at μ_{max}.

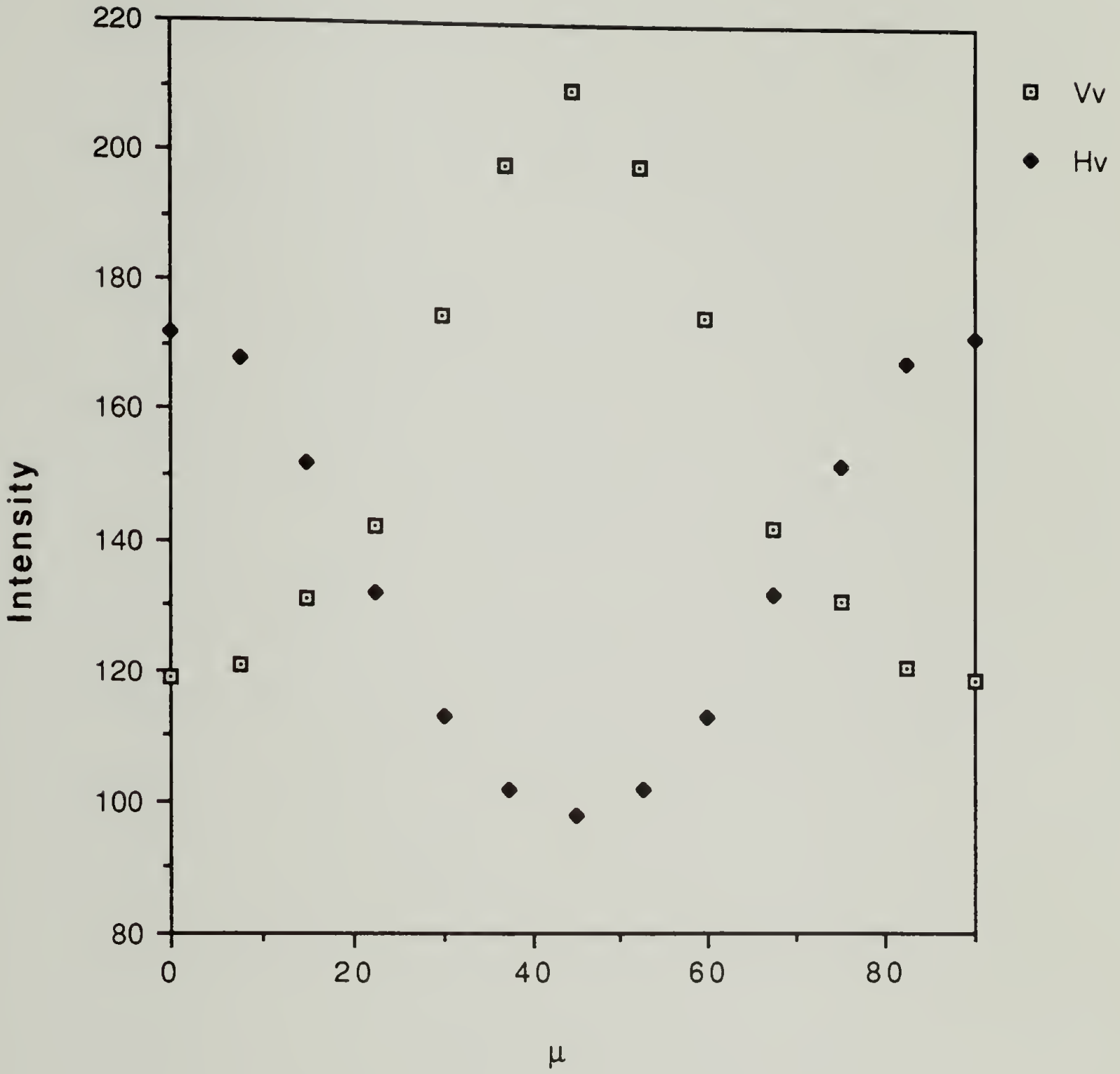

Figure 3.8 Azimuthal dependence of the H_V and V_V intensity at q_{max}.

CHAPTER 4

EFFECT OF THERMAL HISTORY ON THE NEMATIC STATE

4.1 Polymer Characterization

The molecular size of the PSHQ polymer was characterized by a GPC calibrated with polystyrene standards. The measured number average molecular weight is 10,800 g/mol with a polydispersity index of 1.88. This would correspond to an average of 17 repeat units per molecule. The actual values might differ due to the possible difference in the hydrodynamic volume between the PSHQ polymer and polystyrene.

The nematic range temperatures were determined by DSC. The transition temperatures were taken from the second heating run (figure 4.1), performed after slow cooling (0.62°C/min) from 200°C down to room temperature. The measured transition temperatures are T_g=88°C, T_m=112°C and T_{N-I}=173°C. The melting temperature is 12°C higher than the previously reported value.[65] The detail study of the N-I transition is presented in the following section. Also shown in figure 4.1 is the DSC trace obtained by cooling from 200°C down to room temperature at a rate of 10°C/min. The sharp exotherm at 170°C indicates a fast transition into the nematic phase occurring at a relatively small degree of undercooling. The absence of lower temperature exotherms indicates that no significant crystallization develops at the cooling rate used.

4.2 Annealing Studies

4.2.1 The Nematic to Isotropic Transition

Annealing in the nematic phase was found to affect the nematic to isotropic transition studied by DSC. A series of samples were first heat treated in the isotropic phase and subsequently annealed at constant temperature in the range of 140 to 160°C. The annealing steps carried for less than 30 minutes were performed in the DSC apparatus. The longer annealing periods were carried out in an outside oven. Following the heat treatment in the oven, the samples were quenched to room temperature and inserted in the DSC with the temperature cell set to 130°C. Figure 4.2 presents the endotherms obtained at a heating rate of 20°C per minute from samples annealed for 1 minute, 3 hours and 12 hours at 150°C. A shift in the isotropization temperature induced by annealing is observed, along with a sharpening of the endotherm peak. The enthalpy of the transition ΔH, given by the area of the endotherm, was found to be independent of annealing time within the experimental error ($\Delta H = 1.2 \pm 0.15$ cal/gr).

Figure 4.3 shows a plot of the measured isotropization temperature as a function of annealing time in the nematic phase. The points corresponding to the various annealing temperatures can be represented by a single curve, indicating that the effect is practically independent of the annealing temperature in the temperature range studied.

The shift in the isotropization temperature was found to be "reproducible", in the sense that subsequent annealing steps

performed on a single specimen led to isotropization temperatures independent of the previous thermal history. In other words, a sample annealed first for a longer period showed a higher T_{N-I} than after a second shorter annealing step. This observation indicates that the shift in T_{N-I} is not due to a change in the chemical structure of the polymer. The reproducibility occurs provided that the sample is treated at temperatures above T_{N-I} in between the annealing steps performed in the nematic phase. For heat treatments carried out at 210°C, the minimum amount of time necessary to erase the previous thermal history was found to be an increasing function of the time the sample had previously spent in the nematic phase, with a maximum period of 10 minutes for samples previously annealed for 12 hours. These conditions (heating for 10 minutes at 210°C) were adopted as the standard procedure for erasing any previous history of all the samples used for the annealing studies presented in the rest of the present chapter. Hereafter, this procedure is referred to as "heat treatment in the isotropic phase".

In order to check the possibility of either decomposition or post-polymerization taking place during annealing, a test specimen subjected to the heat treatment in the isotropic phase followed by 12 hours at 150°C was investigated by GPC. The results indicated molecular weight and molecular weight distribution essentially identical to the untreated polymer.

4.2.2 Evolution of the Macrostructure

Early observations indicated that the macrostructure of the nematic phase depends upon thermal history. In the present study, the nematic textures were studied as they developed at the phase transition from the isotropic state, followed by annealing at constant temperature within the nematic range. In principle, the phase transition can be induced by a drop in temperature from the stable isotropic phase, or by a temperature jump performed on the "frozen-in" unstable isotropic state. The latter can be achieved either by quenching the isotropic phase to temperatures below the glass transition temperature or by solution casting.

Figure 4.4 shows the effect of annealing on the textures recorded from a 1.0 μm thick PSHQ film studied by hot-stage polarized light microscopy. The annealing temperature is 150°C and the annealing time is measured from the moment the sample was quenched from the isotropic phase. The corresponding unpolarized micrographs are shown in figure 4.5.

Annealing results in a relatively slow coarsening of the fine Schlieren texture, indicated by a decrease in the density of the extinction lines. No significant changes in the textures could be detected for annealing times longer than 24 hours, up to 4 days of annealing. In the context of the terms introduced in the previous chapter, the coarsening of the texture can be defined as a "domain growth" process. The network appearance of the initial texture gradually changes due to annealing resulting in a more open texture, with a closer resemblance to the characteristic Schlieren textures of small molecule nematics.[86] The domain growth

process involves the annihilation of disclination lines, as evidence by the decrease in the density of the dark points observed in the unpolarized micrographs in figure 4.5. This process is correlated with the changes occurring in the SALS patterns. The SALS technique was found to be most sensitive to the coarsening occurring in up to the first 5 hours of annealing at 150°C. Figure 4.6 shows the H_V patterns recorded from films quenched after 1 minute, 30 minutes and 5 hours of annealing at 150°C. Due to annealing, the intensity moves to smaller angles, indicating an increase in the orientation correlation length.

A similar domain growth process was observed in samples of the Polaroid polymer. As the Polaroid polymer does not develop an isotropic phase before its decomposition, the nematic phase was induced by performing a temperature jump on the isotropic as-cast films. Figure 4.7 presents side by side the polarizing micrographs and the corresponding H_V patterns obtained from the quenched nematic state of samples exposed to 200°C for 2, 10 and 20 seconds. No significant changes on the texture of the Polaroid polymer can be observed after 2 minutes, while for the PSHQ samples the analogous process take place in up to 24 hours. The rest of the present chapter presents the quantitative characterization of the kinetics of the domain growth of the PSHQ polymer studied by SALS.

The time dependence of the H_V intensity during annealing was measured for samples of thickness in the range 0.8 to 1.0μm. The general procedure consisted of an initial heat treatment of the

as-cast films in the isotropic phase followed by a rapid transfer of the specimens into a hot-stage pre-set at constant temperature. Figure 4.8 shows a series scattering curves, represented in terms of $I_{Hv} q^2_{max}$ versus scattering vector q, corresponding to increasing annealing times at 150°C. In the first 8 hours, the absolute intensity increases by two order of magnitudes, from an initial value of 30 cm^{-1} up to 4000 cm^{-1}. A sharpening of the peak is also evident. Figure 4.9 presents what will be referred to as a growth curve, obtained by plotting the $1/q_{max}$ values extracted from the curves in figure 4.8, as a function of annealing time. The quantitative growth curve could be reproduced after 10 hours of annealing at 150°C, provided the films were first heat treated in the isotropic phase. The growth curve shows a constant decrease in its slope, with an apparent leveling off after approximately 8 hours reaching a $1/q_{max}$ value of 2.8 μm. From optical microscopy it is known that the size of the domains increases for longer than 10 hours. The leveling off in the size parameter obtained from light scattering is probably a consequence of the increasing effect of multiple scattering during annealing, which limited the resolution of intensity maxima at scattering angles smaller than 2°.

As already suggested by figure 4.8, the increase in the scattering intensity is greater than the contribution due to the increase in the domain size suggesting an increase in the local anisotropy δ. The time dependence of this local ordering process is shown in figure 4.10, in terms of $I_{Hv}q^2_{max}$ at q_{max} ,i.e., assuming

orientation fluctuations in two dimensions. A significant local ordering is observed in the first two hours. The corresponding parameter calculated by assuming a non-planar geometry is plotted in figure 4.11. The initial increase in the local anisotropy is still apparent, however, the explanation for its latter drop is not evident, suggesting a planar geometry of the films.

4.2.3 Temperature Dependence of the Domain Growth

Figure 4.12 presents the growth curves for one hour annealing obtained from samples quenched from 210°C down to 130, 140, 150 and 160°C. The various growth curves intercept the y axis at $1/q_{max}=0.52\pm0.01\ \mu m$, indicating that the initial disclination density is independent of the phase transition temperature. As the rate of the phase transition is comparable to the cooling rates used, it could not be unambiguously established whether the phase transition occurred at isothermal conditions. The temperature independence of the initial disclination density, however, is supported by the observation that the same initial $1/q_{max}$ value (0.52 μm) was obtained from isotropic films subjected to a temperature jump into temperatures within the nematic phase. The latter consisted of either as-cast films or films quenched from the isotropic phase to room temperature.

While the growth curves at 130 and 140°C can be fitted by straight lines, at higher temperatures the behavior is non linear, meaning that the growth rate is a function of the disclination density. It was found that the growth rate, i.e., the tangent of the

growth curve, is only a function of temperature and the instantaneous disclination density (or $1/q_{max}$), meaning that a change in temperature from T_1 to T_2 at a given annealing time t is equivalent to a shift along the time axis from the growth curve at T_1 to that corresponding to T_2. The temperature dependence of the growth rate is represented in figure 4.13 as the initial slope of the growth curve at t = 0, at constant $1/q_{max}$= 0.52μm.

Information about the temperature dependence of the local anisotropy can be obtained by the temperature dependence of the scattered intensity at constant $1/q_{max}$. Figure 4.14 shows a plot of the total H_V scattered intensity as a function of temperature, obtained for a sample annealed at 150°C for 24 hours, at which point the growth rate can be neglected compared to the time of the measurement. In temperatures within the nematic range, the local anisotropy is a small decreasing function of temperature, with a sharp drop occurring at temperatures close to the clearing point.

The combination of the temperature dependence of the scattered intensity and the effect of annealing can give rise to apparent synergistic effects on the optical properties of the system. Figure 4.15 shows the temperature dependence of the H_V intensity obtained during a series of heating and cooling runs. By cooling from 180°C down to 140°C at 10°C per minute, the onset of the H_V intensity occurs at around 168°C, corresponding to the formation of the nematic phase (curve a). If an immediate heating run is subsequently performed at 10°C per minute, the resulting intensity is only slightly temperature dependent up to the

clearing point (curve b). However, if the heating is performed at a slower rate (curve c), the scattered intensity initially increases reaching a maximum value before dropping to zero at the isotropization temperature. Thus, during heating, the scattering intensity can either increase or decrease depending on the relative rate of the ordering occurring at the nematic phase and the rate of the change in temperature.

4.3 A Kinetic Model for the Domain Growth

A simple phenomenological model is proposed in an attempt to describe the kinetics of the annihilation of disclinations in a polydomain texture.

The model assumes a system containing an equal number of S=+1/2 and S=-1/2 disclinations. At any given time t, the total disclination density n_d is

$$n_d = 2\, n_{+1/2} = 2\, n_{-1/2} \quad . \tag{4.1}$$

The annihilation process is treated as a second order reaction of the kind

$$\left[-\frac{1}{2}\ \text{disclination}\right] + \left[+\frac{1}{2}\ \text{disclination}\right] \longrightarrow \ \text{annihilation} \tag{4.2}$$

characterized by a rate constant k_{ann} . The rate of dissapearance of the disclinations is

$$-\frac{dn_d}{dt} = 2\, k_{ann}\, n_d^2 \quad , \tag{4.3}$$

leading to the following time dependence of n_d

$$\frac{1}{n_d} = 2\, k_{ann}\, t + \frac{1}{n_{do}} \quad , \tag{4.4}$$

where n_{do} is the initial disclination density at t=0.

Assuming the correlation length $1/q_{max}$ being proportional to the average distance between neighboring disclinations (dense regime), $1/q_{max}$ should scale as

$$\frac{1}{q_{max}} \approx t^{0.5} \quad . \tag{4.5}$$

At low enough disclination densities the system should approach the "dilute" regime described by de Gennes[79], in which the correlation length is expected to be inversely proportional to the disclination density. That would imply a transition into a linear growth regime.

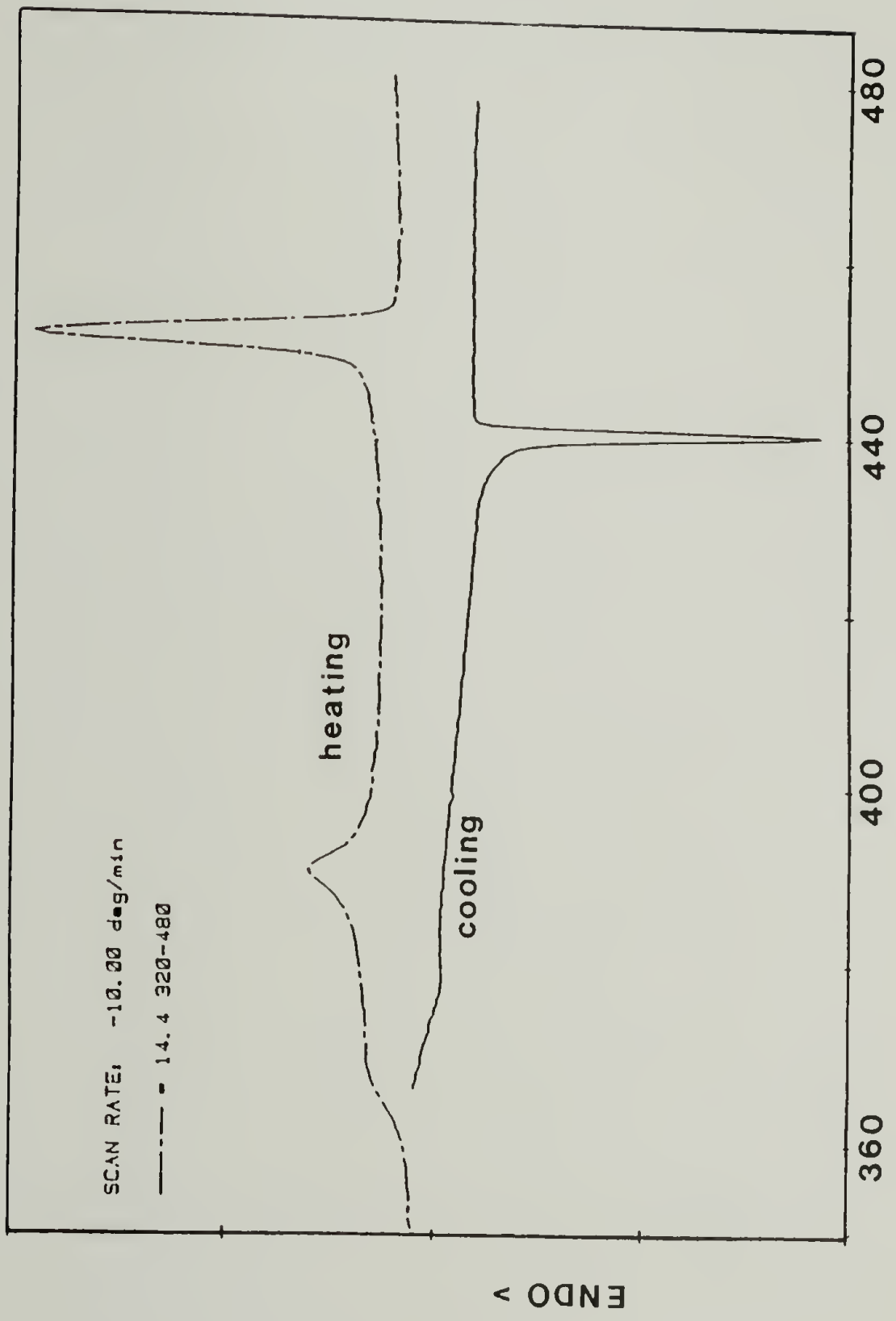

Figure 4.1 DSC thermograms of the PSHQ polymer.

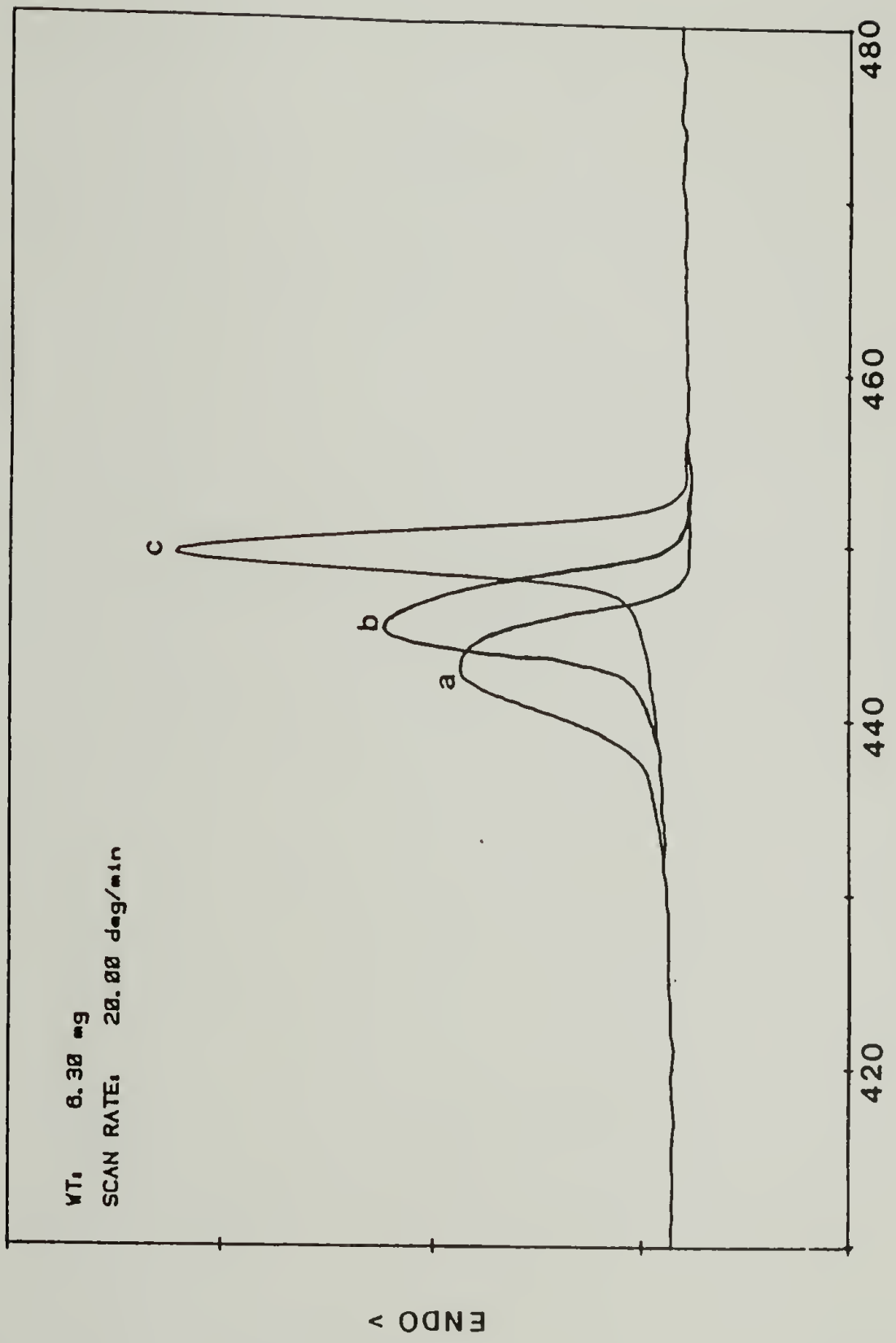

Figure 4.2 DSC endotherms of the N-I transition measured from samples annealed at 150°C for (a) 1 min.; (b) 3 hrs.; (c) 12 hrs.

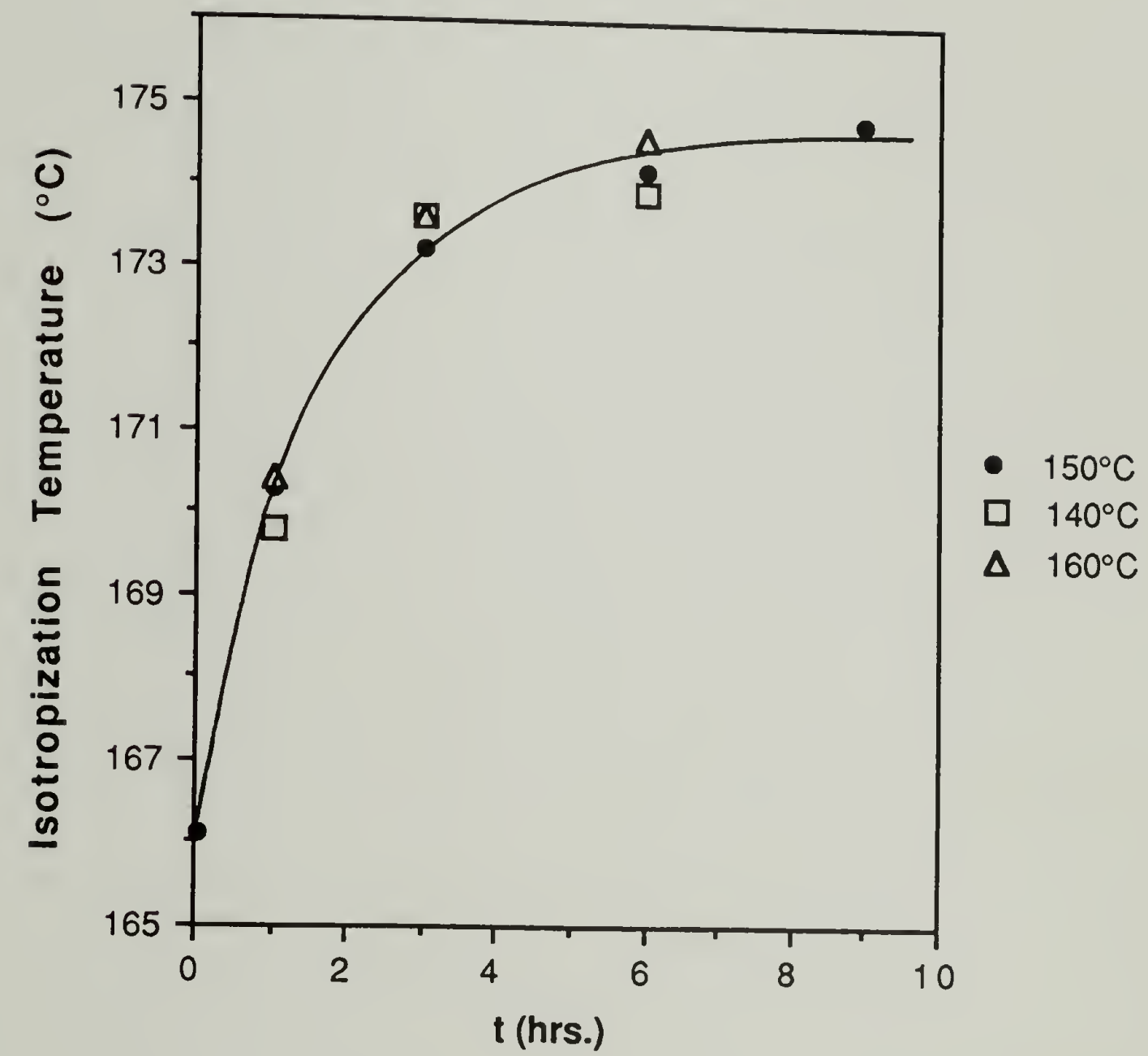

Figure 4.3 T_{N-I} determined from DSC as a function of annealing time.

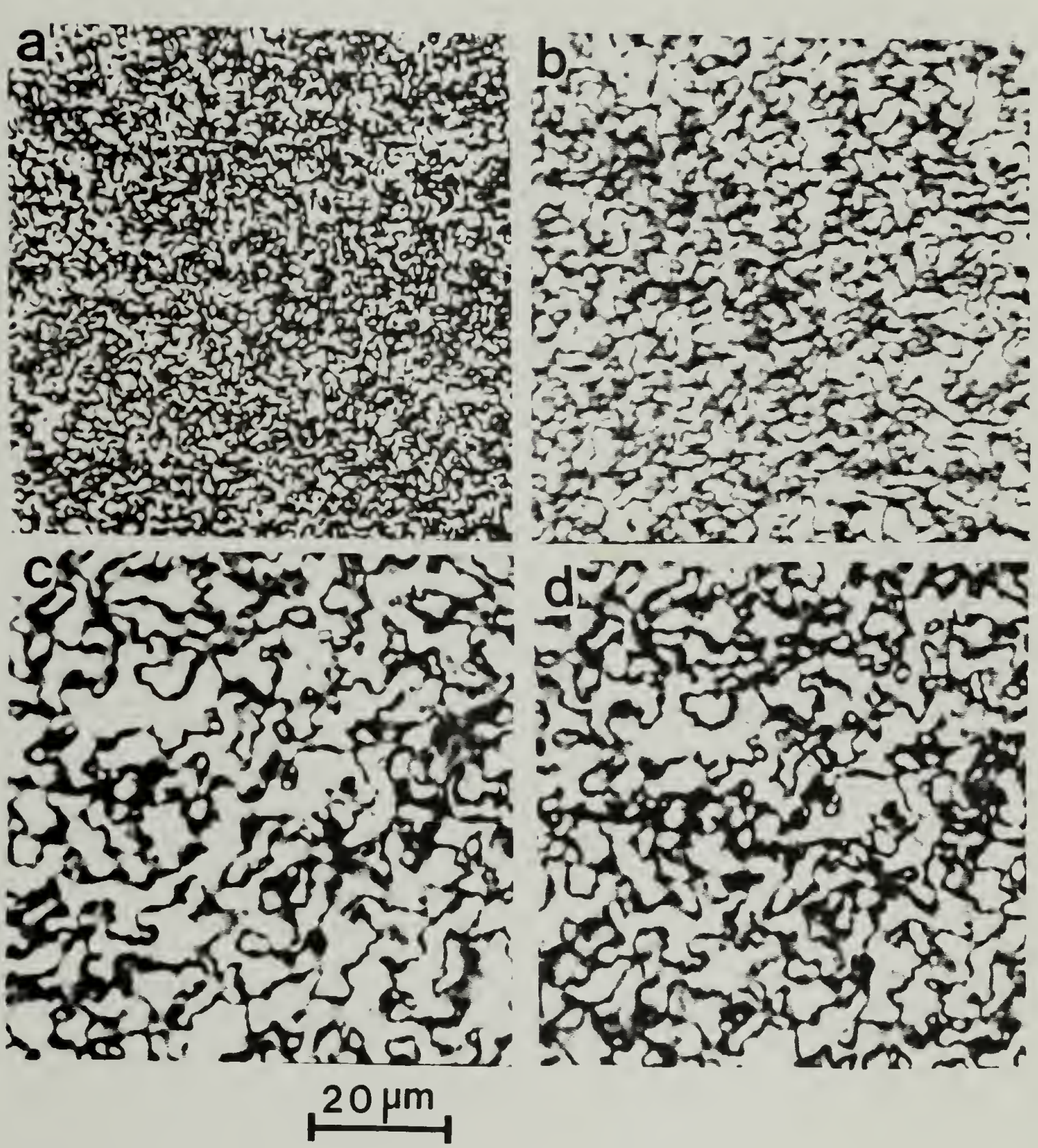

Figure 4.4 Polarizing micrographs of PSHQ as a function of annealing time at 150°C. (a) 1 hr.; (b) 3 hrs. ; (c) 9 hrs. ; (d) 20 hrs.

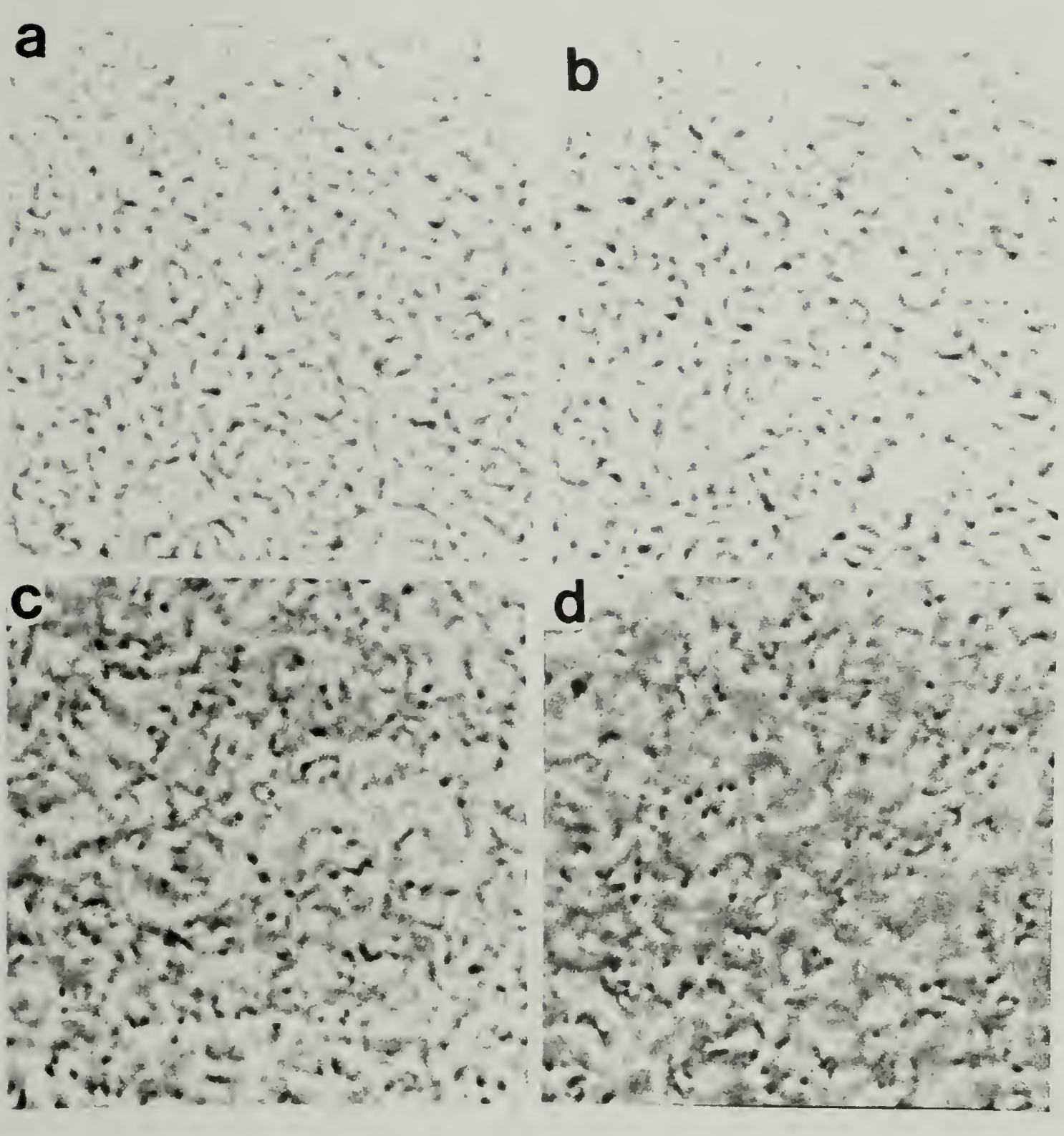

Figure 4.5 Unpolarized micrographs of PSHQ as a function of annealing time at 150°C. (a) 1 hr.; (b) 3 hrs. ; (c) 9 hrs. ; (d) 20 hrs.

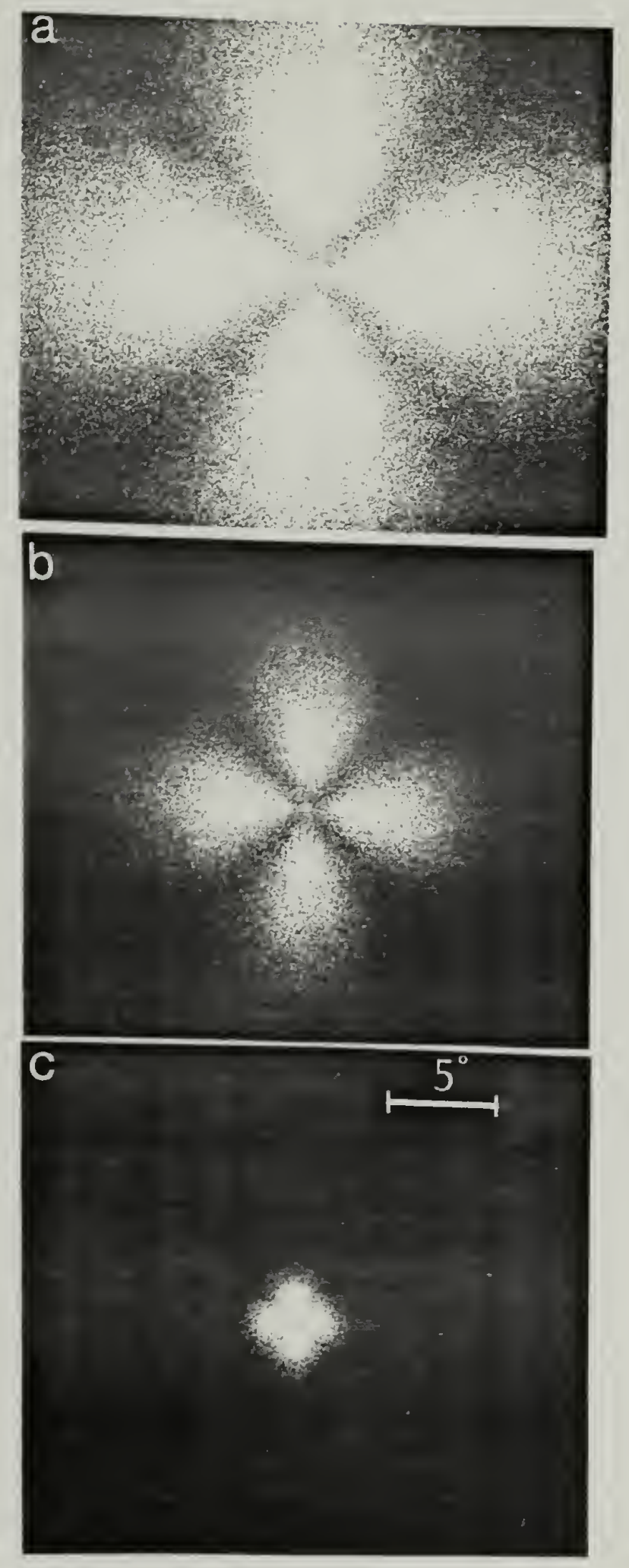

Figure 4.6 H_v SALS patterns from PSHQ films quenched from the nematic phase after various annealing periods at 150°C. (a) 1 min. ; (b) 30 min. ; (c) 5 hrs.

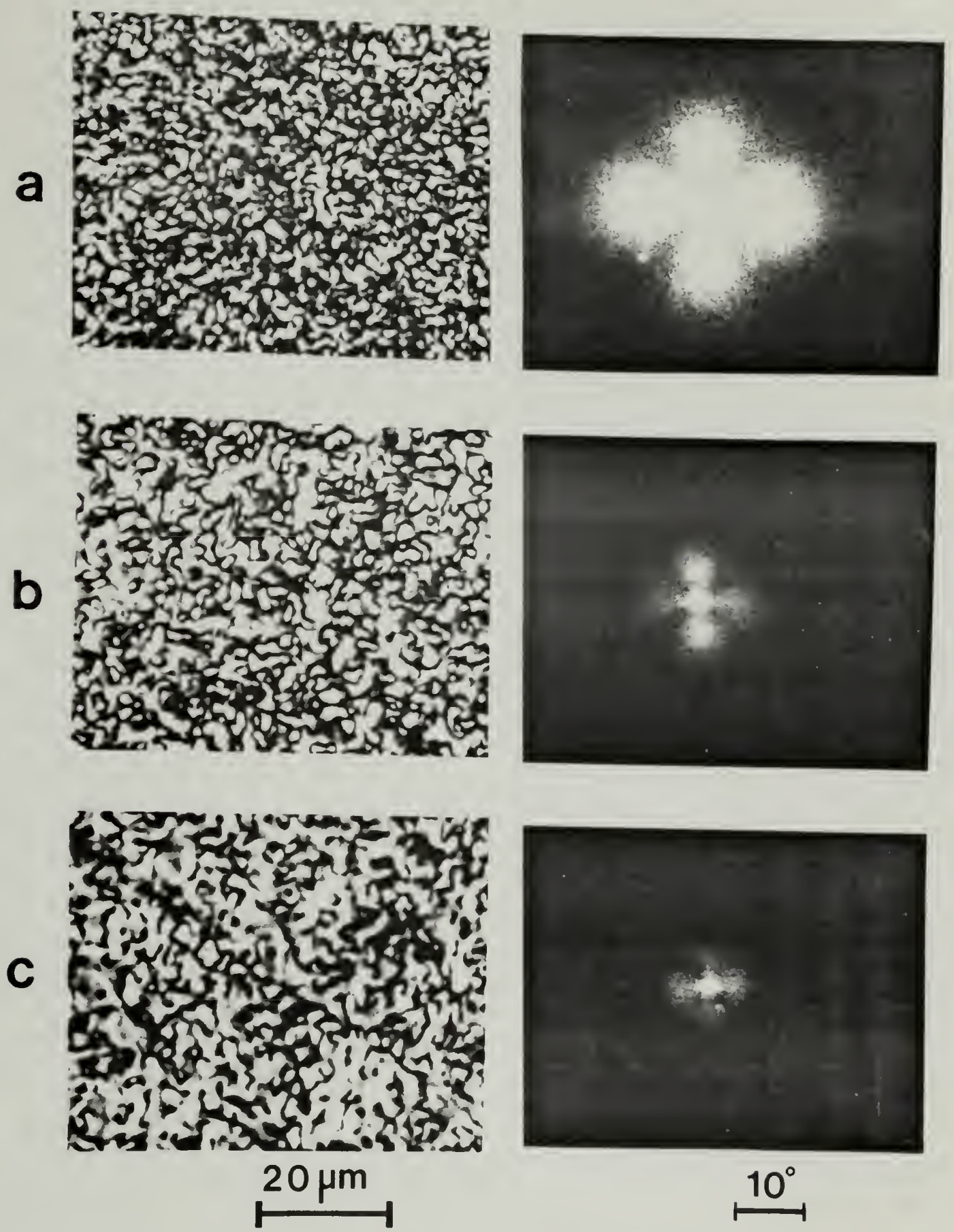

Figure 4.7 Polarized micrographs (left) and H_v SALS patterns (right) of the Polaroid polymer as a function of annealing time at 200°C.
(a) 2 sec. ; (b) 10 sec. ; (c) 20 sec.

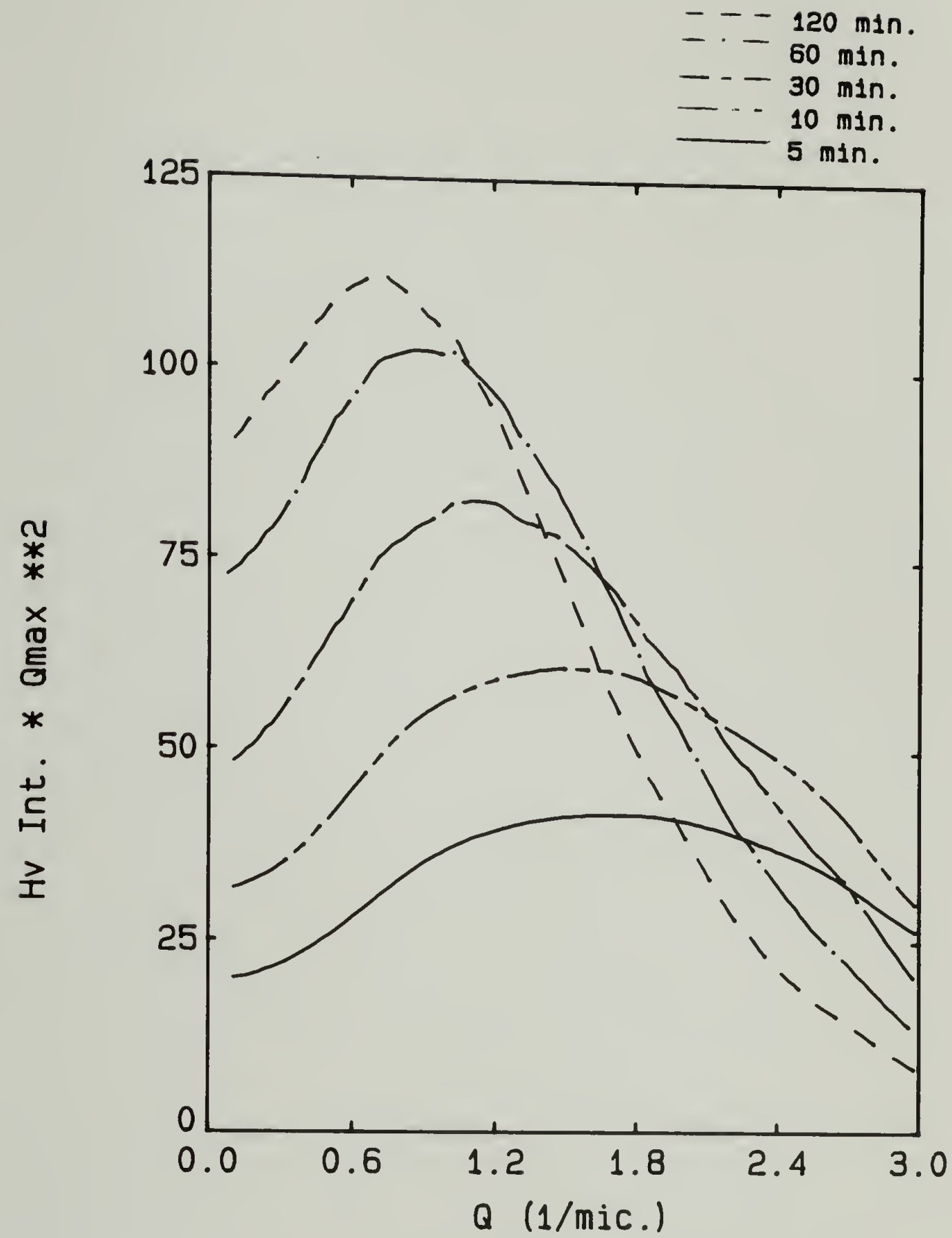

Figure 4.8 H_V intensity distribution at $\mu=0°$ measured at increasing annealing time at 150°C.

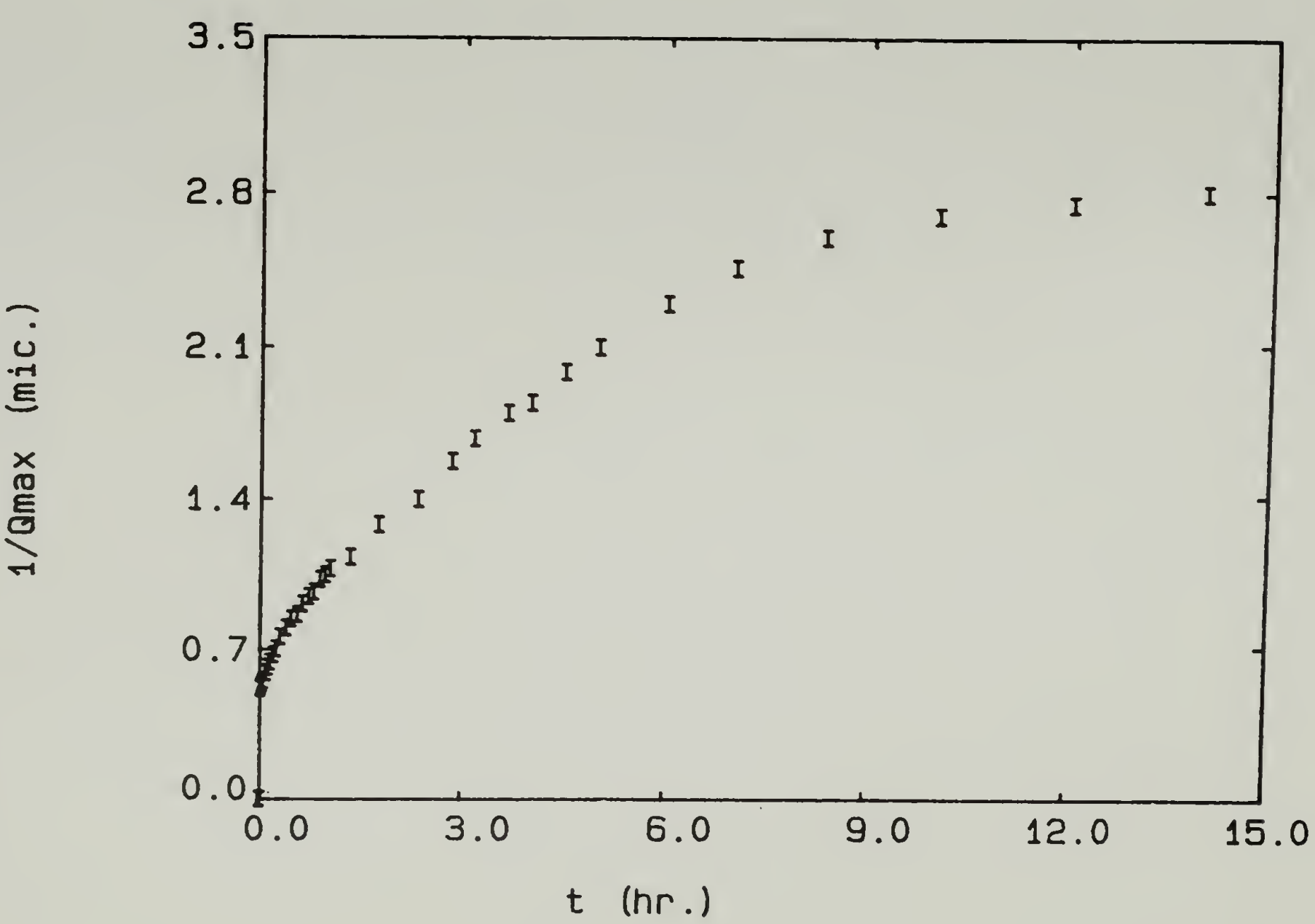

Figure 4.9 Growth curve of PSHQ at 150°C.

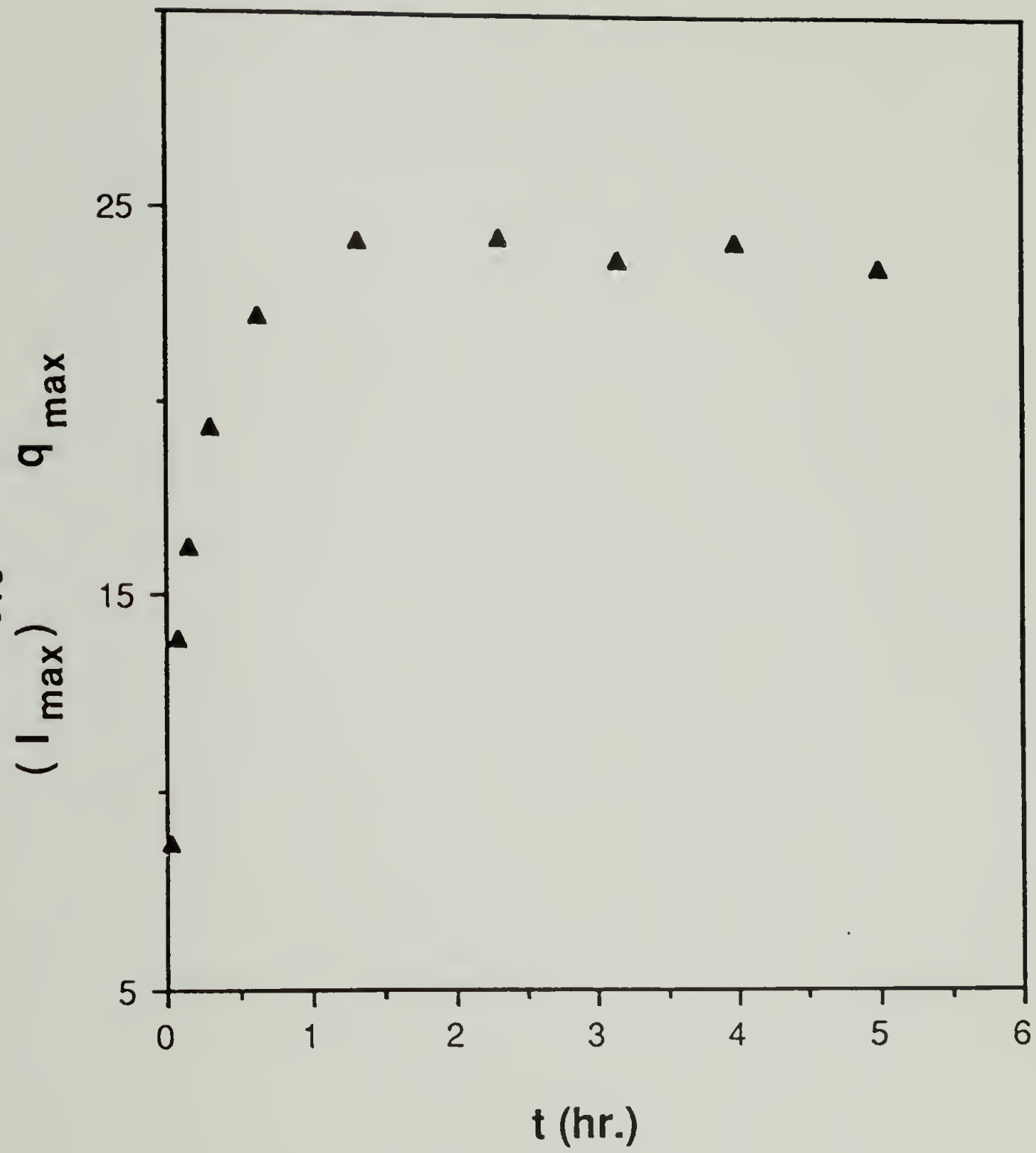

Figure 4.10 Degree of local anisotropy (in arbitrary units) of PSHQ as a function of annealing time at 150°C, assuming orientation fluctuations in two dimensions.

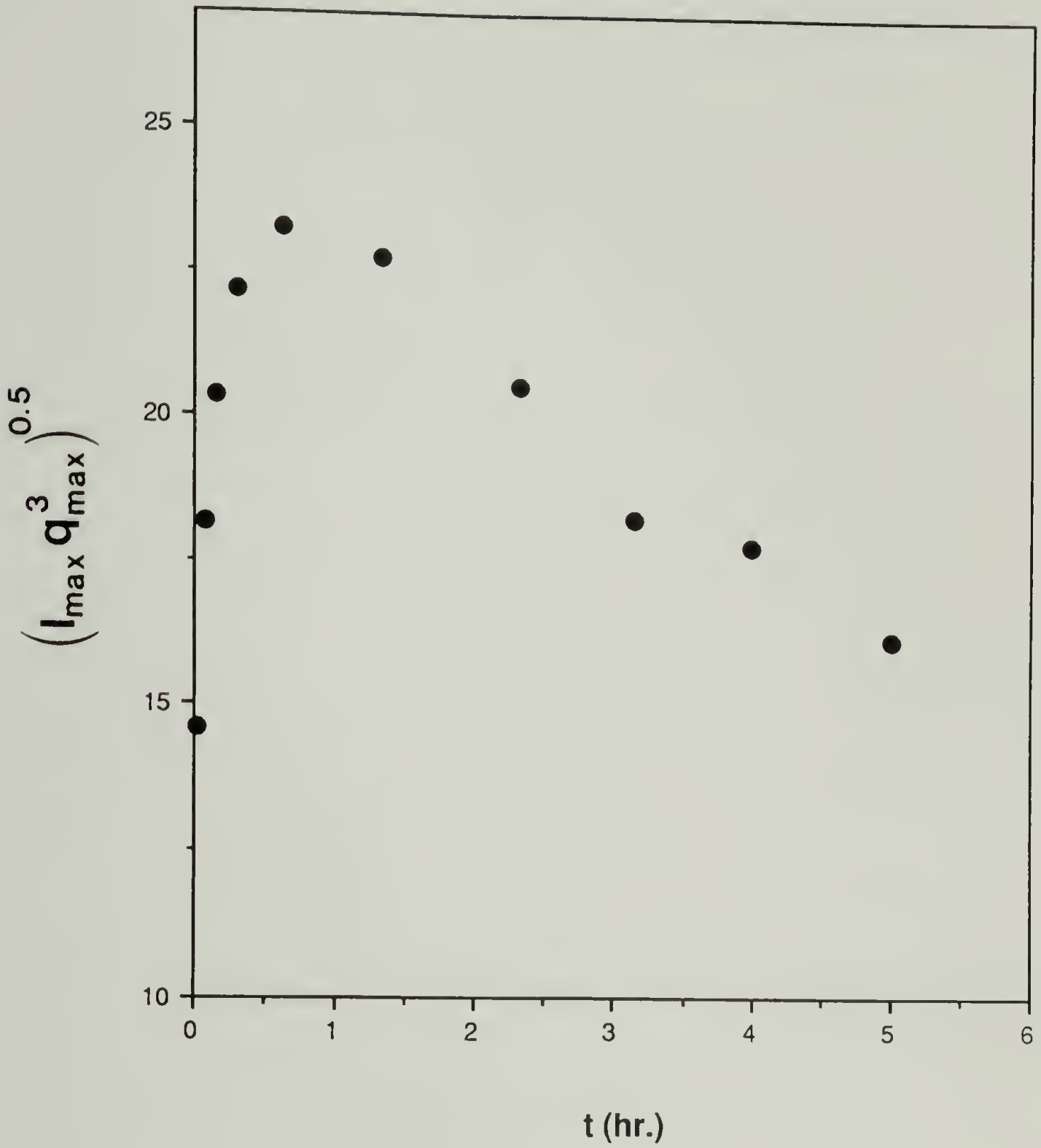

Figure 4.11 Degree of local anisotropy (in arbitrary units) of PSHQ as a function of annealing time at 150°C, assuming orientation fluctuations in three dimensions.

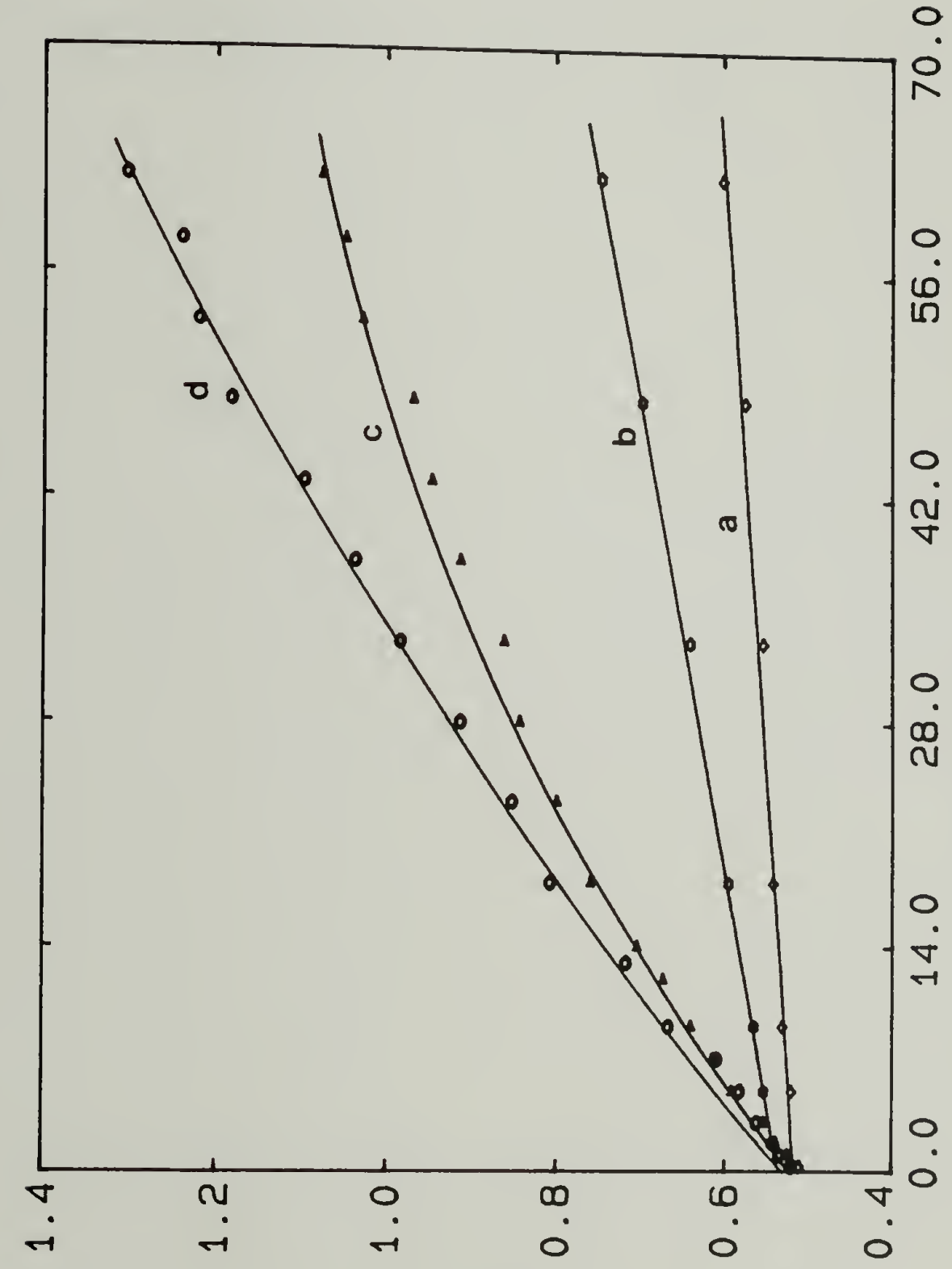

Figure 4.12 Growth curves of PSHQ at various temperatures.
(a) 130°C ; (b) 140°C ; (c) 150°C ; (d) 160°C.

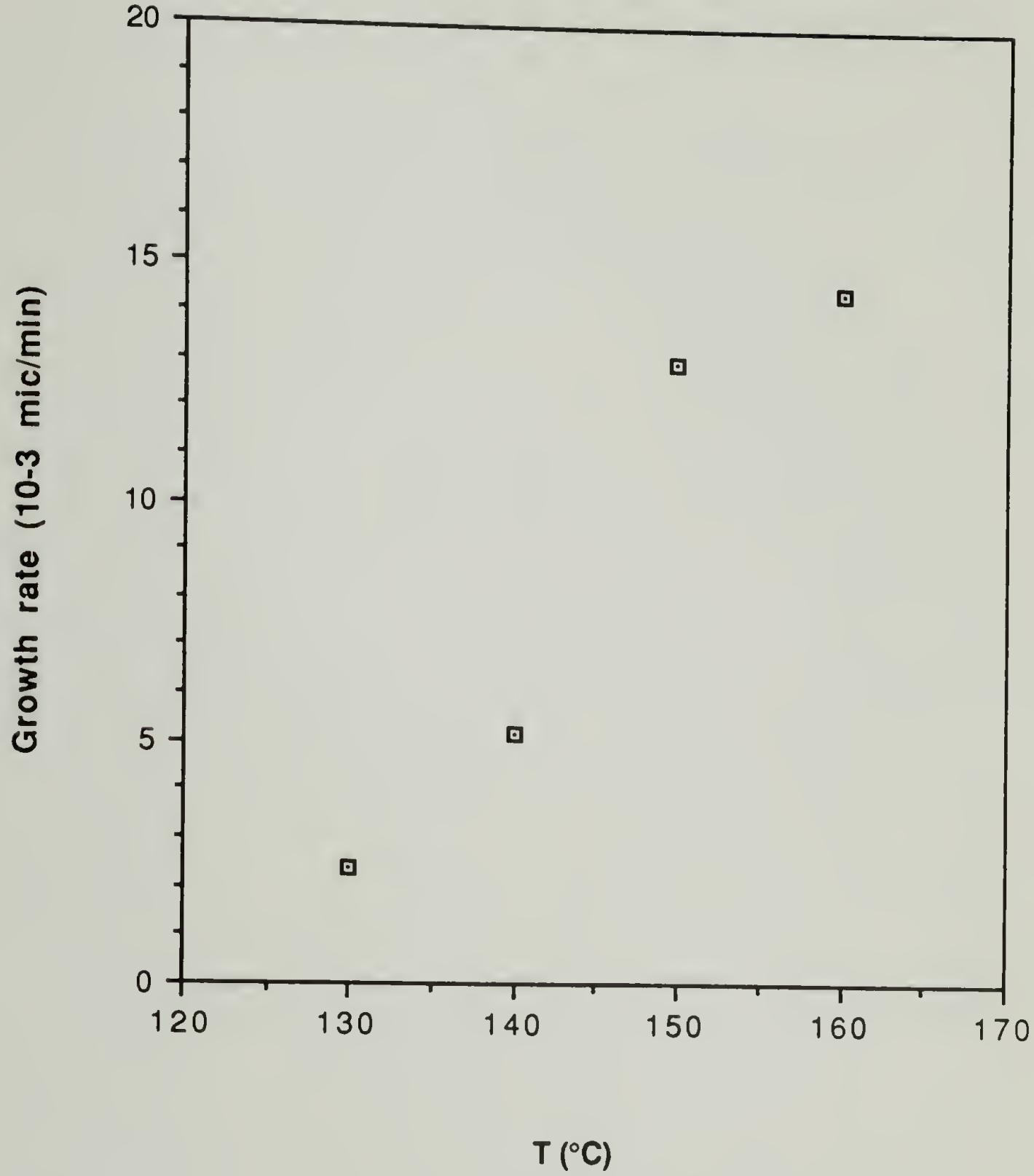

Figure 4.13 Initial growth rate of PSHQ as a function of temperature.

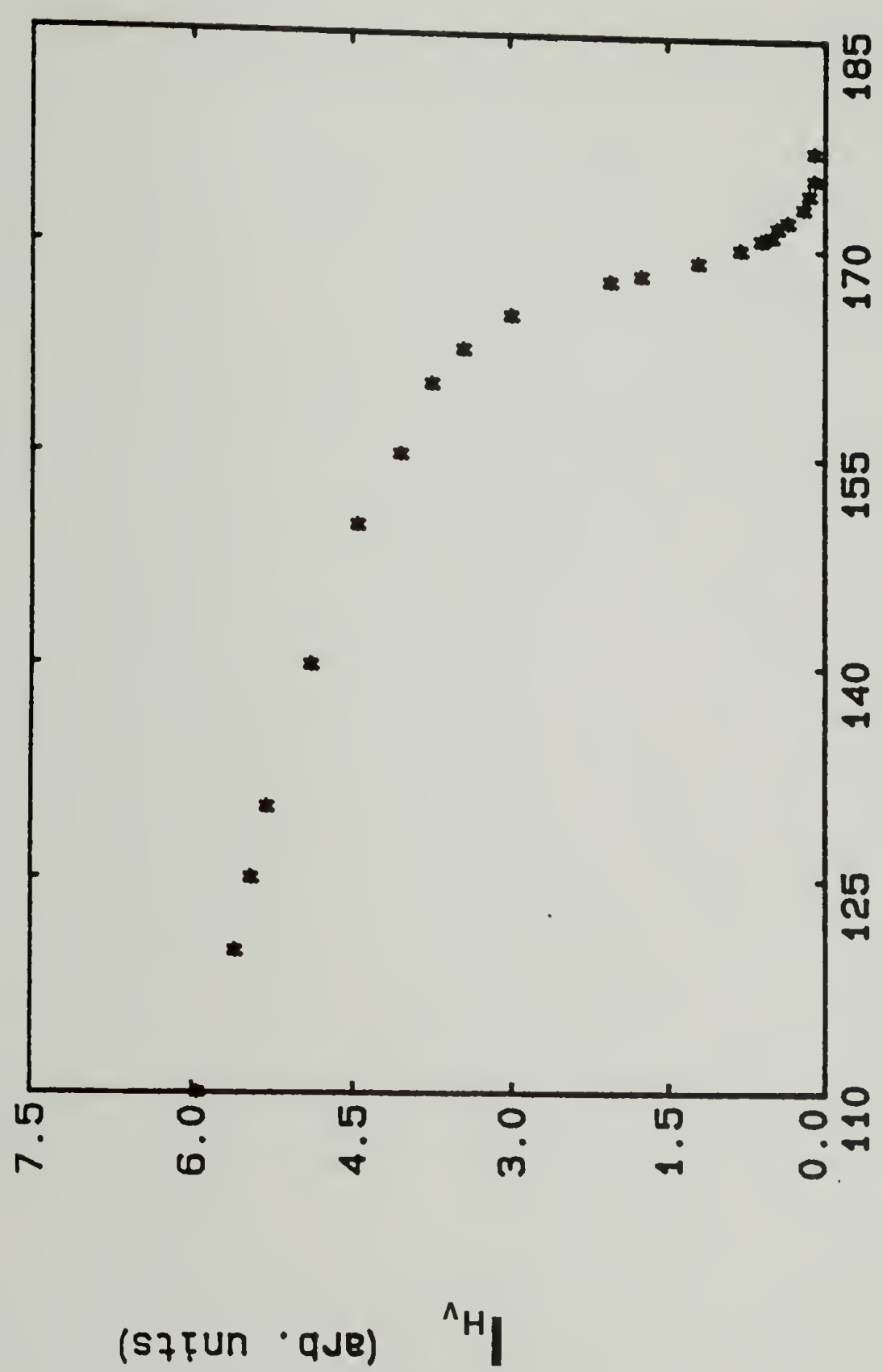

Figure 4.14 Temperature dependence of the total H_v intensity of PSHQ measured after 24 hrs. annealing at 150°C.

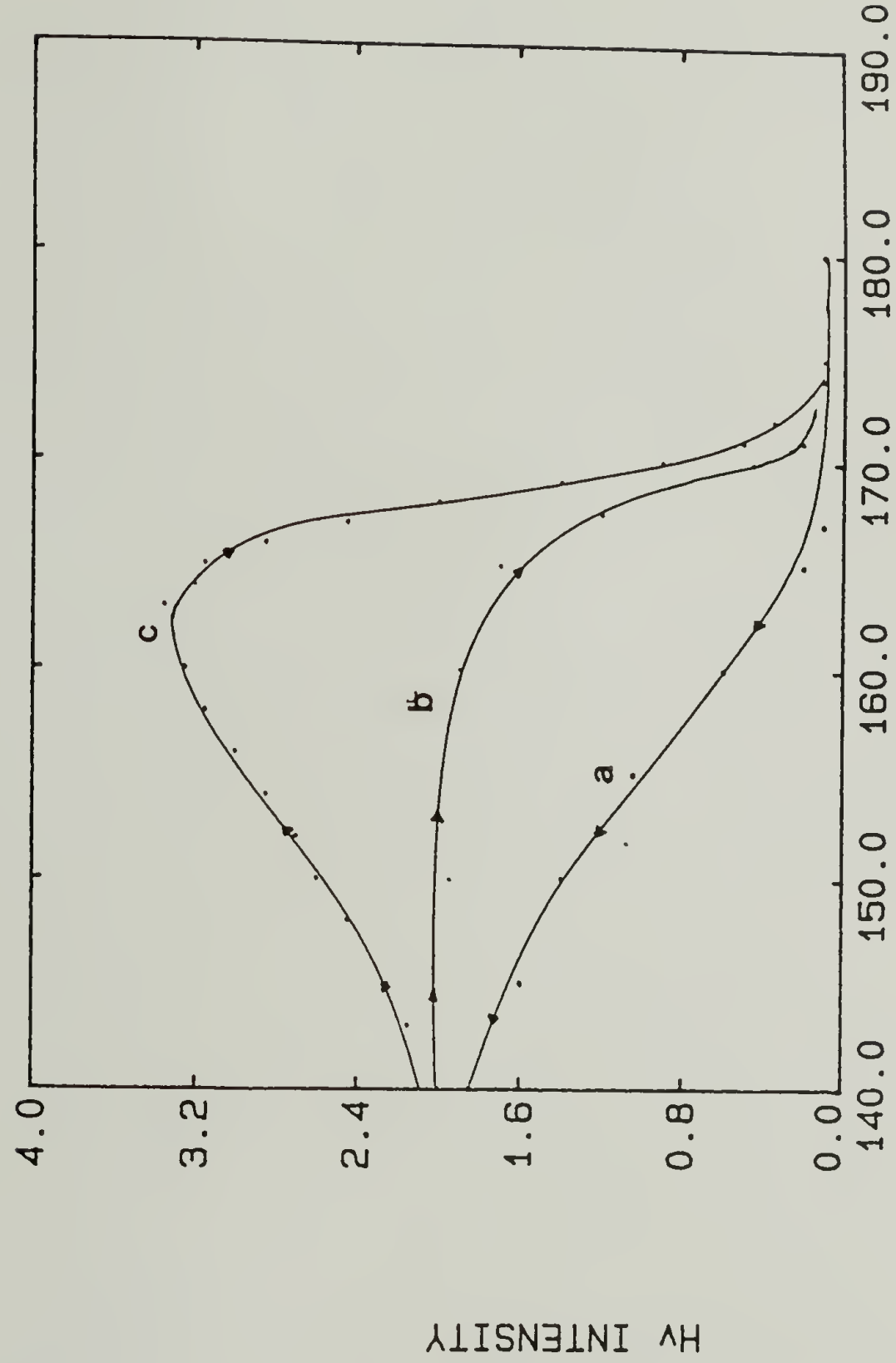

Figure 4.15 Total H_v intensity of PSHQ as a function of temperature measured during heating and cooling. (a) cooling at 10°C/min. ;(b) heating at 10°C/min.(c) heating at 2°C/min.

CHAPTER 5

DEFORMATION STUDIES

The present chapter reports the results of a preliminary study concerning the deformation process of a macroscopically unoriented thermotropic nematic liquid crystal polymer. The "Flow SALS" technique, in which the scattering is measured in-situ during a flow process was used in studying the deformation of the PSHQ polymer. Polarized optical microscopy of pre-sheared samples was performed to identify the corresponding textures.

5.1 Small-Angle Light Scattering

A special sample cell was designed in order to allow the recording of the SALS patterns during the deformation process at elevated temperatures. A schematic diagram of the experimental set-up is given in figure 5.1. The 10 μm thick film is confined between two microscope slides. The lower microscope slide is fixed to the hot-stage while the upper one is allowed to slide by the effect of a constant force. This deformation geometry corresponds to linear shear flow at constant stress. In such type of deformation, the shear rate is not constant hence the quantity used to characterize the amount of deformation is the shear strain, defined as the displacement of the moving slide divided by the length of the gap containing the sample. The shear direction was set parallel to the polarization plane of the analizer. The H_v patterns were continuously recorded during the deformation process by a video camera focused on the SALS patterns as

displayed on the CRT screen of the OMA system. The present study concerns the qualitative features of the scattering patterns only. A relatively small stress of $1500N/m^2$ was used and the stress was applied for approximately two minutes, at which point the shear strain was estimated to be 100 shear units. The deformation was performed at 150°C.

Figure 5.2 shows the evolution of the H_v patterns during the shear flow. Thirty seconds after the application of the stress (figure 5.2b), a distortion of the initial four leaf clover pattern (figure 5.2a) is observed. The lobes parallel to the shear direction (μ=90°) move to smaller angles and their intensity increase relative to the intensity at μ=0°.

Approximately 60 seconds after the application of the shear stress, a splitting of the strong horizontal lobes parallel to the deformation axis takes place, while the intensity st μ=0° takes the form of a thin streak. (figure 5.2c). At 90 seconds, most of the scattering occurs at μ=45°(X shape), with an apparent homogeneous decrease in the intensity at increasing scattering angles (figure 5.2d). No significant scattering is observed at scattering angles larger than 5°, indicating, as expected, that the structure obtained after the deformation contains larger areas of homogeneous orientation than the undeformed initial fine Schlieren texture.

Upon removal of the stress, no significant changes in the H_v pattern occurred in up to 30 minutes, while keeping the temperature constant at 150°C, suggesting a relatively slow

relaxation of the state obtained at the cessation of the shear. A dramatic change in the scattering pattern occurred, however, by lowering the sample temperature. The effect is shown in figure 5.3. The two spots diffraction-like pattern in figure 5.3 developed at around 130°C, 20°C lower than the deformation temperature, still in the nematic phase. An intensification and sharpening of the diffraction pattern was observed upon a further decrease in temperature down to 110°C. As it will be shown in the next section, the diffraction pattern arises from the banded texture, which consists of nearly equidistant extinction lines perpendicular to the shear direction. In analogy to a one dimensional diffraction grating, the diffraction from such a system is given by

$$n\,\lambda = d\,\sin\theta \quad , \qquad (5.1)$$

where d is the spacing of the lines. The first order diffraction in figure 5.3b occurs at $\theta=12°$, corresponding to a spacing of 3.0 μm.

When the temperature was raised back to 150°C, the banded texture's diffraction pattern faded-out as the former one (figure 5.3a) faded-in. Upon further subsequent cooling and heating, the corresponding low and high temperature pattern formed, for at least three heating and cooling cycles. The total time spent in the temperature cycles was 15 minutes. The samples were finally cooled down to room temperature, quenching-in the diffraction pattern.

The observation made by SALS indicated that for at least 40 minutes after the cessation of the shear, the morphology of the

post-shear state depends on the sample temperature only. Moreover, the results suggested an apparent reversible formation of the banded texture induced by temperature. The recovering of the banded texture at low temperatures was possible provided that the sample was not exposed to temperatures higher than the deformation temperature (150°C). Exceeding the deformation temperature rapidly erased the deformation history.

A post-annealing step performed at 130°C showed a slow decrease in the intensity and sharpness of the diffraction pattern. After 3 hours of annealing, no signs of the banded texture pattern could be detected. The H_v pattern observed at that time showed circular symmetry of the intensity. The initial four leaf clover shape was not recovered in the up to 24 hours annealing time range covered by the study.

5.2 Optical Microscopy

Figure 5.4 presents a polarizing micrograph of a specimen quenched to room temperature after subjected to shear for 30 seconds. The texture is characterized by extinction lines running perpendicular to the prior shear direction, giving rise to apparent elongated domains or "worms" The orientation of the worms agrees with the scattering intensity being stronger in the direction parallel to the shear (figure 5.2a). The term "worm texture" was used by Graziano and Mackley[62] to describe the texture observed at small oscillatory shear deformation. In the latter, however, the worms were oriented parallel to the shear. The texture in figure

5.4 appears to retain the characteristics of the quiescent state in the sense that the orientation of the extinction lines to changes while rotating the polarizers. Unlike the textures observed by Graziano and Mackley[62], the dark lines can not be seen with unpolarized light. The induced texture at small extent of deformation can be classified as a "distorted fine Schlieren" or "ordered Schlieren" texture.

Knowing that the relaxation following the cessation of the shear is rather slow (longer than 30 minutes), the post-shear textures and the temperature dependence were studied by hot-stage microscopy of samples sheared for the entire period of 2 minutes. Figure 5.5 presents a micrograph recorded at room temperature from an as-quenched pre-sheared film. The banded texture shows a very regular array of extinction lines with an average spacing of 3.3μm, in close agreement with the value determined for the light diffraction pattern. The bands could be seen with unpolarized light, although the contrast is much lower. Figure 5.6 presents a series of micrographs from a single section at various temperatures, with the polarizer direction set parallel to the prior shear direction. At 150°C, the deformation temperature, the texture shows curled black threads which are not align along a specific direction. Lowering the temperature to 130°C induces an ordering of the extinction lines, in what can be considered a precursor of the banded texture, which fully develops at around 120°C (figure 5.6c). At 110°C, the bands are more distinct and less undulated than at higher temperature, with a close resemblance to the quenched state. In completing a

temperature cycle by heating back to 150°C, the various textures on figure 5.6 were recovered at the same temperature as seen during the cooling run. At temperatures within the mesophase range, the bands could be detected only under cross polarization conditions. Optical microscopy confirmed the earlier indication by the SALS results concerning the apparent reversibility of the bands formation.

Figure 5.7 shows the texture recorded at room temperature, after the post-annealing treatment (3 hours at 130°C). The very fine texture resembles the quiescent texture, although some sections show elongated domains aligned perpendicular to the prior shear direction, similarly to the worm texture observed at small deformation. Similar textures were seen from samples in which the deformation history was erased by heating at temperatures between 160°C and 170°C.

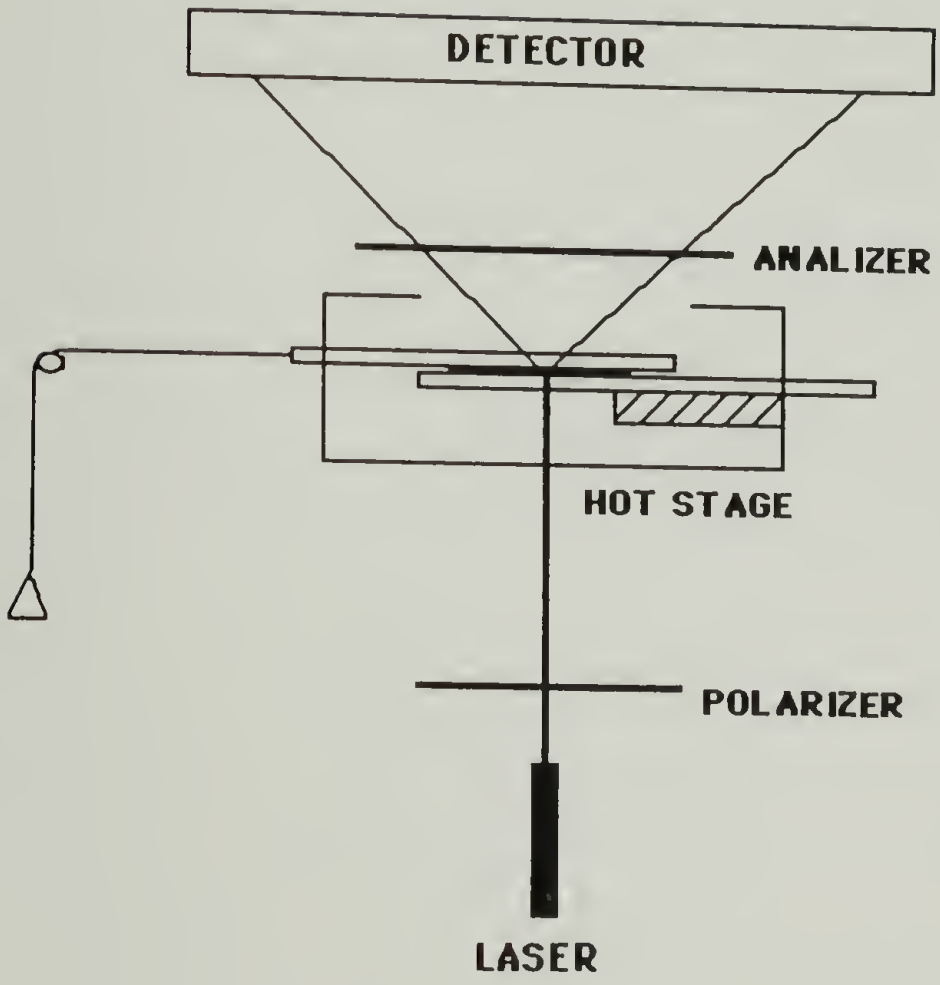

Figure 5.1 Schematic diagram of the Flow-SALS apparatus.

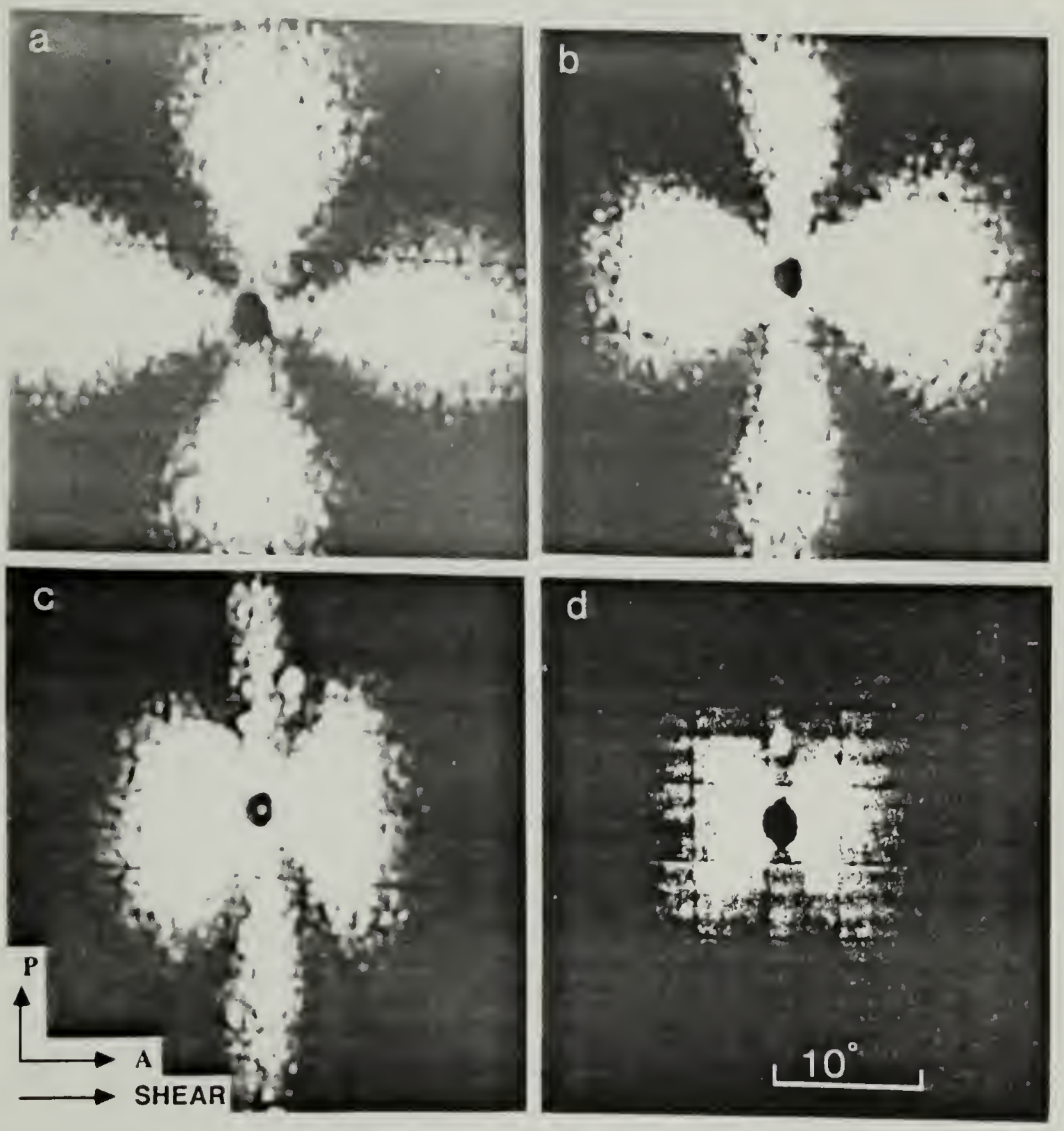

Figure 5.2 H_v SALS patterns of PSHQ as a function of time during shear deformation. (a) quiescent state; (b) 30 sec. ; (c) 60 sec. ; (d) 90 sec.

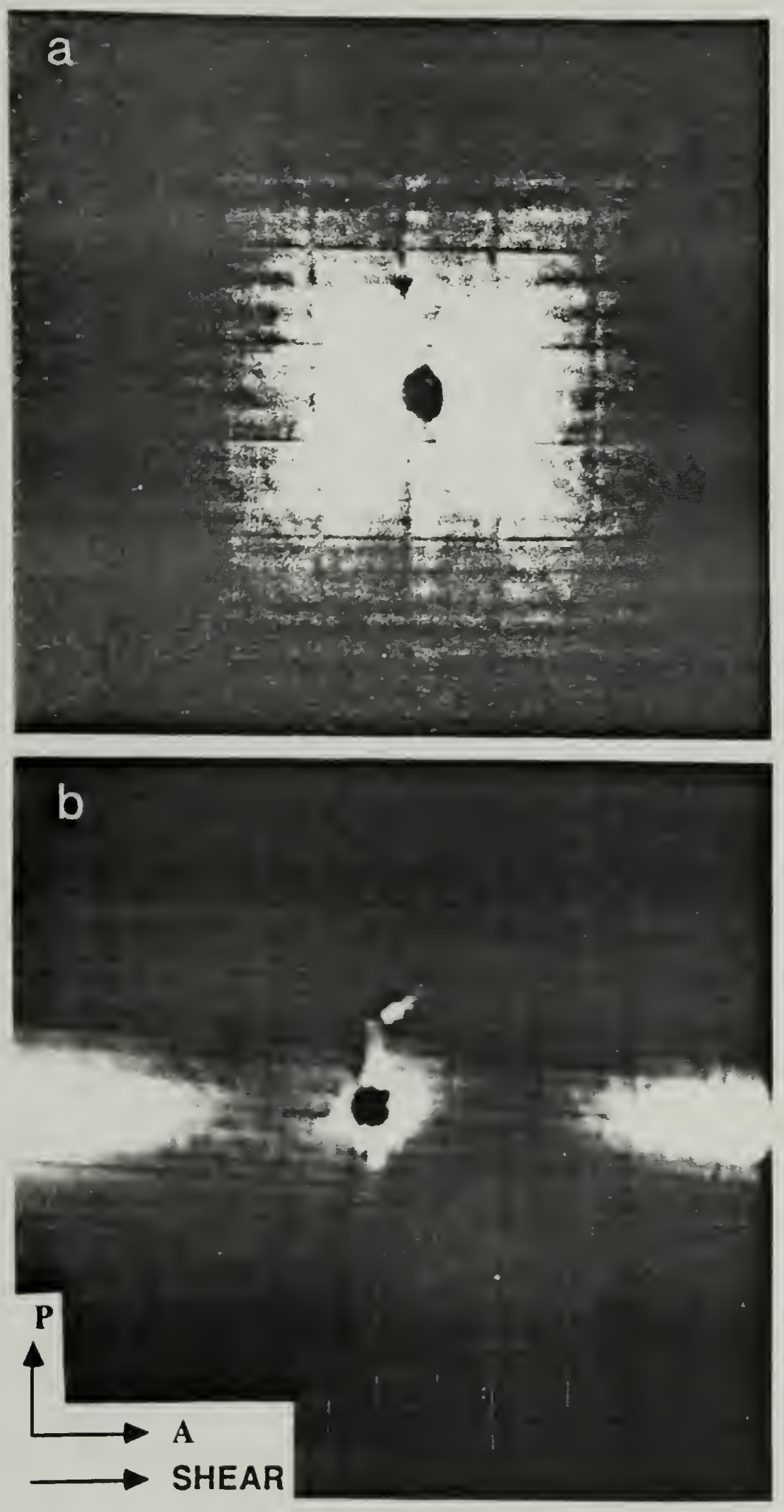

Figure 5.3 H_v SALS patterns of PSHQ after the cessation of the shear. (a) 150°C ; (b) 130°C.

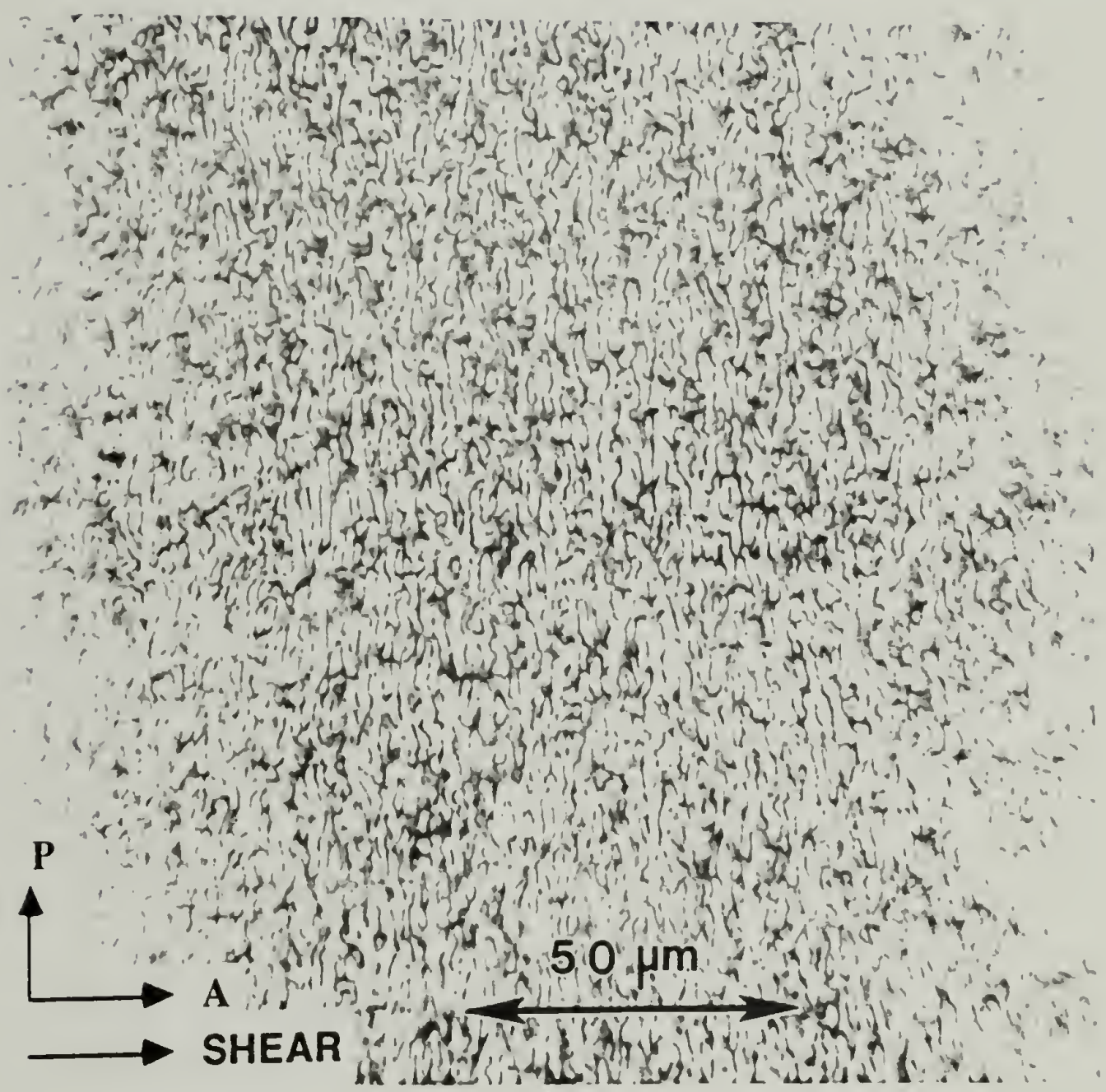

Figure 5.4 Polarized micrograph of a PSHQ film quenched after being sheared for 30 sec.

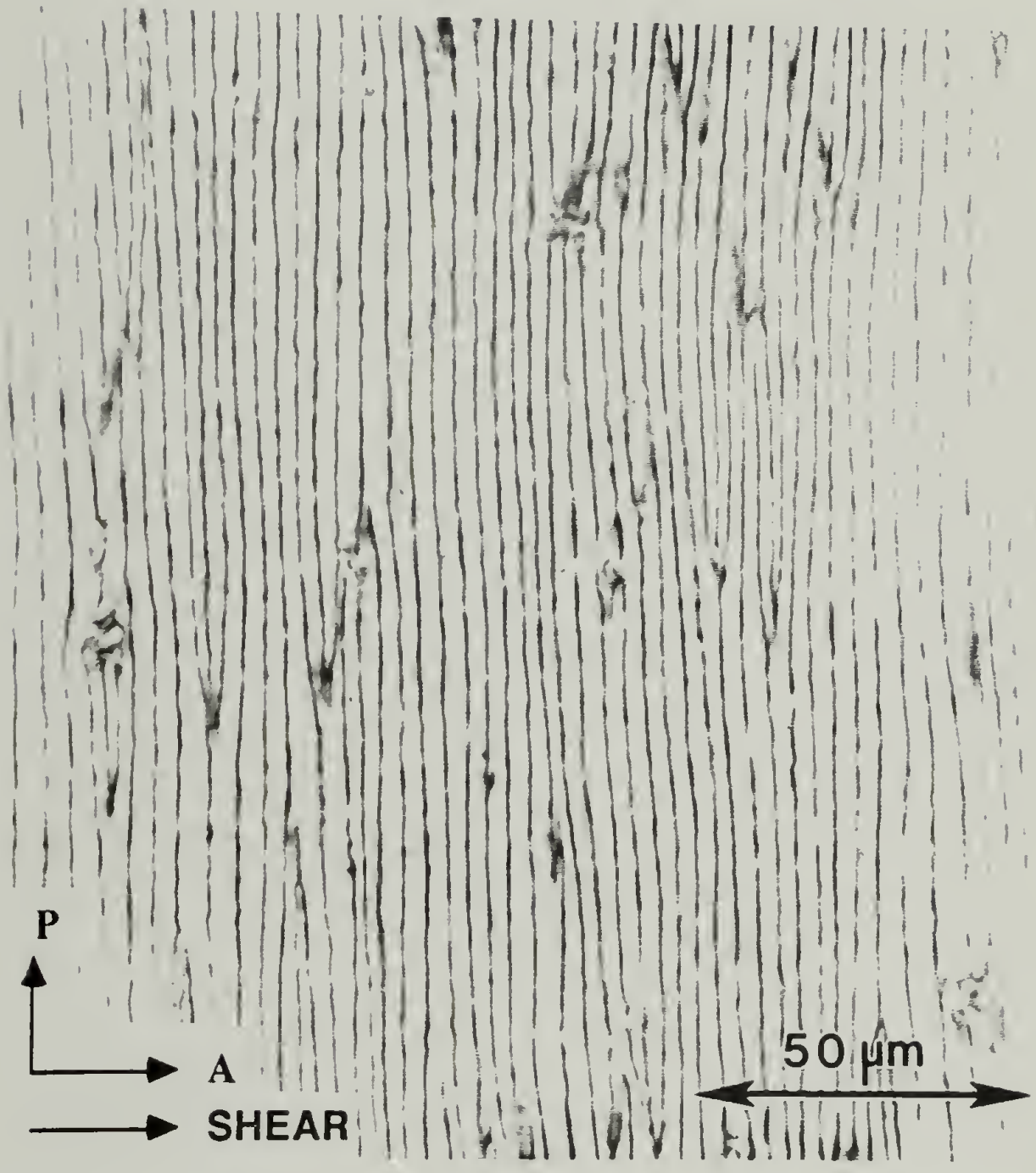

Figure 5.5 Polarized micrograph of a PSHQ film quenched after being sheared for 2 min.

Figure 5.6 Polarized micrographs recorded at various temperatures from a PSHQ film previously sheared for 2 min. (a) 150°C ; (b) 130°C ; (c) 120°C ; (d) 110°C.

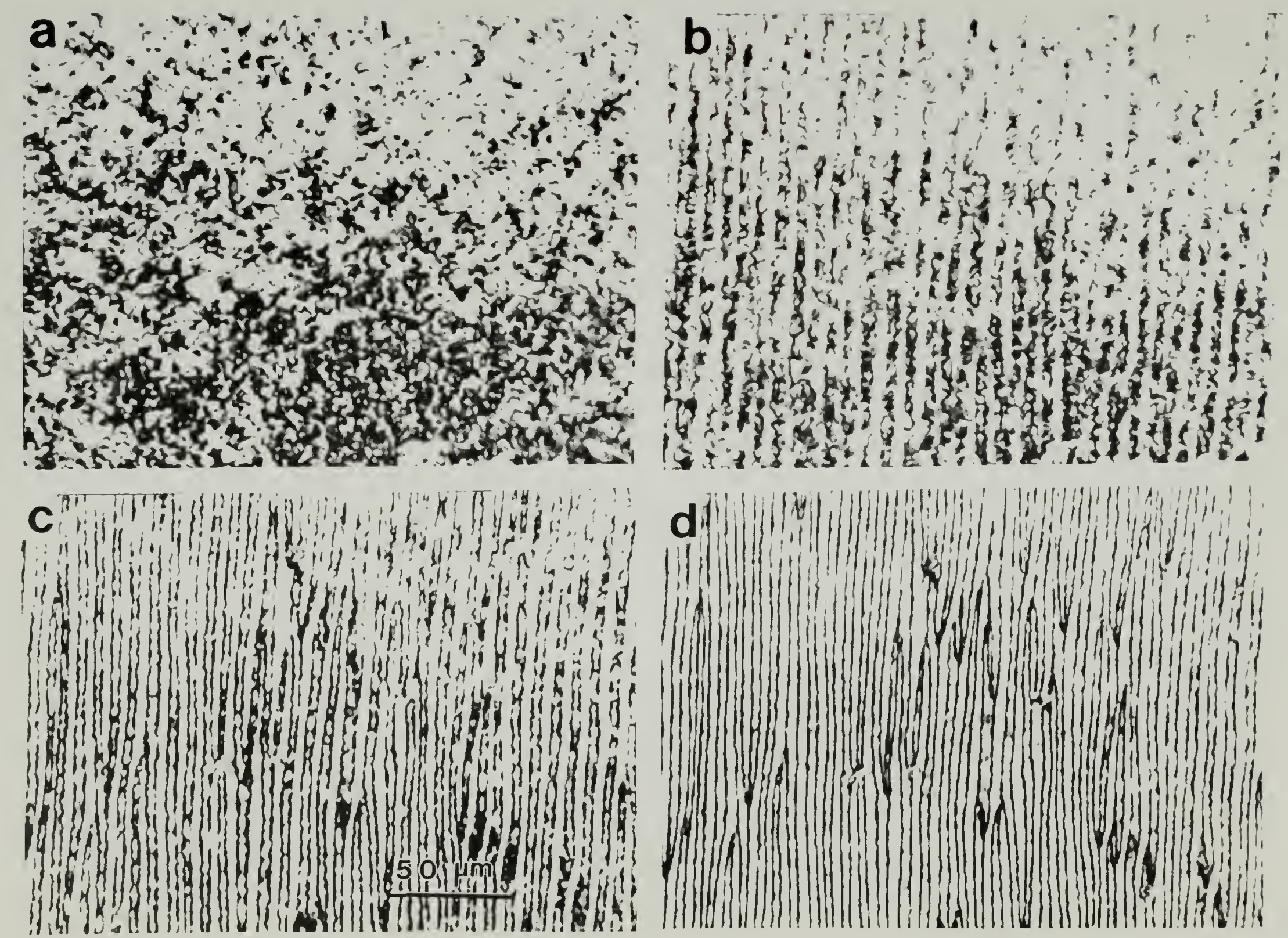
a
b
c
d
50 µm

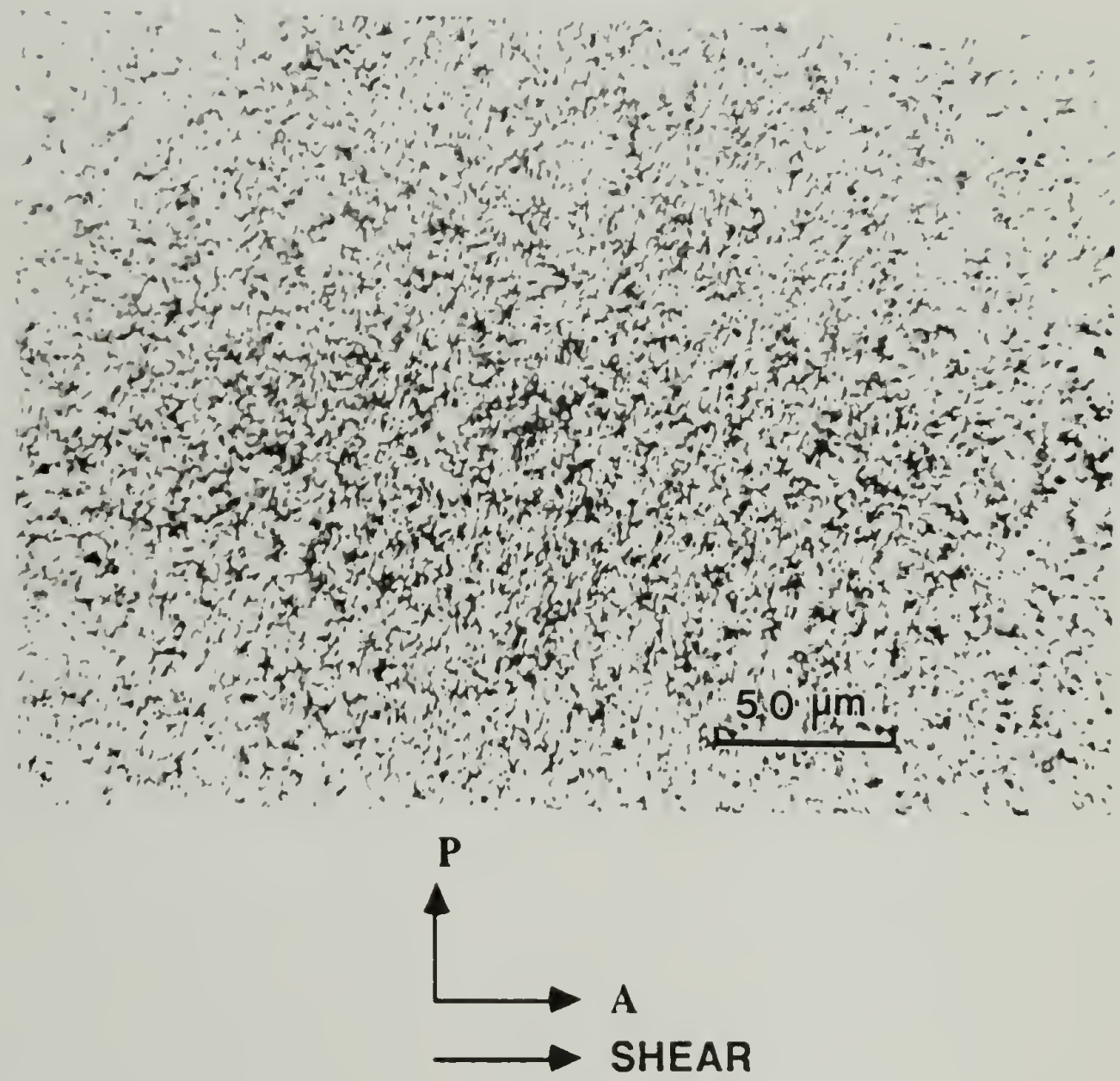

Figure 5.7 Polarized micrograph of a PSHQ film annealed for 3 hrs. at 130°C after being sheared for 2 min.

CHAPTER 6
DISCUSSION OF RESULTS

6.1 Geometry of the Directorfield

The azimuthal dependence of the SALS patterns from the fine Schlieren textures indicates that the geometry of the structure can not be described in terms of "random orientation fluctuations". As it has already pointed out, no theoretical model has so far been able to predict the observed azimuthal dependence of the scattering. It is possible, however, to qualitatively describe some of the implications of the geometry of the SALS patterns concerning the geometry of the directorfield in the fine Schlieren textures and to consider some possible reasons to account for the non-randomness of the fluctuations.

It is worth mentioning that both the H_V and V_V SALS patterns observed from the fine Schlieren textures have a close resemblance to those reported for polytetrafluoroethylene (teflon) films crystallized under certain conditions.[87,88] In the latter, the patterns are interpreted in terms of spherulites in which the optic axes makes an angle of 45° with the radius of the spherulite. This is in agreement with the spherulitic macrostructure with maltese crosses at 45° from the polarizers seen by polarized light optical microscopy. The extinction lines in the nematic textures, however, appear to follow random paths with no specific orientation.

The non-randomness of the directorfield geometry can be rationalized by making a comparison with the random

disclinations model suggested by de Gennes (section 3.2). To recall, the two basic assumptions made by de Gennes relate to the elastic isotropy of the system and the insignificance of the interaction between disclinations. The interactions between disclinations are expected to play a major role in the "dense" textures common to LCPs, affecting the angular distribution of the scattering as well as the relationship between the disclination density and its corresponding correlation length. This factor alone, however, will probably not predict the departure from the random fluctuations. The reason is that even if disclinations are closely packed, for elastic isotropic systems the distortion energy is independent of the relative orientation of neighboring disclinations. Averaging over all the possible configurations should still result in random orientation fluctuations. This will not be the case if either bend or splay deformation is more favorable. The effect of elastic anisotropy on the interaction between a pair of disclinations was qualitatively described in section 1.3.2 . The result of the non-equality of the splay and bend constants is that the c values of neighboring disclinations have to be correlated. It was suggested by de Gennes that the azimuthal dependence of the scattering patterns could be accounted for in terms of the difference in the elastic constants. This would predict the observed decrease in the azimuthal dependence of the scattering at increasing temperatures. The effect of the elastic anisotropy should be particularly strong at high disclination densities. Consequently, the azimuthal dependence of the scattering should decrease as the

annihilation of disclinations takes place. This effect could not be verified experimentally due to the increase in multiple scattering during annealing.

Summarizing, it is possible that the observed azimuthal dependence of the scattering is a consequence of the role the elastic anisotropy plays in imparting specific configurations of the closely packed disclinations and the resulting directorfield.

Concerning the angular dependence of the intensity at μ_{max}, it was demonstrated that the scattering angle θ_{max} corresponding to the position of the maximum of the intensity curve can be used for characterizing the average domain size determined by the disclination density. The SALS technique was found to be particularly sensitive to changes in textures containing large defect densities, in the regime where analysis by optical microscopy is hardly accessible. This makes the SALS technique an appropriate tool for studying the typically fine liquid crystalline textures occurring in polymeric systems.

6.2 Effect of Thermal History

6.2.1 The Initial Nematic Texture

One important result presented in section 4.2.3 concerns the insignificant change on the q_{max} values measured from the initial textures obtained while changing the degree of undercooling from 10°C to 40°C, i.e., for the phase transition occurring in the temperatures in the range of 130°C to 160°C. The temperature

independence of the initial domain size suggests the value of the disclination density obtained at the time of the phase transition being independent of the the degree of undercooling.

Having discarded the above observation being a consequence of the non-isothermal conditions during the phase transition (by comparing with the T-jump experiments), it is still possible that the temperature independence of the "initial" disclination density is only an apparent effect. This would be the case if the actual disclination density obtained at the phase transition is a function of temperature, however, this is followed by a fast annihilation process occurring before the development of the minimum degree of anisotropy required for the measurement of the H_v intensity above the background level, at which point the first scattering curve can be detected. In the experiments, the first H_v curve was measured 5 seconds after the quenching from the isotropic phase.

On the other hand, it is possible that in the temperature range studied, the actual initial disclination density is indeed independent of the phase transition temperature. Such a phenomenon has to be related to the mechanism by which the disclinations are formed. One possible mechanism for the formation of disclinations is presented in the following paragraphs.

The model assumes that the formation of the nematic phase from the isotropic state occurs by a nucleation and growth mechanism. For simplicity, the nematic phase is assumed to growth as two dimensional circular nematic droplets in a

continuous isotropic medium. Moreover, the molecules within the nematic droplets formed from the growth of a single nucleus are assumed to align along a single direction (figure 6.1), meaning that the nuclei grow into monodomain droplets. The orientation of the director within a droplet is determined by the substrate, and assuming that the substrate is isotropic, the direction of molecular orientation of a droplet can take any possible orientation, uncorrelated with the orientation direction of neighboring droplets. As the nematic droplets grow, neighboring droplets impinge on each other. The angle α is defined as the angle between the directors representing the orientation of the impinging droplets. As schematically represented in figure 6.1, the impingement of two nematic droplets can result in either of two competing processes. One is the "droplet coalescence" process, which leads to the formation of a larger nematic droplet characterized by a directorfield corresponding to either a gradual change in the orientation within the droplet or by a larger monodomain. If α is larger than zero, this process involves the reorientation of the molecules in at least one of the impinging droplets. Another possible result of the impingement is the formation of a defect such as a disclination line. As a disclination allows for an abrupt change in orientation, this process can take place without a significant extent of reorientation of molecules in the impinging droplets. In the example shown in figure 6.1, the creation of a S=1/2 disclination can nearly preserve the overall orientation of impinging domains with $\alpha=90°$.

The three main parameters determining the result of the impingement of a pair of droplets are the angle α, and two molecular parameters: the orientational viscosity, which will determine the rate of the reorientation process, and the effective elastic constants of the system, which determines the relative stability of the resulting droplet containing a disclination, compared to the monodomain obtained as a result of the "droplet coalescence". The disclination density obtained at the end of the phase transition ("initial disclination density") will be determined by the relative rate at which the two competing processes occur. Regardless of the relative rate of the formation of disclinations and the droplet coalescence, the initial disclination density will be proportional to the nucleation density. In this context, the temperature dependence of the initial disclination density will depend upon the conditions of the nucleation of the nematic phase. For homogeneous nucleation, the nucleation rate should increase with increasing degree of undercooling, leading to the prediction of a larger initial disclination density formed at lower temperatures. On the other hand, if the nucleation of the nematic phase occurs at predetermined fixed nucleation sites (heterogeneous nucleation), with all the nuclei forming instantaneously, both the number of nuclei and the initial disclination density will be independent of the nucleation temperature.

Thus, the observation of the temperature independence of the initial domain size can be interpreted in terms of the model

presented above, where the formation of the nematic phase from the isotropic one occurs by heterogeneous nucleation. This model for the formation of disclinations can predict the common observation of the larger disclination densities encountered in polymeric systems compared to SMLC, in terms of higher values of the orientational viscosities of the former. In this approach, the differences in disclination densities between LCPs and SMLC concerns the formation of disclinations, in contrast to the idea that the larger disclination densities characteristic of LCPs is due to the slower annihilation of the already formed disclinations.[53]

6.2.2 Domain Growth

The thermal history dependence of the textures studied indicates that the initial structures obtained at the nematic phase formation are not the stable textures. The stable form of the directorfield in liquid crystals can not be defined without defining the boundary conditions. Because of the small magnitude of the Frank elastic constants the director can be affected by small perturbations such as the presence of impurities and surface inhomogeneities. In the case of untreated substrates, such as the ones used in this work, the substrate can favor a specific local molecular orientation, which may randomly vary from point to point. Under such boundary conditions, the energy can be minimized by the presence of a given number of defects such as disclinations. The value of the stable disclination density will be a

function of parameters such as the elastic constants of the material as well as energy of interaction between the substrate and the defects.

The domain growth process observed, involving the annihilation of the disclinations, can be rationalized in terms of a relaxation process driven by a decrease in the excess free energy of the initial texture. The initial disclination density, determined by the mechanism of the nucleation of the nematic phase, is larger than the stable density determined by the substrate. The driving force for the process is the excess elastic free energy due to the curvature of the directorfield imposed by the disclinations.

The kinetics of the domain growth can be interpreted in terms of its driving force and a viscous drag force. It is possible to draw an analogy between the annihilation of disclinations in the polydomain state and the relaxation of the orientation fluctuations in the monodomain state (section 1.3.3). In the latter, the distortions of the directorfield are due to thermal fluctuations and the relaxation rate is proportional to the quantity k/η , where k is a characteristic value of the elastic constants and η is an average viscosity representing the friction related to the twisting of the director. In the polydomain state, the viscosity η should be related to the mobility of the defects in the medium.

In this context, one can qualitatively explain the large difference in the time scale of the domain growth observed between the Polaroid polymer (a few minutes) and the PSHQ polymer (several hours). While the relative "orientational viscosities" viscosities of the two systems can not be assessed, the

observed differences follow the trend expected from considering the difference in the elastic constants. From its para-linked structure, the backbone of the Polaroid polymer is expected to be stiffer than the semiflexible PSHQ polymer, and in turns, it should have larger k values.

Following the concept of the kinetics of the domain growth being proportional to the quantity k/η , one can attempt to interpret the temperature dependence of the initial growth rate of the PSHQ polymer (figure 4.13). The observation of increasing growth rates with increasing temperatures indicates that in the range of temperatures studied, the temperature dependence of the viscosity prevails over the effect of temperature on the driving force. In other words, while both k and η are decreasing functions of temperature, the results obtained indicate that η decreases faster than k at increasing temperatures up to 160°C. However, the values of the elastic constants should rapidly approach zero at temperatures in the proximity of the nematic to isotropic transition, and this effect should lead to a maximum growth rate at some temperature T_{max} , above which the growth should slow down. While a decrease in the domain growth rate at increasing temperatures was not observed in the range of 130°C to 160°C, the leveling-off trend apparent in figure 4.13 at 160°C would indicate T_{max} being close to $T_{N\text{-}I}$ (170°).

For considering the shape of the growth curve at constant temperature, figure 6.2 shows a logarithmic representation of the growth curve measured at 150°C (figure 4.9). The sigmoidal shape

of the logarithmic plot deviates from the behavior predicted by the kinetic model presented in section 4.3. It is recalled that assuming $1/q_{max}$ being proportional to the average distance between neighboring disclinations, the model predicts a single scaling behavior with an exponent of 0.5. Some possible factors responsible for the deviations from the ideal model are considered below.

First, the kinetic model neglects the presence of disclinations of strength higher than $S=\pm 1/2$. In the textures studied, the analysis of the disclination strength was only possible after some extent of annihilation have taken place (see section 3.3) with the conclusion that the vast majority of the disclination corresponded to strength of $S=\pm 1/2$. It is possible, however, that annealing affects not only the disclination density, but also the disclination strength distribution. It is conceivable that if the initial texture would contain a considerably amount of disclinations of strength $S=\pm 1$, those would annihilate faster than the more stable $S=\pm 1/2$ disclinations.

Secondly, since the value of the elastic constants is a function of the order parameter, the observed time dependence of the local degree of order indicates the possibility of an increase in the effective values of the elastic constants during annealing. This would imply an increasing driving force during annealing, affecting the rate constant for the annihilation.

In a study of the domain growth in the X7-G , Hashimoto et al.[82,83] found both $1/q_{max}$ and the average distance between

disclinations to follow a scaling behavior with time with a scaling exponent of 0.35.

6.2.3 Local Ordering

The thermal analysis results presented in section 4.2.1 indicate that the N-I transition does not occur at equilibrium conditions, but the equilibrium conditions can be approached by thermal treatment at temperatures within the nematic range. Assuming that the N-I transition occurs at a constant value of the order parameter, the increase in T_{N-I} upon annealing suggests that at the phase transition from the isotropic to the nematic state, the order parameter does not reach its thermodynamic value. This kinetic effect on the order parameter is supported by the time dependence of the local anisotropy measured by SALS.

The fact that the broadness of the N-I endotherm peak was also found to be affected by thermal history can be interpreted as the existence of a "distribution of the order parameter". Thus, during annealing, the increase in the order parameter is accompanied by a narrowing of its distribution.

For a given structure, the N-I transition temperature is an increasing function of molecular weight, reaching a constant value at high molecular weights.[89,90] Based on this, the broadness encountered in TLCPs is often explained in terms of the polydispersity of the systems. The observation made in the present work indicates that the broadness of the transition might be in part due to the nematic phase not having reached its equilibrium state.

The conclusions drawn concerning the existence of a distribution of molecular order and the thermodynamical stability of the polymeric mesophase can be compared to observations made by other investigators. For example, the NMR spectrum of macroscopically aligned TLCPs often shows a central resonance peak on top of the split bands corresponding to the macroscopically oriented segments. The central peak is usually attributed to an isotropic phase which coexists with the nematic phase.[91] Moor and Stupp[92] studied the effect of molecular weight and annealing on the fraction of "disordered material". They observed a decrease on the fraction of the central peak with increasing annealing time at temperatures within the nematic phase. The observations were not in accordance with the presence of an isotropic fraction, and the authors suggested a "liquid crystal fringed micelle" model, consisting of interconnected "domains" of varying degree of segmental orientational order. While the existence of such domains separated by interphases, as originally formulated, might not represent the actual state, the concept of a non-equilibrium structure with varying degree of local order can be applied to describe the observations presently discussed.

It is possible that these non-equilibrium states are characteristic of polymeric molecules containing flexible segments. Based on a calculation done using the rotational isomeric state, Yoon and Bruckner[93] concluded that in such polymers the stable chain conformation consists of one in which the flexible spacers

adopt an all trans conformation, resulting into the fully extended molecular conformation. This result was found to agree with the experimental determination of the orientation functions of deuterium labeled spacers (by quadrupole deuterium NMR)[94]. It is important to point out that a requisite for carrying these measurement is to macroscopically align the samples by the magnetic field. On the other hand, recent small-angle neutron scattering studies performed on two different TLCPs[95,96] have shown that in the absence of an external field, the molecules in the nematic state are far from being extended. In the system studied by Blumstein, the radius of gyration was found to undergo an insignificant change while going from the isotropic into the nematic phase.

The following model is proposed as a possible molecular mechanism for the N-I transition in semiflexible LCPs, including the ordering induced by annealing. It is assumed that the thermodynamical stable nematic state consists of the fully extended conformation of the flexible spacers and mesogens (figure 6.3). Given the high rate of the transformation from the isotropic to the nematic phase, it is possible that the molecular conformation formed right at the phase transition initially involves the orientational ordering of the mesogenic units only. This would account for the long range order which give rise to the observed birefringence while nearly retaining the overall molecular shape from the isotropic state. This is followed by a slow ordering process involving the displacement of chain

segments through rotation around the flexible bonds leading to the extended chain conformation.

It would be of interest to see whether such a model would account for the negligible effect of annealing temperature on the shift of T_{N-I}.

6.3 Textures Induced by Shear

The texture induced by small deformation, with the elongated domains or worms oriented perpendicular to the shear direction, appears to be a peculiar observation. The common behavior is that the oriented structures obtained by deformation leads to greater correlation in orientation in the direction parallel to the elongation or shear direction. Examples of such systems are deformed spherulites[97], fiber structures[98] and the wormlike texture observed by Graziano and Mackley.[62] On the other hand, the perpendicular orientation observed in this work is not unique. The stress-induced crystallization of polyethylene terephtalate (PET) leads to spherulites elongated in the direction perpendicular to the stress, the corresponding SALS intensity concentrating in the direction parallel to the stress.[99] In fact, the most striking example of perpendicular correlation is the banded texture developing after the cessation of the shear.

The appearance of the textures induced by moderate extents of shear would probably depend on the interactions between the shear field and the defects. Assuming that small deformation does not affect the disclination density, it is possible that, depending on

parameters such as the anchoring energy of the defects and the sample thickness, the disclination lines originally attached to the bottom and top plates could either elongate, slip, or translate. This would cause different distortions of the directorfield, affecting the appearance of the resulting textures.

The SALS patterns observed at higher shear deformation (figure 5.2), closely resembles those observed by Navard[64] and by Hashimoto[100] in lyotropic LCPs at constant shear rates in the shear thinning region. A unique interpretation of the patterns has not yet been established, but it was suggested that it can be accounted for in terms of a large fraction of the material being aligned parallel to the shear, confining the defects into regions of lower effective anisotropy.

The geometry of the molecular alignment giving rise to the banded texture has been established by Windle[58], by optical and electron microscopy studies of quenched films of X7-G. The analysis indicated a serpentine trajectory of the director along the prior shear axis.

The structure obtained at the highest shear deformation performed in the present study was found to be relatively stable. The general trend observed in various systems (not necessarily LCPs) is that the relaxation time of the post-shear state decreases with increasing the shear rate applied. Therefore, the stability observed might be a result of the low shear rates employed.

Most interesting is the observation made concerning the effect of temperature on the formation of the banded texture. The

fact that the banded texture did not developed at the deformation temperature could be due to the low shear stress applied, which at 150°C, did not reach the minimum shear rate necessary for the bands formation. However, the formation of the bands at lower temperatures indicates that the conditions for the band formation are not an absolute function of the amount of deformation applied, and are probably determined by the ratio between the amount of energy supplied during the deformation and the elastic energy of the material. The latter would be directly related to the values of the elastic constants. In this context, the formation of the banded texture during cooling can be interpreted in terms of a minimum value of the elastic constants necessary for the bands formation. Under the shear conditions used, these are reached at 130°C. This interpretation is compatible with the observation made by, Graziano and Mackley[62], who concluded that the banded texture is a "low temperature, high shear relaxation phenomenon".

The role of the elastic constants of the material on the band formation was considered by a model proposed by Marrucci.[101] The banded texture is explained as an ordered tumbling effect, where the condition for the tumbling is determined, between other parameters, by what Marrucci describes as the "Frank elasticity". While Marrucci's model was found of limited application, it is conceivable that the elastic constants play a significant role on the conditions for the band formation. The ability to recover the banded texture at lower temperatures during subsequent temperature cycles indicates the banded texture being a thermodynamical metastable state.

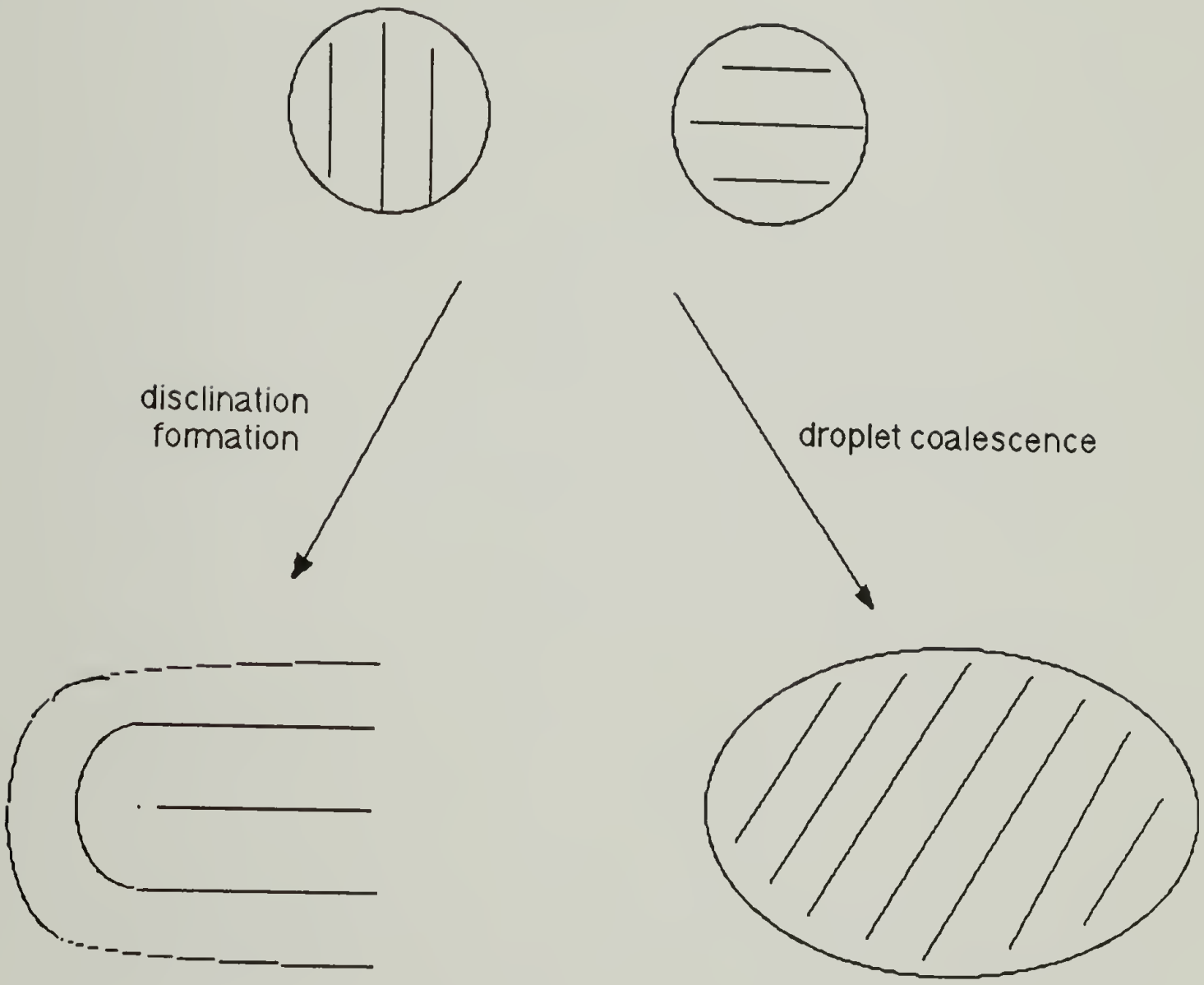

Figure 6.1 Schematic representation of a possible mechanism for the formation of disclinations during the phase transition from the isotropic phase.

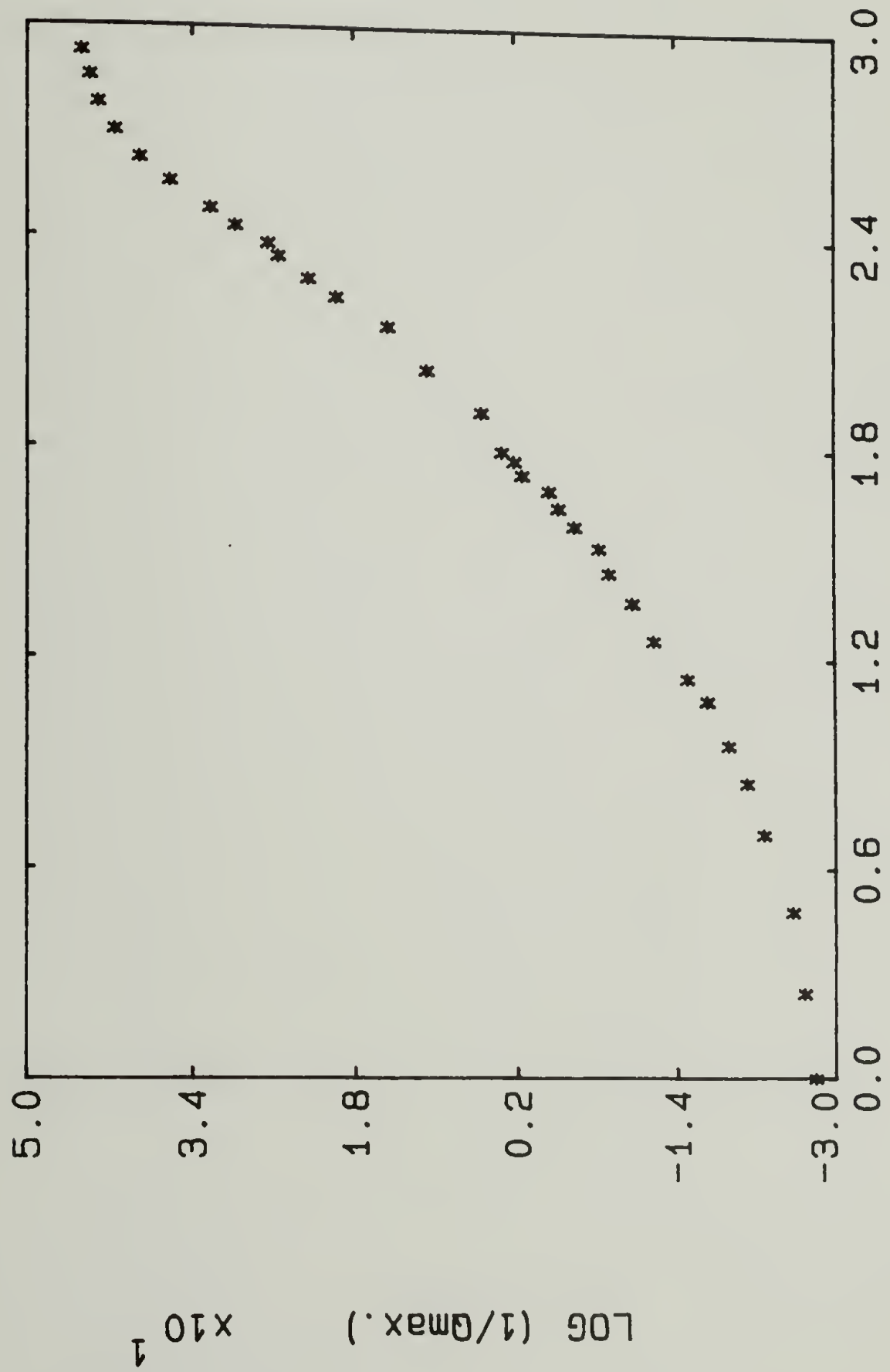

Figure 6.2 Logarithmic plot of the growth curve of PSHQ at 150°C.

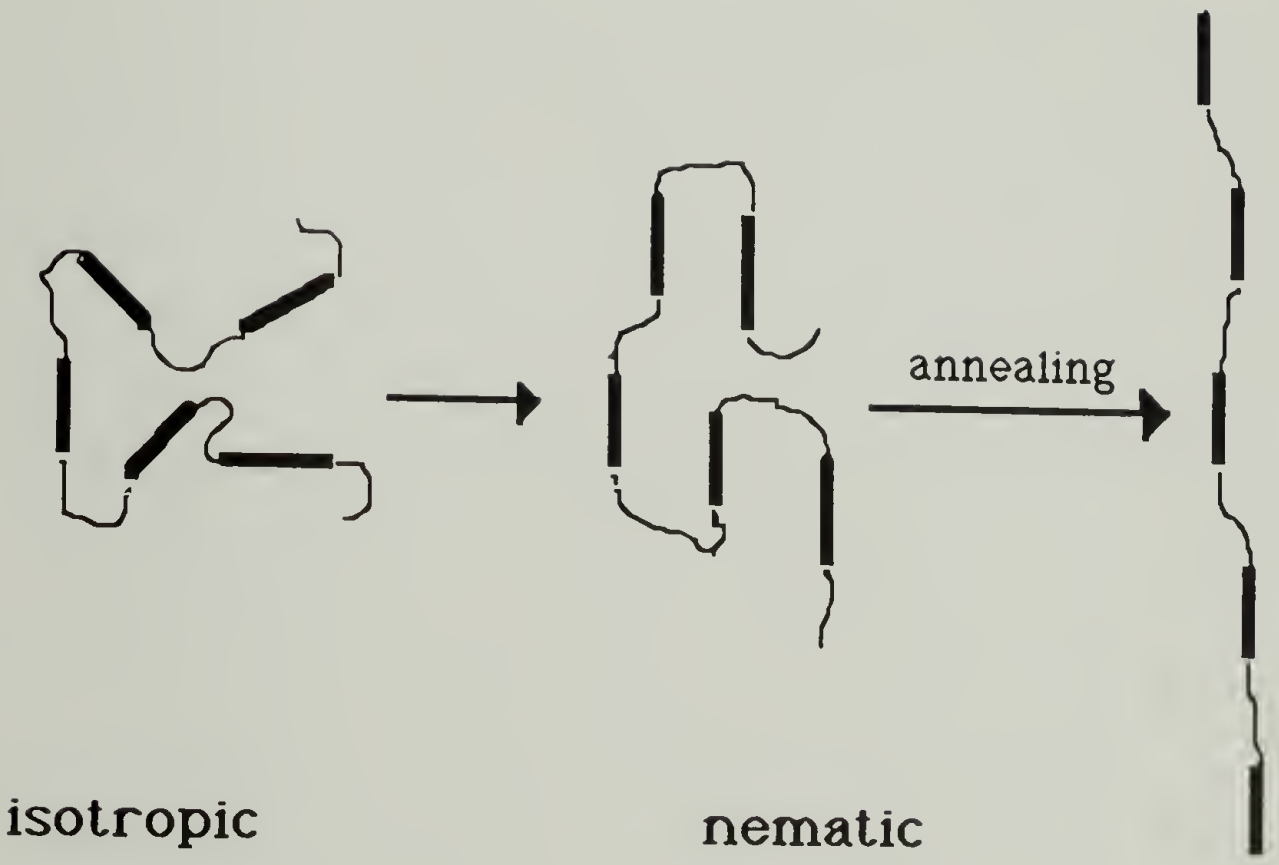

Figure 6.3 Schematic representation of the proposed model for the configurational changes occurring at the nematic phase formation and during annealing.

CHAPTER 7
CONCLUSIONS AND SUGGESTIONS FOR FUTURE WORK

7.1 Conclusions

One major conclusion is that, unlike small molecule liquid crystalline systems, the mesomorphic state of polymeric systems under usual circumstances is not necessarily in its equilibrium state. The study carried on a semiflexible polymer showed that the initial nematic state obtained following the fast transition from the isotropic phase does not reach its maximum possible degree of order. The equilibrium state, however, can be approached by annealing at temperatures within the nematic range. Aging results in an increase in the degree of local anisotropy along with a macrostructural rearrangement involving the annihilation of defects. The increase in the nematic to isotropic transition occurring during annealing was interpreted as an increase in order in a molecular scale and it is suspected to involve a change in the chain conformation. The kinetics of the local ordering process was found to be independent of the annealing temperature, in the 20°C range studied. In the same temperature range, the kinetics of the domain growth depends strongly on temperature, with increasing rates of annihilation of disclinations at increasing temperature.

In spite of the apparent randomness of the nematic textures as visualized by optical microscopy, the small-angle light scattering patterns indicate the directorfield adopts a specific,

non-random geometry. The latter is believed to be a consequence of the role played by the elastic anisotropy in the interaction between disclinations.

A preliminary study of the textures induced by shear deformation carried out by rheo-optical techniques revealed the possibility of a reversible formation of the banded texture. The observed behavior indicates the banded texture being a thermodynamical metastable state. The elucidation of the deformation and relaxation mechanisms of liquid crystal polymers is still in its primitive steps and deserves the focus of additional experimental investigation.

7.2 Suggestions for Future Work

7.2.1 Small-Angle Light Scattering

Although the SALS technique was shown to be a useful tool for characterizing the nematic textures in the quiescent state, the analysis was done on a semiempirical bases. The development of a theoretical model describing the orientation fluctuations in such textures would allow to extract additional information about the corresponding textures. For example, one open question is the quantitative relationship between the measured correlation length and the average disclination density of the system. Such a model should be also able to account for the observed azimuthal dependence of the scattered intensities. While it was postulated that the observed azimuthal dependence of the intensity is a

consequence of the non-equality of the elastic constants, it is not known whether the functionality will differ if either splay of bend deformation would prevail. The non-particulate nature of the textures would suggest the statistical approach to be the most appropriate for treating the orientation fluctuations. This leads to the conclusion that the treatment of statistical non-random fluctuations proposed by Stein et al.[78], found of limited use to describe systems of defined geometries, can be very appropriate for describing the liquid crystalline textures. This model could be used for proposing orientation correlation functions representing either splay or bend deformation and evaluating the azimuthal dependence expected from each mode. Such a model might enable the evaluation of the ratio of the elastic constants from the SALS data. In order to check the validity of the proposed argument concerning the nature of the non-randomness of the fluctuations, a simpler alternative would be to calculate the scattering amplitude from the directorfield imposed by single pairs of disclinations in configurations favoring either splay or bend deformation.

7.2.2 The Conformation of Semiflexible Liquid Crystal Polymers

In the discussion of the effect of annealing on the N-I transition temperature, it was suggested that the local ordering induced by annealing is related to changes in the conformation of the flexible spacers. It is possible that such a relaxation process might be responsible for the observation of non-equilibrium properties of semiflexible TLCPs made by other investigators.[92]

While it has been established that the thermodynamical stable state should be favored by the flexible spacers assuming a mostly extended conformation, the question is whether such a state is instantaneously achieved at the phase transition from the isotropic phase. The technique of choice to study molecular conformations is small-angle neutron scattering (SANS) from deuterium labeled molecules. One limitation of the technique is the inability (at least at the present time) to monitor changes occurring in relatively short time scales. It would be of interest to see whether indeed the conformation in the mesophase is affected by aging. The feasibility of the SANS measurements depends on the extent of the hydrogen content necessary for the contrast, which is usually relatively low in the aromatic polyesters.

7.2.3 Deformation Studies

The deformation study reported in this thesis is only a first step. The ultimate goal is to elucidate the mechanism by which the quiescent textures transform into the highly oriented structures required for obtaining the desired mechanical properties. Some of the pending questions concern the role of the defects in the quiescent state on the unique rheological properties observed at small shear rates and how the system gets rid of the disclinations at high shear rates, where the molecules are homogeneously aligned along the shear direction.

Valuable information could be obtained by measuring the scattered intensities corresponding to other polarization conditions

(H_H, V_H) not measured in the present thesis. It would be desirable to design the geometry of the deformation experiment so to accommodate steady state conditions. Another possibility would be to modify the system used in this thesis so one of the glass plates containing the sample is subjected to an oscillatory displacement. This would allow to vary the effective shear rates while keeping a constant gap between the glass plates.

As it has been shown in this thesis, while some of the features displayed by TLCPs subjected to shear appear to be analogous to the deformation process of lyotropic LPCs, the possibility of controlling the elastic constants by simply varying the temperature means that the study of thermotropic systems can provide additional valuable information on the behavior of LCPs in general.

REFERENCES

1. Maret G. and Blumstein A., Mol. Cryst. Liq. Cryst., **88**, 295 (1982).

2. Done D. and Baird D. G., Polym Eng . Sci. ,**27**, 818 (1987).

3. Reinitzer F., Montash. Chem., **9**, 421 (1888).

4. Stein R. S., J. Polym Sci., Part C, **15**, 185 (1966).

5. Kiss G. and Porter R. S., Mol. Cryst. Liq. Cryst., **60**, 267 (1980).

6. Asada T. and Onogi S., Polym. Eng. Rev., **3**, 324 (1983).

7. Hashimoto T., Takebe T. and Suehiro S., Polymer J., **18**, 123 (1986).

8. Friedel G., Ann. Physique, **18**, 273 (1972).

9. Saupe A., Angew. Chem. Int. Ed., **7**, 97 (1968).

10. Tsvetkov V., Acte Physicochim., **16**, 132 (1942).

11. Saupe A. and Maier W., Z. Naturforsch., **16**a, 816 (1961).

12. Spence R. D., Gutowsky H. S. and Holon C. H., J. Chem. Phys., **21**, 380 (1953).

13. Samulski E. T., Polymer, **26**B, 177 (1985).

14. de Gennes P. G., "The Physics of Liquid Crystals", Clarendon Press, Oxford (1974).

15. Chandrasekhar S., "Liquid Crystals", Cambridge University Press, Cambridge (1977).

16. Onsager L., Ann. N.Y. Acad. Sci., **51**, 627 (1956).

17. Flory P. J., Proc. Roy. Soc., A**234**, 73 (1956).

18. Flory P. J., Adv. Polym. Sci., **59**, 2 (1984).

19. Maier W. and Saupe A., Z. Naturforsch., **14**a, 882 (1959).

20. Stinson T. W. and Lister J. D., Phys. Rev. Lett., **25**, 503 (1970).

21. Tolstoi N. A. and Fedotov L. N., J. Exp. Theor. Phys.(USSR), **17**, 564 (1947).

22. de Gennes P. G., Mol. Cryst. Liq. Cryst., **12**, 193 (1971).

23. Landau L. D. and Lifshitz E. M., "Statistical Physics", Pergamon Press, Oxford (1969).

24. Gramsbergen E. F., Longw C. and de Jeu W. H., Phys. Rep., **135**, 195 (1986).

25. Stinson T. W. and Lister L. D., Phys. Rev. Lett., **30**, 688 (1973).

26. Oseen C. W., Trans. Faraday Soc., **29**, 883 (1933).

27. Frank F. C., Disc. Faraday Soc., **25**, 19 (1958).

28. Saupe A., Z. Natirforsch., **15**a, 810 (1960).

29. Priest R. G., Phys. Rev., A7, 720 (1973).

30. Lee S. and Meyer R. B., J. Chem. Phys., **84**, 3443 (1986).

31. Taratula V., Hurd A. J. and Meyer R. B., Phys. Rev. Lett., **55**, 246 (1985).

32. Hara M., Hirakata J., Toyooka T., Takezoe H. and Fukuda A., Mol. Cryst. Liq. Cryst., **122**, 161 (1985).

33. Chandrasekhar S. and Ranganath G. S., Adv. Phys., **35**, 507 (1986).

34. Meyer R. B., Mol. Cryst. Liq. Cryst., **16**, 355 (1973).

35. Nehring J. and Saupe A., J. Chem. Soc., Faraday Trans., **68**, 1 (1972).

36. Hudson S. D., submitted to Phys. Rev. Lett.

37. Ranganath G. S., Proc. Int. Conf. on Liq. Cry., Bangalore (1979).

38. Chatelain P., Acta Cryst.,**1**, 315 (1948).

39. de Gennes P. G., Mol. Cryst. Liq. Cryst., **7**, 325 (1969).

40. Van EckD. C. and Perdeck M., Mol. Cryst. Liq. Cryst., **49**, 39 (1978).

41. Haller I. and Lister J. D., in "Liquid Crystals", vol.3 (eds. G. H. Brown and M. M. Labes) p.85, Gordon and Breach (1972).

42. Orsay Liquid Crystal Group, J. Chem. Phys., **51**, 816 (1969).

43. Vorlander D., Z. Phys. Chem., **105**, 211 (1923).

44. Dobb M. G. and McIntyre J. E., Adv. Polym. Sci., **60**, 63 (1984).

45. Jin J. I., Antoun S., Ober C. and Lenz R. W., Brit. Polymer J., **12**, 132 (1980).

46. B. Wunderlich and J. Gebowicz, Adv. Poly. Sci., **60**, 1 (1984).

47. d'Allest J. F. , Sixou P., Blumstein A. and Blumstein R., Mol. Cryst. Liq. Cryst., **157**, 229 (1988).

48. de Gennes P. G., Mol. Cryst. Liq. Cryst., **34**, 177 (1977).

49. Mackley M. R., Pinaud F. and Siekmann G., Polymer, **22**, 437 (1981).

50. Viney C. and Windle A. H., J. Mat. Sci., **17**, 2661 (1982).

51. Kleman M., Liebert L. and Strzelecki L., Polymer, **24**, 295 (1983).

52. Mazelet G. and Kleman M., Polymer, **27**, 714 (1986).

53. Wood B., Ph.D. Thesis, Univ. of Massachusetts (1985).

54. Shiwaku T., Nakai A., Hasegawa H. and Hashimoto T., Polym. Commun., **28**, 174 (1987).

55. Hudson S. D., Thomas E. L. and Lenz R. W., Mol. Cryst. Liq. Cryst., **153**, 63 (1987).

56. Horio H., Ishikawa S. and Oda K., Appl. Polym. Symp., **41**, 269 (1985)

57. Aharoni S. M., Macromol., **12**, 94 (1979).

58. Navard P., J. Polym. Sci. Phys. Ed., **24**, 435 (1986).

59. Zachariades A. E. and Logan J. A., Polym. Eng. Sci., **23**, 797 (1983).

60. Donald A. M., Viney C. and Windle A. H., Polymer, **24**, 155 (1983).

61. Viney C., Donald A. M. and Windle A. H., Polymer, **26**, 870 (1985).

62. Graziano D. G. and Mackley M. R., Mol. Cryst. Liq. Cryst., **106**, 73 (1984).

63. Marsano E., Carpaneto L. and Ciferri A., Mol. Cryst. Liq. Cryst., **158**, 267 (1988).

64. Ernst B. and Navard P., to be published.

65. Furukawa A. and Lenz R. W., Macromol. Chem. Macromol. Symp., **2**, 3 (1986).

66. Sinta R., Gaudiana R. A., Minns R. A. and Rogers H. G., Macromol, **20**, 2374 (1987).

67. Weeks N., personal communication.

68. Hsiao B., personal communication.

69. Prud'homme R. E., Bourland L., Natarajan R. T. and Stein R. S., J. Polym. Sci. Polym. Phys. Ed., **12**, 1955 (1974).

70. Natarajan R. T., Prud'homme R. E., Bourland L. and Stein R. S., J. Polym. Sci. Polym. Phys. Ed., **14**, 1541 (1976).

71. Stein R. S. in "Static and Dynamic Properties of the Polymeric Solid State", (eds. R. A. Pethrick and R. W. Richards) p.109, D. Reidel (1982).

72. Guinier A., "Small-Angle Scattering of X-Rays", Wiley, New York (1955).

73. Van de Hulst H. C., "Light Scattering by Small Particles", Wiley, New York (1957).

74. Stein R. S. and Rhodes M. B., J. Appl. Phys., **31**, 1873 (1960).

75. Debye P. and Bueche B., J. Appl. Phys., **20**, 518 (1949).

76. Goldstein M. and Michalik E. R., J. Appl. Phys., **26**, 1450 (1955).

77. Stein R. S. and Wilson P. R, J. Appl. Phys., **33**, 1914 (1962).

78. Stein R. S., Erhardt P. F., Clough S. B. and Adams G., J. Appl. Phys., **37**, 3980 (1966).

79 Bouligand Y., J. Phys., Paris, **33**, 525 (1972).

80. de Gennes P. G., J,. Physique Lett., **35**, 217 (1974).

81. Windle A. H., Faraday Discuss. Chem. Soc., **79**, 186 (1985).

82. Shiwaku T., Nakai A., Hasegawa H. and Hashimoto T., Polym. Commun., **28**, 174 (1987).

83. Hashimoto T., to be published.

84. Stein R. S. and Stidham S. N., J. Appl. Phys., **35**, 42 (1964).

85. Clough S., van Aartsen J. J. and Stein R. S., J. Appl. Phys., **36**, 3072 (1965).

86. Demus D. and Richter L., "Textures of Liquid Crystals", Verlag Chemie, Weinheim (1978).

87. Rhodes M. B. and Stein R. S., J. Polym. Sci., **62**, 84 (1962).

88. Rhodes M. B. and Stein R. S., Polym. Lett., **1**, 663 (1963).

89. van Luyes D. and Strzelecki L., Europ. Polym. J., **16**, 303 (1980).

90. Dowell F., Mol. Cryst. Liq. Cryst., **157**, 203 (1988).

91. Schmiedel H., Hillner B., Grande S., Losche A. and Limmer S., J. Magn. Reson., **40**, 369 (1980).

92. Moore J. S. and Stupp S. I., Macromol., **20**, 282 (1987).

93. Yoon D. Y. and Bruckner S., Macromol., **18**, 651 (1985).

94. Bruckner S., Scott J. C., Yoon D. Y. and Griffin A. C., Macromol., **18**, 2709 (1985).

95. Blumstein R., to be published.

96. Buchner S., Chen D., Gehrke R. and Zachmann H. G., Mol. Cryst. Liq. Cryst., **155**, 357 (1988).

97. van Aartsen J. J. and Stein R. S., Polym. Lett., **5**, 901 (1967).

98. Stein R. S., Erhardt P., van Aartsen J. J., Clough S. and Rhodes M., J. Polym. Sci. Part C, **13**, 1 (1966).

99. Stein R. S., Polym. Eng. Sci., **16**, 152 (1976).

100. Hashimoto T. and Takebe T., to be published.

101. Marrucci G., Pure Appl. Chem, **57**, 1545 (1985).